Elsevier Editorial System(tm) for Chemical Engineering Journal

Manuscript Draft

Manuscript Number: CEJ-D-19-09387R1

Title: Comparison of acid-resistant ceramic and polymeric nanofiltration membranes for acid mine waters treatment

Article Type: Research Paper

Keywords: acid mine waters; rare earth elements; nanofiltration; TiO2 active layer; MPF-34; sulphuric acid recovery

Corresponding Author: Mr. Julio López,

Corresponding Author's Institution:

First Author: Julio López

Order of Authors: Julio López; Mònica Reig; Xanel Vecino; Oriol Gibert; José Luis Cortina

Abstract: Acid-resistant ceramic and polymeric nanofiltration (NF) membranes have been identified as relevant materials for sustainable management of acidic streams. NF properties such as a high passage of single-charged ions and high rejection of multi-charged ions make NF membranes suitable for acid recovery and metal concentration. In this work, the performance of two acid-resistant membranes: TiO2 ceramic and MPF-34 (proprietary layer) was tested with solutions mimicking acidic mine waters. Model solutions were composed by Al, Fe, Ca, Cu, Zn and rare earth elements (REEs) such as La, Dy, Sm, Nd, Pr and Yb. The effect of acidity (from pH 1.5 to 1.0), Al(III) (from 0.6 to 1.8 g/L) and Fe(III) (from 0.5 to 2.1 g/L) concentrations was studied. Both membranes allowed the transport of H+ (negative rejections were obtained), but exhibited differences related to the metallic ions transport. While MPF-34 presented metal rejections around 80% and independent on the concentration of the major components (Al(III) and Fe(III)), the TiO2 membrane provided a sequence of rejection values from 5 to 30%, with highest values for trivalent transition metals. These differences in the sequence of rejections suggested that the chemical properties of the TiO2 layer played a relevant role, and the differences in rejections could only be explained by dielectric effects. From the observed rejections, it was estimated that MPF-34 provided concentration factors for metals up to 4.2 and <1 for the H2SO4.

Response to Reviewers: -Reviewer 1
We would like to thank the reviewer for her/his detailed and accurate revision of the manuscript. All the queries have been taken into account and, accordingly, the required modifications have been made.
This work compared the TiO2 ceramic and polymeric nanofiltration membranes for acid recovery and metal concentration during the treatment of acid mine waters. The experimental results are of great practical significance. The topic is suitable for the journal audience. Therefore, I will recommend this work to be published in "Chemical Engineering Journal". However, the experimental data in the present manuscript are

insufficient. The paper needs some work to improve the quality. The authors should consider the following comments.

1. Introduction was not well written and did not highlight the importance of the study.

As indicated by the reviewer, the introduction was modified accordingly, and the importance of the study was highlighted.

2. The 'Limitations on acid purification and its recovery' in the title was not well represented in the abstract and conclusion.

As indicated by the reviewer, the title was modified accordingly to "Comparison of acid-resistant ceramic and polymeric nanofiltration membranes for acid mine waters treatment".

3. Page 4 line 2, It is suggested to investigate the actual water body in Iberian Pyrite Belt.

The Iberian Pyrite Belt is one of the most important polymetallic sulphide deposits of the world that has been exploited since before the Roman Empire. The intense mining, along with the low neutralization capacity of the minerals of their basins, has caused these rivers to develop extreme acidity and high concentrations of toxic elements. As a result, more than 150 types of Acid Mine Drainage can be found in the Odiel and Tinto river basins.

Feed composition is based on the mean composition of La Poderosa Mine at the Iberian Pyrite Belt along one year. More information was provided in the text.

4. Page 11 line 47, why did the rejection followed the sequence Al(III)>REE(III)?

Size exclusion cannot be responsible for higher Al(III) rejections than REEs(III). The higher REEs(III) molecular weight (from 139 to 162 Da), and consequently larger size, than Al(III) (27 Da) did not explain this tendency. Then, the electric and dielectric effects are responsible for the lower rejections. The ion polarizabilities, which are defined as the ability of an ion to relocate its electrical charge to minimize the interaction energy with the environment, can explain the sequence Al(III)>REE(III). The polarizability of Al3+ is within the range 0.05–0.07 Å3, whereas for REEs (La3+) is from 1.0 to 1.3 Å3. Then, higher rejections for Al(III) than REEs(III) were obtained. This information was provided in the manuscript (Page 12, lines 17-22).

5. Page 17 line 29, According to the author, a ceramic membrane with a smaller pore size should be used. However, in introduction, ZrO_2 has smaller pore size and narrower pore size distribution. Why did authors not use this? It might work well with this.

The transport of ions in nanofiltration is a sum of diffusion (gradient of concentration), convection (coupling between solvent and ions) and electrodiffusion (the different diffusivities of ions generate a potential gradient inside the membrane). The TiO_2 used in this study presents a large pore size. Therefore, there is a predominance of the convection term over the diffusive and electrodiffusive ones. The contribution of the convective term, which is responsible for the low rejections, can be diminished by using a membrane with smaller pore size and narrower pore size distribution. Then, it could be possible to obtain higher rejections.

As indicated by the reviewer, the use of a ZrO_2 membrane can be more suitable for this application. However, the ceramic membranes were fabricated by an external laboratory and delivered to test its applicability with acidic waters. An extended review of ceramic NF membrane producers was carried out and a reduced number of them were found. The selected provider was able to provide tubular NF membranes, with two ranges of pore sizes.

6. Many parts of the chart needed to be improved, such as Fig. 3 and Fig. 4. There was overlap between the abscissa and data points. In addition, the abscissa ruler should be placed at the low end and the valence state of the ion should be given.
As indicated by the reviewer, the chart was improved.
7. The experimental device diagram and the reaction mechanism diagram of the two membranes should be showed.
As indicated by the reviewer, diagrams of the nanofiltration experimental set-up (Figure 1) and membranes (Figure 4) were provided in the manuscript.
8. The concentrations of Fe and Al are different. Why did authors choose that concentration?
The Iberian Pyrite Belt site is rich in sulphide minerals, especially those containing iron (i.e. pyrite) while those based on zinc and copper are present at a lower extent. Moreover, aluminosilicates can be found in large quantities. As a result, the main elements in the acidic waters from the Iberian Pyrite Belt are iron and aluminium. As indicated, the solution composition was based on the mean composition of La Poderosa Mine at the Iberian Pyrite Belt along one year. Elements with concentrations lower than 10 mg/L were not included in the solution, such as arsenic, cadmium, cobalt and potassium, among others. The main variations in the composition from La Poderosa Mine were for aluminium and iron, with mean values 300 mg/L Al and 1100 mg/L Fe. From the analysis of the acid mine waters, it was reported 75th percentile values of 1800 mg/L Al and 2125 mg/L Fe. Therefore, and since the performance of nanofiltration membranes is highly influenced by the major elements in solution, different scenarios of Fe and Al concentrations were evaluated. More information was provided in the text (Page 5, lines 1-10).
9. The title is inconsistent with the research content. So, the title is suggested to be modified.
As indicated by the reviewer, the title was modified accordingly to "Comparison of acid-resistant ceramic and polymeric nanofiltration membranes for acid mine waters treatment".
10. The experiment section needed to be supplemented in more detail, Including formulas of acid recovery and metal concentration. Furthermore, was the 30 L solution for each reaction? What was the volume of each reaction? Was the reaction continuous flow reaction or batch reaction? How much metal was trapped on the membrane for calculating metal concentration? It is suggested to supplement the results of the used membrane XPS or SEM-mapping for further proving the experimental results and mechanism.
As indicated by the reviewer, the experiment section was supplemented in more detail:
- The equation for rejection and metal concentation factor were provided in the manuscript (see eq. 1 in Page 7, lines 3-9).
- Each experiment was performed with 30 L of feed solution to minimize changes in its composition when permeate samples were taken. This was clarified in the experiment.
- Two kinds of reactions can be found during the experiment; those related to equilibria in aqueous solution (see Table 2) which take place in the 30 L of the feed solution, and those related to the protonation/deprotonation of the active layer functional groups. In the latter case, these reactions take place in the membrane itself, but only in the active layer. The ones related to the ceramic membrane are present in equations 2 and 3 (Page 8, lines 11-15). For the MPF-34 membrane, the membrane was analyzed by XPS, which suggested the membrane has any kind of amide as functional group (Page 10, lines 14-20).

- Two feed samples were taken along with the experiment, one at the beginning before sampling and another one at the end of the experiment. Moreover, mass balances were performed with the composition of feed and permeate samples to determine if any metal was trapped on the membrane. Differences below 1% in the mass balances were found, which were related to analytical errors instead of metal entrapment. Moreover, a solubility analysis was performed with the Hydra/Medusa code (reference 34 in the manuscript), and no precipitation occurs at pH<1.5. This information was provided in the manuscript (Page 14, lines 24-28).
- After finishing one experiment, the set-up (including the membrane), was cleaned with a diluted sulphuric acid solution (pH = 1.0) and with deionised water during 1 h each one to remove any impurity. By cleaning the system only with deionised water, it can lead to an increase in pH of the solution that is still in the set-up and iron precipitation may occur inside the system. However, a first cleaning with a diluted sulphuric acid solution allowed to remove completely the solution from the system. Nevertheless, if there is any kind of scaling is removed due to the acidity of the cleaning solution. Then, the used membrane was not analysed previously by XPS or SEM-mapping.

-Reviewer 3

We would like to thank the reviewer for her/his detailed and accurate revision of the manuscript, especially the discussion devoted to improve the performance of the ceramic membranes in terms of membrane transport. While a large effort of transport models on polymeric membranes can be found, the modelling efforts on ceramic membranes are still needed. All the queries have been taken into account and, accordingly, the required modifications have been made.

This manuscript mainly presents and compares two commercial acid-resistant nanofiltration (NF) membranes of TiO2 ceramic one and the polymeric one named MPF-34 in the performance of acid recovery and metal rejection in acid mine water treatment. The results showed that both of the two membranes could partly reject the metal ions. MPF-34 showed a better rejection than TiO2 ceramic membrane, but it still let ~20% metal ions permeate and hardly assure a high purity of the acid.

As described by the reviewer the evaluation of the performance of a TiO2 ceramic membrane in acidic water was one objective, especially the assessment of its stability in acidic media, but no information was reported on the performance of complex streams as acid mine waters.

In previous works, we have evaluated different kinds of polymeric membranes for the treatment of acidic waters from the Iberian Pyrite Belt. Three commercial nanofiltration membranes: two polyamide-based (NF270 and Desal DL) and one sulphonated poly-ethersulphone-based (HydraCoRe 70pHT) were evaluated under the same conditions. The latter exhibited the worst performance because of their lower permeate flux and metal rejections (around 90%). The polyamide-based membranes exhibited the best performance with higher permeate flux and metal rejections (>98%), lower H+ rejections (<40%, with even negative values). However, after evaluating their stabilities in acidic conditions (1 month in 1 M H2O4), the polyamide-based membranes exhibited a loss of their selectivity (metal rejections around 90%) and higher permeate flux (almost the double the same pressure) due to hydrolysis of the active layer.

The low stability of polyamide-based membranes has made that we decided to evaluate different acid-resistant membranes for the treatment of acidic waters.

López, J., Reig, M., Gibert, O., Torres, E., Ayora, C., Cortina, J.L. "Application of nanofiltration for acidic waters containing rare earth

elements: Influence of transition elements, acidity and membrane stability" Desalination 430 (2018) 33 - 44
López, J., Reig, M., Gibert, O., Cortina, J.L. "Integration of nanofiltration membranes in recovery options of rare earth elements from acidic mine waters" Journal of Cleaner Production 210 (2019) 1249 - 1260
López, J., Reig, M., Gibert, O., Cortina, J.L. "Recovery of sulphuric acid and added value metals (Zn, Cu and rare earths) from acidic mine waters using nanofiltration membranes" Separation and Purification Technology 212 (2019) 180 - 190
In the analysis process of the effects of pH, Al3+, and Fe3+ on metal rejection and acid recovery, authors found the significant difference between the two membranes and revealed the possible mechanism of rejection and separation. However, in my opinion, the mechanism analysis is insufficient for the acid mine water with the complicated composition, referring lots of other research papers only and lacking systematic investigation.
This study follows up four years of research on the treatment of acidic mine waters by NF (see reference list above). The methodology for the evaluation and study of the transport mechanism was based on the Solution-Diffusion- Electromigration Model, which can be applied for solutions containing a dominant salt and different trace salts but not for complex systems such as acid mine waters. The concept of the reactive transport was introduced successfully for polymeric based NF-membranes and was tried to be applied in this work, but the properties of the active surface layer (where the pore size approaches to the free-volume size of the polymeric membranes) make necessary a reformulation of the model before application. This new model is under development, and results will deserve a publication full dedicated to this effort. It could be seen as described by the reviewer at this stage that the "mechanism analysis is insufficient for the acid mine water with the complicated composition" but the fact that any model has not been reported in the literature is an indication of the challenge faced.
Please explain why MPF-34 with 10 times thinner active layer rejected metal ions more efficiently than TiO2 ceramic membrane, showed a similar rejection level for most of the metal ions, and had a clear increase with the flux increase. Maybe, these results implied the density or the porosity of membrane is critical to the interaction strength of metal ions with active sites on the membrane surface and in membrane channel, especially along with the change of ion form. That is to say, the membrane matrix and porosity determines the role of geometric dimension exclusion, Donnan exclusion, and dielectric exclusion. The experimental design of this manuscript hardly digs out the filtration mechanism.
We fully agree with your statement that the membrane matrix and porosity determines the role of size, Donnan, and dielectric exclusions. In the case of polymeric membranes, efforts to characterize the free volume sizes has been achieved by the use of Positron Annihilation Spectroscopy and Rutherford Back Scattering techniques have been postulated recently to provide this information. However, limited effort has been reported for ceramic membranes and main efforts have been directed to pore size characterization. In this case, the mean pore size is determined by filtering organic compounds of different molecular weight. However, the obtained pore size will not be the same at different pH values, since the membrane properties are dependent on solution pH. Moreover, it is established that the intermediate layer has a significant effect on the ion separation. Furthermore, the relatively small thickness of the active layer makes impossible to separate it from the rest of the membrane without damaging it.

Both membranes are quite different. One of them is made of a polymeric material, most likely an amide with a dense active layer, whereas the other membrane is made of titania with a relatively open geometry (pore size of 1 nm according to the manufacturer) and higher thickness. The differences in porosity can explain the different behaviour.
The ion flux across the membrane (i.e. rejections) can be explained by a combination of diffusion (concentration gradient), electromigration (the differences in ion transport generate a potential gradient inside the membrane) and convection (coupling between solvent and ions). For dense polymeric membranes (e.g. MPF-34), the contribution of convection can be neglected. Thus, ion transport is governed by diffusion and electromigration. The fact that convection predominates over the diffusion and electromigration, as the case of the TiO2 ceramic membrane, makes rejection lower since more water is transported due to coupling between ion and solvent (i.e. water). Moreover, the effect of dielectric exclusion is high for dense membranes, and its effect diminished at large pore sizes. In this case, the large pore size of the ceramic membrane (1 nm according to the manufacturer) makes dielectric exclusion weaker. This is also responsible for the higher rejections of MPF-34.
Many reports (referred in this manuscript) had indicated the limitation of NF membrane in acid mine water treatment, showing low metal rejection and bad selectivity between metal ions and acid. Notably, in this manuscript, the MPF-34 showed superior H+ permeability, especially under a high concentration Fe3+. If you further filter the permeate, the purity of the acid may improve remarkably. As a result, the acid can be separated and recovered for reuse. I think you should focus on acid recovery and conduct additional and systematic experiments. After a major revision, I think the manuscript can be reviewed again.
As indicated by the reviewer, there are limitations of the tested NF membranes to treat acidic mine waters. MPF-34 showed better metal rejections than the TiO2 ceramic membrane, but 20% of the metals were able to permeate. This fact resulted in a lower purity of the obtained acid. Moreover, the high H+ permeability with negative rejections favoured a permeate richer in sulphuric acid than the feed stream. As suggested, by further filtering the permeate, the purity of the acid will improve. However, with the performed experiments, it was shown that the metal rejections were around 80% and barely changed with solution composition. Instead, we have made an estimation of the concentration factors if the feed solution is continuously filtered at different permeate recoveries (Section 3.4).
The proposal and recommendation provided by the reviewer is under evaluation on a project at pilot scale in two mines facilities where the main target selected is acid recovery because in some cases: i) acid may be reused internally in the processing stages (e.g. leaching stages) even if the quality is not very high; ii) acid extraction reduces the need of alkali for neutralization of these acid mine waters.

Refer to some papers from CEJ
More papers from CEJ were cited

Departament d'Enginyeria Química
UNIVERSITAT POLITÈCNICA DE CATALUNYA

Dr. Professor Tejraj M Aminabhavi

Editor on Chemical Engineering Journal,

Barcelona, 06/09/2019

Dear Mr,

Please find enclosed the revised version of our manuscript: "*Comparison of acid-resistant ceramic and polymeric nanofiltration membranes for acid mine waters treatment"* by: Julio López, Mònica Reig, Xanel Vecino, Oriol Gibert and José Luis Cortina (**Reference CEJ-D-19-09387**).

We have considered all the comments and suggestions made by the reviewers and we hope that the manuscript will now be suitable for publication in **Chemical Engineering Journal.**

A listed response to the reviewer's comments and a marked original copy is provided on separate sheets.

I look forward to hearing from you.

Yours faithfully,

Mr. Julio López (corresponding author)

Departament d'Enginyeria Química EEBE,

Universitat Politècnica de Catalunya-BarcelonaTech

Av. D'Eduard Maristany 10-14, 08019 Barcelona, Spain

Phone: (+34) 93 401 6997

e-mail: julio.lopez.rodriguez@upc.edu

Suggested reviewers

First name	Last name	Department	Institution	E-mail adress	Reason
Ricardo	Navarro	Departamento de Química	Universidad de Guanajuato	navarrm@ugto.mx	Experience in the membrane field, including nanofiltration membranes
Míriam C. S.	Amaral	Department of Sanitary and Environmental Engineering	Federal University of Minas Gerais	miriam@desa.ufmg.br	Experience on the treatment of acidic waters with nanofiltration membranes
Patrick	Dutourné	Institut de Science des Matériaux de Mulhouse	Université de Haute Alsace	patrick.dutournie@uha.fr	Experience on the treatment of the nanofiltration field, including ceramic membranes

Ref: CEJ-D-19-09387

Title: Comparison of acid-resistant ceramic and polymeric nanofiltration membranes for acid mine waters treatment: Limitations on acid purification and its recovery

Journal: Separation and Purification Technology

Dear Proff. Tejraj Aminabhavi,

Thank you for your invitation to resubmit our manuscript after addressing all reviewer comments. We have completed the review of your manuscript, and a summary of the raised comments and the comments and changes made could be found in the next pages below. We have considered all issues mentioned in the reviewers' comments, and we have outlined every change made point by point, and provide suitable rebuttals for any comments not addressed.

I look forward to receiving your comments.

Kind regards,

Julio Lopez

Comments from the editors and reviewers:

-Reviewer 1

We would like to thank the reviewer for her/his detailed and accurate revision of the manuscript. All the queries have been taken into account and, accordingly, the required modifications have been made.

This work compared the TiO2 ceramic and polymeric nanofiltration membranes for acid recovery and metal concentration during the treatment of acid mine waters. The experimental results are of great practical significance. The topic is suitable for the journal audience. Therefore, I will recommend this work to be published in "Chemical Engineering Journal". However, the experimental data in the present manuscript are insufficient. The paper needs some work to improve the quality. The authors should consider the following comments.

1. Introduction was not well written and did not highlight the importance of the study.

As indicated by the reviewer, the introduction was modified accordingly, and the importance of the study was highlighted.

2. The 'Limitations on acid purification and its recovery' in the title was not well represented in the abstract and conclusion.

As indicated by the reviewer, the title was modified accordingly to “Comparison of acid-resistant ceramic and polymeric nanofiltration membranes for acid mine waters treatment”.

3. Page 4 line 2, It is suggested to investigate the actual water body in Iberian Pyrite Belt.

The Iberian Pyrite Belt is one of the most important polymetallic sulphide deposits of the world that has been exploited since before the Roman Empire. The intense mining, along with the low neutralization capacity of the minerals of their basins, has caused these rivers to develop extreme acidity and high concentrations of toxic elements. As a result, more than 150 types of Acid Mine Drainage can be found in the Odiel and Tinto river basins.

Feed composition is based on the mean composition of La Poderosa Mine at the Iberian Pyrite Belt along one year. More information was provided in the text.

4. Page 11 line 47, why did the rejection followed the sequence Al(III)>REE(III)?

Size exclusion cannot be responsible for higher Al(III) rejections than REEs(III). The higher REEs(III) molecular weight (from 139 to 162 Da), and consequently larger size, than Al(III) (27 Da) did not explain this tendency. Then, the electric and dielectric effects are responsible for the lower rejections. The ion polarizabilities, which are defined as the ability of an ion to relocate its electrical charge to minimize the interaction energy with the environment, can explain the sequence Al(III)>REE(III). The polarizability of Al^{3+} is within the range 0.05–0.07 $Å^3$, whereas for REEs (La^{3+}) is from 1.0 to 1.3 $Å^3$. Then, higher rejections for Al(III) than REEs(III) were obtained. This information was provided in the manuscript (**Page 12, lines 17-22**).

5. Page 17 line 29, According to the author, a ceramic membrane with a smaller pore size should be used. However, in introduction, ZrO2 has smaller pore size and narrower pore size distribution. Why did authors not use this? It might work well with this.

The transport of ions in nanofiltration is a sum of diffusion (gradient of concentration), convection (coupling between solvent and ions) and electrodiffusion (the different diffusivities of ions generate a potential gradient inside the membrane). The TiO_2 used in this study presents a large pore size. Therefore, there is a predominance of the convection term over the diffusive and electrodiffusive ones. The contribution of the convective term, which is responsible for the low rejections, can be diminished by using a membrane with smaller pore size and narrower pore size distribution. Then, it could be possible to obtain higher rejections.

As indicated by the reviewer, the use of a ZrO_2 membrane can be more suitable for this application. However, the ceramic membranes were fabricated by an external laboratory and delivered to test its applicability with acidic waters. An extended review of ceramic NF membrane producers was carried out and a reduced number of them were found.

The selected provider was able to provide tubular NF membranes, with two ranges of pore sizes.

6. Many parts of the chart needed to be improved, such as Fig. 3 and Fig. 4. There was overlap between the abscissa and data points. In addition, the abscissa ruler should be placed at the low end and the valence state of the ion should be given.

As indicated by the reviewer, the chart was improved.

7. The experimental device diagram and the reaction mechanism diagram of the two membranes should be showed.

As indicated by the reviewer, diagrams of the nanofiltration experimental set-up (**Figure 1**) and membranes (**Figure 4**) were provided in the manuscript.

8. The concentrations of Fe and Al are different. Why did authors choose that concentration?

The Iberian Pyrite Belt site is rich in sulphide minerals, especially those containing iron (i.e. pyrite) while those based on zinc and copper are present at a lower extent. Moreover, aluminosilicates can be found in large quantities. As a result, the main elements in the acidic waters from the Iberian Pyrite Belt are iron and aluminium. As indicated, the solution composition was based on the mean composition of La Poderosa Mine at the Iberian Pyrite Belt along one year. Elements with concentrations lower than 10 mg/L were not included in the solution, such as arsenic, cadmium, cobalt and potassium, among others. The main variations in the composition from La Poderosa Mine were for aluminium and iron, with mean values 300 mg/L Al and 1100 mg/L Fe. From the analysis of the acid mine waters, it was reported 75th percentile values of 1800 mg/L Al and 2125 mg/L Fe. Therefore, and since the performance of nanofiltration membranes is highly influenced by the major elements in solution, different scenarios of Fe and Al concentrations were evaluated. More information was provided in the text (**Page 5, lines 1-10**).

9. The title is inconsistent with the research content. So, the title is suggested to be modified.

As indicated by the reviewer, the title was modified accordingly to "Comparison of acid-resistant ceramic and polymeric nanofiltration membranes for acid mine waters treatment".

10. The experiment section needed to be supplemented in more detail, Including formulas of acid recovery and metal concentration. Furthermore, was the 30 L solution for each reaction? What was the volume of each reaction? Was the reaction continuous flow reaction or batch reaction? How much metal was trapped on the membrane for calculating metal concentration? It is suggested to supplement the results of the used membrane XPS or SEM-mapping for further proving the experimental results and mechanism.

As indicated by the reviewer, the experiment section was supplemented in more detail:

- The equation for rejection and metal concentation factor were provided in the manuscript (see eq. 1 in **Page 7, lines 3-9**).
- Each experiment was performed with 30 L of feed solution to minimize changes in its composition when permeate samples were taken. This was clarified in the experiment.
- Two kinds of reactions can be found during the experiment; those related to equilibria in aqueous solution (see Table 2) which take place in the 30 L of the feed solution, and those related to the protonation/deprotonation of the active layer functional groups. In the latter case, these reactions take place in the membrane itself, but only in the active layer. The ones related to the ceramic membrane are present in equations 2 and 3 (**Page 8, lines 11-15**). For the MPF-34 membrane, the membrane was analyzed by XPS, which suggested the membrane has any kind of amide as functional group (**Page 10, lines 14-20**).
- Two feed samples were taken along with the experiment, one at the beginning before sampling and another one at the end of the experiment. Moreover, mass balances were performed with the composition of feed and permeate samples to determine if any metal was trapped on the membrane. Differences below 1% in the mass balances were found, which were related to analytical errors instead of metal entrapment. Moreover, a solubility analysis was performed with the Hydra/Medusa code (**reference 34** in the manuscript), and no precipitation occurs at pH<1.5. This information was provided in the manuscript (**Page 14, lines 24-28**).
- After finishing one experiment, the set-up (including the membrane), was cleaned with a diluted sulphuric acid solution (pH = 1.0) and with deionised water during 1 h each one to remove any impurity. By cleaning the system only with deionised water, it can lead to an increase in pH of the solution that is still in the set-up and iron precipitation may occur inside the system. However, a first cleaning with a diluted sulphuric acid solution allowed to remove completely the solution from the system. Nevertheless, if there is any kind of scaling is removed due to the acidity of the cleaning solution. Then, the used membrane was not analysed previously by XPS or SEM-mapping.

-Reviewer 3

We would like to thank the reviewer for her/his detailed and accurate revision of the manuscript, especially the discussion devoted to improve the performance of the ceramic membranes in terms of membrane transport. While a large effort of transport models on polymeric membranes can be found, the modelling efforts on ceramic membranes are still needed. All the queries have been taken into account and, accordingly, the required modifications have been made.

This manuscript mainly presents and compares two commercial acid-resistant nanofiltration (NF) membranes of TiO_2 ceramic one and the polymeric one named MPF-34 in the performance of acid recovery and metal rejection in acid mine water treatment. The results showed that both of the two membranes could partly reject the metal ions. MPF-34 showed a better rejection than TiO_2 ceramic membrane, but it still let ~20% metal ions permeate and hardly assure a high purity of the acid.

As described by the reviewer the evaluation of the performance of a TiO2 ceramic membrane in acidic water was one objective, especially the assessment of its stability in acidic media, but no information was reported on the performance of complex streams as acid mine waters.

In previous works, we have evaluated different kinds of polymeric membranes for the treatment of acidic waters from the Iberian Pyrite Belt. Three commercial nanofiltration membranes: two polyamide-based (NF270 and Desal DL) and one sulphonated poly-ethersulphone-based (HydraCoRe 70pHT) were evaluated under the same conditions. The latter exhibited the worst performance because of their lower permeate flux and metal rejections (around 90%). The polyamide-based membranes exhibited the best performance with higher permeate flux and metal rejections (>98%), lower H^+ rejections (<40%, with even negative values). However, after evaluating their stabilities in acidic conditions (1 month in 1 M H_2O_4), the polyamide-based membranes exhibited a loss of their selectivity (metal rejections around 90%) and higher permeate flux (almost the double the same pressure) due to hydrolysis of the active layer.

The low stability of polyamide-based membranes has made that we decided to evaluate different acid-resistant membranes for the treatment of acidic waters.

López, J., Reig, M., Gibert, O., Torres, E., Ayora, C., Cortina, J.L. "*Application of nanofiltration for acidic waters containing rare earth elements: Influence of transition elements, acidity and membrane stability*" Desalination 430 (2018) 33 - 44

López, J., Reig, M., Gibert, O., Cortina, J.L. "*Integration of nanofiltration membranes in recovery options of rare earth elements from acidic mine waters*" Journal of Cleaner Production 210 (2019) 1249 - 1260

López, J., Reig, M., Gibert, O., Cortina, J.L. "*Recovery of sulphuric acid and added value metals (Zn, Cu and rare earths) from acidic mine waters using nanofiltration membranes*" Separation and Purification Technology 212 (2019) 180 - 190

In the analysis process of the effects of pH, Al^{3+}, and Fe^{3+} on metal rejection and acid recovery, authors found the significant difference between the two membranes and revealed the possible mechanism of rejection and separation. However, in my opinion, the mechanism analysis is insufficient for the acid mine water with the complicated composition, referring lots of other research papers only and lacking systematic investigation.

This study follows up four years of research on the treatment of acidic mine waters by NF (see reference list above). The methodology for the evaluation and study of the transport mechanism was based on the Solution-Diffusion- Electromigration Model, which can be applied for solutions containing a dominant salt and different trace salts but not for complex systems such as acid mine waters. The concept of the reactive transport was introduced successfully for polymeric based NF-membranes and was tried to be applied in this work, but the properties of the active surface layer (where the pore

size approaches to the free-volume size of the polymeric membranes) make necessary a reformulation of the model before application. This new model is under development, and results will deserve a publication full dedicated to this effort. It could be seen as described by the reviewer at this stage that the "mechanism analysis is insufficient for the acid mine water with the complicated composition" but the fact that any model has not been reported in the literature is an indication of the challenge faced.

Please explain why MPF-34 with 10 times thinner active layer rejected metal ions more efficiently than TiO_2 ceramic membrane, showed a similar rejection level for most of the metal ions, and had a clear increase with the flux increase. Maybe, these results implied the density or the porosity of membrane is critical to the interaction strength of metal ions with active sites on the membrane surface and in membrane channel, especially along with the change of ion form. That is to say, the membrane matrix and porosity determines the role of geometric dimension exclusion, Donnan exclusion, and dielectric exclusion. The experimental design of this manuscript hardly digs out the filtration mechanism.

We fully agree with your statement that the membrane matrix and porosity determines the role of size, Donnan, and dielectric exclusions. In the case of polymeric membranes, efforts to characterize the free volume sizes has been achieved by the use of Positron Annihilation Spectroscopy and Rutherford Back Scattering techniques have been postulated recently to provide this information. However, limited effort has been reported for ceramic membranes and main efforts have been directed to pore size characterization. In this case, the mean pore size is determined by filtering organic compounds of different molecular weight. However, the obtained pore size will not be the same at different pH values, since the membrane properties are dependent on solution pH. Moreover, it is established that the intermediate layer has a significant effect on the ion separation. Furthermore, the relatively small thickness of the active layer makes impossible to separate it from the rest of the membrane without damaging it.

Both membranes are quite different. One of them is made of a polymeric material, most likely an amide with a dense active layer, whereas the other membrane is made of titania with a relatively open geometry (pore size of 1 nm according to the manufacturer) and higher thickness. The differences in porosity can explain the different behaviour.

The ion flux across the membrane (i.e. rejections) can be explained by a combination of diffusion (concentration gradient), electromigration (the differences in ion transport generate a potential gradient inside the membrane) and convection (coupling between solvent and ions). For dense polymeric membranes (e.g. MPF-34), the contribution of convection can be neglected. Thus, ion transport is governed by diffusion and electromigration. The fact that convection predominates over the diffusion and electromigration, as the case of the TiO_2 ceramic membrane, makes rejection lower since more water is transported due to coupling between ion and solvent (i.e. water).

Moreover, the effect of dielectric exclusion is high for dense membranes, and its effect diminished at large pore sizes. In this case, the large pore size of the ceramic membrane (1 nm according to the manufacturer) makes dielectric exclusion weaker. This is also responsible for the higher rejections of MPF-34.

Many reports (referred in this manuscript) had indicated the limitation of NF membrane in acid mine water treatment, showing low metal rejection and bad selectivity between metal ions and acid. Notably, in this manuscript, the MPF-34 showed superior H^+ permeability, especially under a high concentration Fe^{3+}. If you further filter the permeate, the purity of the acid may improve remarkably. As a result, the acid can be separated and recovered for reuse. I think you should focus on acid recovery and conduct additional and systematic experiments. After a major revision, I think the manuscript can be reviewed again.

As indicated by the reviewer, there are limitations of the tested NF membranes to treat acidic mine waters. MPF-34 showed better metal rejections than the TiO_2 ceramic membrane, but 20% of the metals were able to permeate. This fact resulted in a lower purity of the obtained acid. Moreover, the high H^+ permeability with negative rejections favoured a permeate richer in sulphuric acid than the feed stream. As suggested, by further filtering the permeate, the purity of the acid will improve. However, with the performed experiments, it was shown that the metal rejections were around 80% and barely changed with solution composition. Instead, we have made an estimation of the concentration factors if the feed solution is continuously filtered at different permeate recoveries (**Section 3.4**).

The proposal and recommendation provided by the reviewer is under evaluation on a project at pilot scale in two mines facilities where the main target selected is acid recovery because in some cases: i) acid may be reused internally in the processing stages (e.g. leaching stages) even if the quality is not very high; ii) acid extraction reduces the need of alkali for neutralization of these acid mine waters.

Refer to some papers from CEJ

More references from CEJ were added to the manuscript.

Highlights

Nanofiltration membranes for acid recovery and metal concentration from acidic streams

Need of resistant nanofiltration membranes in acidic media

Evaluation of ceramic (TiO_2) and polymeric (MPF–34) acid-resistant membranes

Comparison of acid-resistant ceramic and polymeric nanofiltration membranes for acid mine waters treatment

J. López [a*], M. Reig [a], X. Vecino [a], O. Gibert [a], J. L. Cortina [a,b]

[a] *Chemical Engineering Department and Barcelona Research Center for Multiscale Science and Engineering, UPC-BarcelonaTECH, C/ Eduard Maristany, 10-14 (Campus Diagonal-Besòs), 08930 Barcelona, Spain*

[b] *Water Technology Center CETaqua, Carretera d'Esplugues 75, 08940 Cornellà de Llobregat, Spain*

* julio.lopez.rodriguez@upc.edu

Abstract

Acid-resistant ceramic and polymeric nanofiltration (NF) membranes have been identified as relevant materials for sustainable management of acidic streams. NF properties such as a high passage of single-charged ions and high rejection of multi-charged ions make NF membranes suitable for acid recovery and metal concentration. In this work, the performance of two acid-resistant membranes: TiO_2 ceramic and MPF–34 (proprietary layer) was tested with solutions mimicking acidic mine waters. Model solutions were composed by Al, Fe, Ca, Cu, Zn and rare earth elements (REEs) such as La, Dy, Sm, Nd, Pr and Yb. The effect of acidity (from pH 1.5 to 1.0), Al(III) (from 0.6 to 1.8 g/L) and Fe(III) (from 0.5 to 2.1 g/L) concentrations was studied. Both membranes allowed the transport of H^+ (negative rejections were obtained), but exhibited differences related to the metallic ions transport. While MPF–34 presented metal rejections around 80% and independent on the concentration of the major components (Al(III) and Fe(III)), the TiO_2 membrane provided a sequence of rejection values from 5 to 30%, with highest values for trivalent transition metals. These differences in the sequence of rejections suggested that the chemical properties of the TiO_2 layer played a relevant role, and that they could only be explained by dielectric effects. From the observed rejections, it was estimated that MPF–34 provided concentration factors for metals up to 4.2 and <1 for the H_2SO_4.

Keywords: acid mine waters; rare earth elements; nanofiltration; TiO_2 active layer; MPF–34; sulphuric acid recovery.

1. Introduction

Mining activities generate a large number of toxic effluents, including acid mine waters (AMW). These streams are characterised by a low pH (<2) and by the presence of dissolved metallic ions (e.g. Al, Fe, and Cu). Among these dissolved metals, rare earth elements (REEs) can be found. The concentration of REEs in AMW can vary between 4 to 80 mmol/L, which is two orders of magnitude higher than in natural waters [1–3]. Nowadays REEs, which are widely used in the high-tech industry [4,5], are mainly produced in China , while the European Union has a lack of mining sites to exploit REEs. Within this framework/context circular economy schemes are being proposed for their recovery.

Nowadays, management of AMW is focused on the recovery of valuable elements (e.g. H^+, REEs, Cu and Zn) by different methods, such as selective precipitation [6], treatment with natural zeolites [7] and membrane technologies (reverse osmosis [8], forward osmosis [9,10], among others). Among the different membrane technologies, nanofiltration (NF) membranes have shown a good performance because of their capacity of allowing the permeance of single-charged ions while rejecting the multi-charged ones. Different studies have demostrated that this selectivity of NF may allow to separate and recover acid (which permeates through the membrane) from metallic impurities (which are retained by the membrane). The latter can be further concentrated and recovered with other technologies [11–17]. Although the recovery of acid is not having a direct economic benefit, it has an indirect cost in the reduction of alkali consumption in the acidy neutralization stages.

The most widely used NF membranes are the thin-film composite (TFC) polymeric ones incorporating a polyamide active layer. However, at the long–term acid exposure, the polyamide active layer can suffer from hydrolysis leading to a loss in selectivity [18–20]. To solve this problem, acid-resistant TFC NF membranes have been developed and commercialised, such as the Duracid (proprietary, from GE Osmonics), MPF–34 (proprietary, from Koch Membrane Systems) and Hydracore 70pHT (proprietary from Hydranautics) ones, which offer as good rejections as the polyamide ones do [8,14,21].

In most of the cases, the composition of the membrane active layer is proprietary, but sulphamides or sulphonated polyethersulphones are used because of their resistance in acidic media. The stability of this acid-resistant membranes has been studied in literature. For example, Manis et al. [22] filtered a copper electroplating effluent with MPF–34 to separate Cu(II) from the H_2SO_4. As H_2SO_4 concentration increased from 0 to 2 M, copper (from 85% to 45%) and H_2SO_4 (from 20% to 15%) rejections decreased. Moreover, they performed a stability test with a polyamide NF membrane (DK) and the MPF–34 in 2 M H_2SO_4 for 8 weeks. After immersion, the DK showed an increase of permeate flux and a decrease in copper rejection, while MPF–34 was able to keep their properties.

In parallel, ceramic membranes, initially developed for ultrafiltration applications, are emerging as an alternative to the polymeric ones due to their higher chemical, mechanical and thermal stability, resulting in a longer duration. Nevertheless, they have to face their high fabrication cost and low selectivity. These facts have made that ceramic NF membranes are still not applied in applications at large scale [23,24]. The most common materials of their active layer are zirconia (ZrO_2) or titania (TiO_2), while the support is usually made of alumina (Al_2O_3). Only a few studies are found in literature with the applicability of ceramic NF membranes. For instance, Benfer et al. [25] evaluated the performance of ZrO_2 and TiO_2 NF membranes synthesised by the sol-gel method. The former exhibited higher rejections for salts (NaCl and Na_2SO_4), while the latter had better solvent fluxes. Pore size measurements revealed that ZrO_2 membrane had smaller pore size and narrower pore size distribution (0.75 – 1.75 nm) than TiO_2 membrane (0.5 – 2.5 nm). Voigt et al. [26] were able to develop TiO_2 NF membranes with a molecular weight cut-off (MWCO) of 250 Da and water flux of 10 L/(m^2·h·bar) by a two-step coating process. The application of TiO_2 membranes (pore size 0.9 nm, MWCO 450 Da) to treat textile wastewater was also evaluated, achieving a decolouring of 70-100% [27]. Wadekar and Vidic [28] compared the performance of a ceramic (TiO_2, MWCO ~ 500 Da, Cerahelix) and a polymeric (NF270, MWCO ~200 to 400 Da) membranes to treat the drainage of an abandoned coal mine (pH 7.8). NF270 was able to reject more than 96% of all the multi-charged ions, except for arsenic (33%), present as a non-charged form of As(III) (H_3AsO_3). On the other hand, the ceramic membrane exhibited much lower rejections (between 50 and 70%), and an arsenic rejection of 20%. No published studies were found about the performance of ceramic NF membranes in complex acidic media as AMW in the scientific literature.

The increasing price and lack of primary resources of REEs have made other sources such as AMWs to be evaluated. NF membranes have proven to be effective for the treatment of AMWs. However, commercial polyamide membranes can suffer hydrolysis, and therefore acid-resistant membranes (polymeric or ceramic) may be preferred. No studies of the performance of ceramic membranes to treat acidic waters are found in literature. The main objective of this work was to evaluate the performance of two acid-resistant NF membranes: a ceramic one containing titania (TiO_2) as a selective layer and polymeric one (MPF–34) to treat metal-containing sulphuric solutions mimicking AMWs from the Iberian Pyrite Belt. This solution presented an acidic pH (<2) and was characterised by the presence of metals (e.g. Al, Fe, Ca, Cu and Zn) and other elements at a low concentration such as REEs (e.g. La, Pr, Nd, Sm, Dy and Yb). The effects of pH (1.5 to 1.0), Al(III) (from 0.6 to 1.8 g/L) and Fe(III) (from 0.5 to 2.1 g/L) concentration in the AMW were studied in terms of acid and metal rejections. Furthermore, both membranes were characterised by different analytical techniques to study their composition and structure. Experimental results were explained with regard to the membrane active layer and its structure, as well as to the solution composition and the effect of complexation reactions. Moreover, a prediction of concentration factors when an AMW was filtered was carried out for both membranes.

2. Materials and Experimental Methodology

2.1. Membrane and solutions

A ceramic membrane with an active area of 44.92 cm^2 was tested. This membrane has a tubular configuration with an internal diameter of 6.5 mm and a thickness of 2 mm. This membrane presents an active layer of TiO_2 supported on Al_2O_3 with a mean pore size of 1 nm. An acid-resistant flat–sheet (140 cm^2) polymeric NF membrane from Koch Membrane Systems (MPF–34) was also tested. The composition of the active layer is patented, and there are no data about its structure in the literature. This membrane presents an MWCO of 200 Da and an isoelectric point (IEP) between 4.5 and 5.5 [29–32].

First of all, experiments were performed with 0.01 M Na_2SO_4 from pH 1 to 11 to determine the IEP of the ceramic NF membrane. Then, solutions mimicking AMWs

generated in a polysulphide mine in Río Tinto (La Poderosa), Huelva province (Southwest of Spain) were tested in the NF membrane set–up. These solutions reproduced the typical compositions of the effluents from the Iberian Pyrite Belt (Southwest of Spain), which is one of the main sulphide deposits worldwide [33]. Feed composition was based on the mean values along one year. Elements with concentrations lower than 10 mg/L were not included in the solution, such as arsenic, cadmium, cobalt and potassium, among others. The composition of these synthetic solutions is given in **Table 1**. The main variations in the composition were for Al and Fe, and then the effect of different variables such as pH and concentration of Al and Fe on the membrane performance was studied. The presence of Fe, usually as a mixture of Fe(II) and Fe(III), may limit the recovery of REEs in the hydrometallurgical industry. For this reason, Fe(II) is usually oxidised to Fe(III) with air and then removed with a low-cost alkali (e.g. CaO or $CaCO_3$) as hydroxide or hydroxyl–sulphate. Then, two scenarios could be found: one with Fe(III) and another one without this metal. In the present study, Fe in solution was Fe(III) (>99,5%). **Fig. S1** in Supplementary Information collects the speciation diagrams of the different elements in solution.

The following solutions and salts were used to prepare the synthetic solutions: Na_2SO_4 (>99%, Sigma-Aldrich); H_2SO_4 (96 wt%, Sigma-Aldrich); $Al_2(SO_4)_3{\cdot}18H_2O$ (55%, Panreac); $Fe_2(SO_4){\cdot}5H_2O$ (98%, Sigma-Aldrich); $CaSO_4{\cdot}2H_2O$ (100%, Scharlau); $CuSO_4$ (100%, Panreac); $ZnSO_4{\cdot}7H_2O$ (100%, Panreac); $La_2(SO_4)_3{\cdot}9H_2O$ (99.9%, Alfa Aesar); $Pr(NO_3)_3{\cdot}6H_2O$ (100% Fluka AG); $NdCl_3{\cdot}6H_2O$ (100%, Fluka AG); $SmCl_3$ (100%, Fluka AG); Dy_2O_3 (99.9%, Fluka AG) and Yb_2O_3 (99.9% Fluka AG).

In order to take into account the solution chemistry, a speciation analysis was performed with the Hydra/Medusa code [34]. **Table 2** collects the main ion–sulphate complexes in solution for all metals present in the synthetic solutions. Al, Fe and REE were found either as free ions (e.g. Al^{3+}, Fe^{3+}, La^{3+}) or complexed with sulphate (e.g. $AlSO_4^+$, $Fe(SO_4)_2^-$, $LaSO_4^+$, $La(SO_4)_2^-$). As seen in Table 1, complexation of all metals with sulphate gives rise to a wide variety of single- and double- charged species (e.g. $AlSO_4^+$, $FeHSO_4^{2+}$). Other metals such as Ca(II), Cu(II) and Zn(II) can also be present in solution either as a free ion (e.g. Ca^{2+}) or forming neutral species with sulphate (e.g. $CaSO_4$).

2.2. Experimental set–up

The set–ups for the polymeric and ceramic membrane tests were the same differing only in their membrane module. **Figure 1** shows a scheme of the experimental set-up. The experiments with the polymeric membrane were carried out with a flat–sheet membrane placed in a cross-flow test cell (GE SEPA™ CF II) with a spacer-filled feed channel, whereas the experiments with the ceramic membrane were performed with a tubular membrane placed on a stainless steel module (from Fraunhofer IKTS).

The NF experimental set–up was equipped with a by–pass (before the entrance of the feed solution in the module) and a needle valve (in the concentrate line), which allowed to vary the cross-flow velocity (cfv) and the trans–membrane pressure (TMP). The feed solution (30 L) was kept in a thermostatic tank at a constant temperature (25 ± 2 °C) and was pumped to the set–up with a high–pressure diaphragm pump (Hydra-Cell, USA). Both outputs of the membrane (permeate and concentrate) were recycled back to the feed tank to keep the same concentration during the whole experiment. Two manometers were allocated before and after the module to monitor the TMP. Just before the discharge of the concentrate in the feed tank, a flow–meter and a pre–filter cartridge were placed. The pre-filter (100 μm, polypropylene) avoided that any erosion product reached the pump. Permeate samples were collected with a three-way valve. Pipes were made of stainless steel.

Before carrying out an experiment, the TiO_2 membrane was tested with deionised water at 13 bar and cfv of 3.5 m/s for 1 h to determine its hydraulic permeability to water. After compactation of the membrane with the solution at the same condition, the experiments were carried out at a pre-fixed cfv (3.5 m/s) and varying TMP from 6 to 13 bar. On the other hand, the MPF–34 membrane was compacted at 22 bar and cfv of 1 m/s, while during the experiments the TMP was varied from 6 to 20 bar at 0.7 m/s. Once the experiment was finished, both set–ups were cleaned with a diluted sulphuric acid solution (pH = 1.0) and with deionised water to remove any impurity that may be left inside.

2.3. Analytical analysis and membrane characterization

Permeate and feed samples were analysed by Inductively Coupled Plasma Mass Spectrometry (7800 ICP-MS from Agilent Technologies) and Optical Emission Spectrometry (5100 ICP-OES from Agilent Technologies). Before ICP analysis,

samples were filtered (0.2 µm) and acidified with 2% HNO_3. Samples taken during the experiments were analysed with a pH–meter (GLP 22, Crison) and a conductivity–meter (GLP 31, Crison) for monitoring purposes. From the measured concentrations, rejection (R) of a given element regardless of its speciation was calculated as follows (Eq. 1):

$$R = 1 - \frac{C_p}{C_f} \quad (1)$$

Where C_p and C_f represent the total concentration regardless of its speciation given by ICP measurements in the feed and permeate streams, respectively. From the obtained rejections, concentration factors were estimated as the ratio between feed concentrations at one %permeate recovery respect to the initial concentration ($C_{\%p,r}/C_f$).

The morphology of the TiO_2 ceramic and MPF–34 membranes was analysed by Scanning Electron Microscopy (SEM) with a JEOL JSM–7001F microscope, operating at an acceleration voltage of 20.0 keV for secondary-electron imaging (SEI). Samples were previously metalised with an alloy of Pt/Pd. Moreover, MPF–34 was analysed by Fourier-transform infrared spectroscopy (FTIR) and X-ray photoelectron spectroscopy (XPS). FTIR was performed by using the Attenuated Total Reflection mode (ATR) directly on the pristine membrane. The FTIR-ATR spectrum was recorded between 4000 and 600 cm^{-1}. (XPS, SPECS) was used to determine the elementary composition of the MPF–34 active layer with an Al anode XR50 source operating at 150 W and a Phoibos MCD-9 detector at vacuum lower than 10^{-8} mbar. The area of analysis was 0.8 mm^2 with a binding energy accuracy of 0.1 eV. Membrane samples were previously dried at 35°C for 12 h before its analysis.

3. Results and Discussion

3.1. Characterisation of the TiO_2 ceramic membrane

3.1.1. Determination of IEP of the TiO_2 membrane

Figure 1 collects the rejection of 0.01 M Na_2SO_4 solution for pH values ranging from 1.0 to 11.0 and for two different TMP values (6 and 13 bar). Solution acidity ranged from pH values below pK_a (HSO_4^-/SO_4^{-2}) = 2.0 (where the predominant species is HSO_4^-) to values above the pK_a (where the predominant species is SO_4^{2-}). Na_2SO_4

rejection values showed a S-shaped curve. At the lower pH values (<3), Na_2SO_4 rejections were around 15% (at 6 bar of TMP) and 20% (at 13 bar of TMP). The increase of pH led to higher rejections values with an inflexion point around pH 5.4±0.5 to reach a plateau with constant rejections values above pH 6 of 72±3% and 85±2% at 6 and 13 bar of TMP, respectively.

The performance of ceramic membranes containing TiO_2 active layers treating 0.01 M Na_2SO_4 solutions has been studied previously [35,36]. Van Gestel et al. [36] also observed the same trend with a TiO_2 with a pore size between 1 and 2 nm, but Na_2SO_4 rejection started to increase at pH 5.5. Puhlfürß et al. [35] observed the transition from low to high rejection values at pH 2 with a TiO_2 membrane (IEP of 3.1) with a mean pore size of 0.55 nm at 6 bar. Values of Na_2SO_4 rejections from both studies are plotted for comparison in **Figure 2**.

The Na_2SO_4 rejection by the membrane can be related to the protonation/deprotonation of the titania active layer surface groups (R–TiOH), which shift from a protonated and positively charged form ($R–TiOH_2^+$) at acid pH to a deprotonated and negatively charged form ($R–TiO^-$) at basic pH, as it is described in equations (2) and (3) [36]:

$$R - TiOH_2^+ \leftrightarrow R - TiOH + H^+ \quad (2)$$

$$R - TiOH \leftrightarrow R - TiO^- + H^+ \quad (3)$$

Van Gestel et al. [36] and Dutounié et al. [37] characterized the acid-base properties of TiO_2 powder by determining the IEP from zeta potential measurements. The IEP value reported by these studies is around 6. As it can be seen in **Figure 2**, the determined IEP values correspond approximately with the pH of the inflexion point of the rejection/pH functions. The IEP determined in the present study for both TMPs tested was 5.4+/-0.5, which fell in the range of reported values by Puhlfürβ et al. [35] and Van Gestel et al. [36].

Table 3 compares the characteristics of TiO_2-based ceramic NF membranes with different average pore sizes of the reported studies. While it does not seem to exist any dependence of water permeability on laver thickness, a relationship between IEP values and average pore size seemed apparent. The decrease of pore size is associated with an increase of the acidity of the TiOH surface groups and consequently a reduction of their pK_a values. The dependence of the acidity of functional groups in TFC NF and reverse osmosis membranes on the free volume has been reported by Coronell et al. [38]. For

polyamide active layer based-membranes, the reduction of the free volume (pore size) is accompanied by a decrease of the acidity of the functional groups.

3.1.2. SEM analysis of the TiO_2 membrane

SEM analysis was performed on various pieces of the ceramic membrane. The top view of the membrane layers is shown in **Figure 3.a** (for the TiO_2 layer) and **3.b** (for the Al_2O_3 layer) at x300. As also described by Dutounié et al. [37] when analysing a similar TiO_2 based membrane, its active layer is constituted by an agglomerate of TiO_2 nanoparticles. This agglomeration was associated with particle sintering arising during thermal treatment.

Figures 3.c and 3.d show a cross-section observation of the tubular membrane at two different enlargements. The membrane profile (**Fig. 3.c**) allowed to see both layers and also the transition zone between them. First, both SEM micrographs showed that the membrane support (α-Al_2O_3) was constituted by several layers with different porosities. The active layer thickness was found to be 21.1 ± 4.6 µm. Moreover, the TiO_2 layer was found to be smooth, and no visible pores were detected in the layer either at magnifications of x300 (Fig 2c) nor x1000 (**Fig. 3.d**).

3.2. Characterisation of the polymeric MPF–34 membrane

MPF–34 is a polymeric membrane with a proprietary active layer of unknown composition. This layer was analysed in the present study by SEM, FTIR-ATR and XPS. **Figure S2 (supplementary information)** shows the SEM images of the MPF–34 membrane. The membrane profile (**Fig. S2.a, b**) allowed to see the three layers of the membrane, including the polyester, the support and the active layer. The following amplification (**Fig S2.c, d**) allowed to see with more detail the support and the active layer, whose thickness was found to be 1.06 ± 0.03 µm. The analysis by SEM-EDX of the MPF–34 membrane revealed the presence of C, N, O and S in the pristine membrane.

In order to determine the functional groups of the membrane, FTIR-ATR and XPS were used. The obtained FTIR-ATR spectrum showed a superposition of the active and the intermediate layers (**Figure S3** and **Table S1** in supplementary information), which was due to a radiation penetration depth higher than the thickness of the active layer. In practice, due to the relative thickness of the two layers, the main signal was from the intermediate layer. From the membrane FTIR-ATR spectra, it was drawn that the

intermediate layer was made of polyether-sulphone or polysulphone, as these two polymers have quite close FTIR spectra. Contrarily, the use of XPS allowed to analyse mainly the active layer and to determine its composition. From the elementary analysis with XPS, it was observed that the active layer was mainly composed by C (69.5%), N (16.8%), O (10.8%) and a minor presence of S (2.1%) and Cl (0.8%). No presence of Si was detected, which discarded the hypothesis that the membrane active layer is polydimethylsiloxane. The high ratios of N/C and the low content of S allowed to postulate as a primary hypothesis the presence of an amide as a functional group in the active layer (**Figure S4** and **Table S2** in Supplementary information). It is discarded the presence of sulphonated groups, due to the lower amount of S. The presence of such groups (R-SO_3^-) provides the membrane a negative surface charge and IEPs below 1, as in the case of the acid-resistant HydraCoRe 70pHT NF membrane. For the case of the MPF–34, IEPs values range between 4.5 and 5.5, which approach most of the polyamide NF membranes [29–32]. Accordingly, the membrane charge will be given by the protonation/deprotonation of the amine and carboxylic groups, as it is described by equations (4) and (5).

$$R - NH_2^+ \leftrightarrow R - NH + H^+ \quad (4)$$

$$R - COOH \leftrightarrow R - COO^- + H^+ \quad (5)$$

Figure 4 shows a scheme of how membrane charge due to the protonation/deprotonation of functional groups affects separation for both membranes. The presence of a positive membrane charge will favour the transport of anions, whereas a negative one will attract the cations in solution.

3.3. Ions rejection from metal-containing AMWs solutions

3.3.1. Influence of solution acidity on membrane performance

The influence of acidity on membrane performance was studied by decreasing the pH of the solution from 1.5 to 1.0 by adding H_2SO_4. **Figures 5.a** and **6.a** show the ion rejection curves as a function of the trans-membrane flux for the solution at pH 1.5 for the TiO_2 and MPF–34 membranes, respectively.

For both membranes, the rejection of H^+ was below 10% (with even negative rejections in the case of MFP-34). With regard to the dominant anionic species (HSO_4^-), rejections were below 20% for TiO_2 membrane and below 52% for the case MPF–34. When the

metal rejections were compared, much higher values (ca. 80%) were measured for MPF–34 than the TiO_2 membrane (values below 30%). Additionally, metal rejections values for the ceramic membrane were dependent on the metal ions properties, being Al(III) the highest rejected, followed by REEs and finally by the transition metal ions (Cu(II), Zn(II)) and Ca(II). Overall, the transport of ions through both membranes was clearly influenced by the active layer membrane properties.

The transport of ions across polymeric NF membranes is described as a combination of diffusion, electromigration and convection processes [39]. Usually, the rejections values tend to increase over the trans–membrane flux. However, in the present study, the rejections given by the TiO_2 membrane barely increased over the evaluated trans–membrane flux, which can be explained by a high contribution of the convection term (i.e. coupling between solvent and ions). Moreover, the difference of dominant ions diffusivities inside the membrane (i.e. Al, SO_4 and H^+) generated an electric potential, which in turn drove the transport of ions traces (i.e. REEs, Ca, Cu and Zn). Dutounié et al. [37] modelled the transport of ions across a TiO_2 membrane assuming the transport as a combination of steric, electric and dielectric effects. Moreover, equilibrium partitioning that implies the equality of generalized chemical potentials on both sides of the membrane-solution interfaces was considered.

As explained in section 3.1, it is expected that, at acidic pH, the TiO_2 layer presented a positively charged sites due to the protonated $TiOH_2^+$ groups. According to the Donnan exclusion phenomenon [40], the transport of cations will be impeded (i.e. metals, protons), while the passage of anions will be favoured (i.e. hydrogen sulphate). The rejections for Al(III) were the highest ones, ranging from 25 to 30% at pH 1.5. REEs(III) rejections varied between 15 and 20%, while Cu(II), Ca(II) and Zn(II) rejections were between 10 and 15%. Although all the metals were partially complexed with sulphate ions (see **Fig. S1** in Supplementary Information), still a significant fraction of them were positively charged. The lowest rejection was for the H^+ (below 5%), due to its small ionic radius (2.82 Å) and high diffusion coefficient ($9.3 \cdot 10^{-9}$ m^2/s) [41].

Dutounié et al. [37] reported similar salt rejection rates, from 20 to 30% for pure salt-water solutions (NaI, NaF, NaCl) at neutral to slightly basic pH values with three TiO_2 based membranes with average pore radius from 1.4 to 2.4 nm. At these pH values, the TiO_2 groups were totally dissociated (R-TiO^- groups), and then a negative charge along

the membrane was expected. In such a scenario, Na^+ ions were preferably transported, and then counter-anions in solution (F^-, Cl^-, I^-) were co-transported to reach electroneutrality conditions. Then, membranes with different pore size distribution provided similar rejections for the three halide salts (around 40% for NaF, 20% for NaCl and <5% for NaI). On the contrary, for non-charged solutes, rejection increased up to 60%. However, they concluded when the salt rejections were compared, the sequence NaF>NaCl>NaI could not be explained by the Stokes radii of halide ions (0.166, 0.121 and 0.120 nm for F^-, Cl^- and I^- respectively) [42], suggesting that, in the present case, steric effects were not the determining phenomenon for salt exclusion. As stressed, the selectivity of ionic species is governed by three phenomena: steric, electric and dielectric exclusion. Since steric exclusion cannot be responsible for ion rejections, the combination of electric and dielectric effects, as well as the acid-base and complexing properties of the TiO_2 groups might have an important influence on the ion rejections. The presence of the protonated TiO_2 groups ($R\text{-}TiO_2^+$) makes that the membrane approaches an anion exchange membrane, so the electric and dielectric effects are responsible for the ion rejections. Then, the rejection followed the sequence Al(III)>REE(III)>Ca(II),Zn(II),Cu(II)>H^+. The higher rejections of Al(III) than of REEs(III) can be explained with the electric and dielectric effects. Ion polarizabilities, defined as the ion ability to relocate its electrical charge to minimize the interaction energy with its environment, can explain the sequence Al(III)>REE(III). The polarizability of Al^{3+} is within the range 0.05–0.07 $Å^3$, whereas for REEs (e.g. La^{3+}) is from 1.0 to 1.3 $Å^3$ [43]. Then, higher rejections for Al(III) than REEs(III) were obtained.

On the contrary, MPF–34 provided higher rejections of all metals (around 80%), whereas sulphate rejection increased from 45 to 52%. Nevertheless, the permeate flux was much lower for the polymeric membrane than for the ceramic one. The rejections from the polymeric membrane were strongly influenced by the Donnan and the dielectric exclusion [40,44]. The pH of the solution is below the IEP (4.5-5.5 [30,31]), so the membrane presented a positively charged surface, which rejected the cations and allowed the anions to permeate. The dielectric exclusion phenomenon is caused because of the interactions between ions and the charged induced in the membrane at the interface solution/membrane with different dielectric constants (i.e. polymeric matrix/bulk solution). The effect of dielectric exclusion is more pronounced than Donnan exclusion since the exclusion energy is proportional to the square of the ion charge, whereas Donnan exclusion is linear with it [44]. Thus, the dielectric exclusion

could explain why the transport of metal-based species, non-complexed (i.e. M^{n+}: Al^{3+}, Ca^{2+} and Cu^{2+}) and complexed forms (i.e. $M(SO_4)_m^{(n-2\cdot m)}$) was more impeded than the one of H^+. However, it should be stressed that metal rejections were independent of their properties (e.g. ionic radii and polarizability), and no differences were observed between divalent and trivalent metal ions. The effect of dielectric exclusion was not used to explain the experimental results of the TiO_2 membrane because its mean pore size was around 1 nm, which makes this phenomenon weak. Rejection values obtained with the MPF-34 membrane in the present study (80%) were lower than those obtained with other polymeric membranes with semi-aromatic polyamides (>98%) as an active layer (e.g. NF270 and Desal DL) reported in a previous study [45].

Figures 5.b and **6.b** show the ion rejection curves for the solution at pH 1.0 for the TiO_2 and MPF–34 membranes, respectively. For the TiO_2 membrane, the shift in pH led to lower rejections of sulphate (4–12 %) and aluminium (21–31%). These variations in rejections could be explained from the speciation diagrams. This variation in the pH in the solution implied a change in the metal-sulphate complexation as it is described in **Figure 7**. When pH decreased from 1.5 to 1.0, the fraction of HSO_4^- increased while the ones of SO_4^{2-}, $AlSO_4^+$ and $Al(SO_4)_2^-$ decreased. The higher amount of HSO_4^- and the positively charged membrane ($R\text{-}TiOH_2^+$) led to lower rejections of sulphate.

Besides, rejections for Ca(II), Cu(II) and Zn(II) with the TiO_2 also decreased to values between 2 and 12% when the acidity of the solution was increased (from pH 1.5 to 1.0). Due to a higher sulphate permeation, more H^+ was transported across the TiO_2 membrane, which conducted to lower rejections than at pH 1.5 (from –2 to 5%). MPF–34 membrane only showed differences in sulphate and H^+ rejections, while metal rejections barely varied (~80%). Sulphate rejections decreased from 45–52% at pH 1.5 to 29–41% at pH 1.0, which was related to the effect of dielectric exclusion phenomena. The fact that at pH 1.0, the sulphate was mainly present as HSO_4^- made it prone to be transported, due to lower exclusion energy than for SO_4^{2-}. This shift in speciation, in addition to the positively charged membrane surface, allowed the transport of sulphate (as HSO_4^-) across the membrane.

Membrane performances were compared with results obtained for similar AMWs when using a semi-aromatic poly(piperazine amides): NF270 [12], Desal DL [46] and a sulphonated polyethersulphone (HydraCoRe 70pHT) [46]. The effect of decreasing the pH (from pH 1.5 to 1.0) was also studied. Both polyamides membranes (NF270 and

Desal DL) at acidic pHs were positively charged, and then metals (i.e. Al, REEs, Cu, among others) were effectively rejected (>95%) by the membranes at the pH range studied (1.5 to 1.0). Moreover, a decrease in sulphate rejection (from 55 to 45% for NF270 and from 80 to 55% for Desal DL) was observed due to the presence of the species HSO_4^- [12,46]. For dense polymeric active layers, the dielectric exclusion mechanism prevails. Because its effect is more pronounced in multivalent ions (e.g. Al^{3+} or SO_4^{2-}) than in monovalent ions (e.g. HSO_4^-), lower sulphate rejections were observed [44]. On the other hand, HydraCoRe 70pHT membrane, which is characterised by a negatively charged surface, was able to reject sulphate at both pHs at a 75%, while metal rejections decreased from 90 to 75% when working at pH 1.5 and 1.0, respectively. Polymeric membranes allowed to obtain higher rejections than the ceramic membrane tested in this study, but the latter was able to obtain higher trans-membrane fluxes at the same TMP.

MPF–34 performances when treating AMWs or acidic solutions containing metals from hydrometallurgical industries were compared [8,47] (**Table 4**). Ricci et al. [8] treated an AMW from a gold mine at pH 1.5 containing metallic impurities (Mg, Fe, Ca, Ni and Cu, among others) with the MPF–34 membrane and obtained metal rejections between 72 and 82%. Tanninen et al. [47] treated an acidic effluent composed by H_2SO_4 and $CuSO_4$. MPF–34 was able to reject an 82% of $CuSO_4$ at 0.1 M H_2SO_4, while acid rejection was near zero. An increase in acid concentration led to lower $CuSO_4$ and higher H_2SO_4 rejections. In both cases, reported metal rejection values were similar to the values reported in this study. No studies of the application of ceramic membranes for treating acidic waters were found.

Mass balances were performed with the composition of feed and permeate samples to determine if any metal was trapped on the membrane. Differences below 1% were found, which were related to analytical errors rather than to metal entrapment and scaling. Moreover, solubility analysis performed with the Hydra/Medusa code [34] revealed that no metal precipitation is expected to occur at pH<1.5.

3.3.2. Influence of Al(III) and Fe(III) concentration

One of the main parameters in the management of AMW is the presence of Al(III) and Fe(III). Both cations have strong acidic properties due to their strong hydrolytic properties in solution. Actually, the acidity of acid mine waters is defined by their concentration in solution. **Figures 5.c-d** and **6.c-d** show the ion rejection curves for the

solution containing 0.6 g/L Al(III) and 1.8 g/L Al(III) for the TiO_2 and MPF–34 membranes, respectively at pH 1.0.

For the TiO_2 membrane, the increase in Al(III) concentration led to higher sulphate rejections, from 4–12 % (**Figure 5.c**) to 13–19% (**Figure 5.d**).This finding was related to an increase in the sulphate fractions of aluminium–sulphate complexes, such as $AlSO_4^+$ and $Al(SO_4)_2^-$ (see **Figure 8**). The addition of Al(III) to the solution was beneficial in terms of acid recovery in the permeate, because it allowed to obtain even lower H^+ rejections, while metal rejections slightly increased. The fact that the dominant ions (i.e. Al, SO_4 and H^+) in solution controlled the transport of traces (i.e. REEs(III), Ca(II), Cu(II) and Zn(II)) resulted in higher rejections of those traces than at the lowest Al(III) concentration tested. For example, REEs(III) rejections varied between 11 to 20% at 1.8 g/L Al(III) (**Figure 5.d**), while ranged between 13 and 21% at 0.60 g/L (**Figure 5.c**). On the other hand, Ca(II), Cu(II) and Zn(II) rejections increased to 13–19%, whereas at 0.6 g/L those rejections were between 4 and 12%.

However, for the MPF–34 the increase in Al concentration barely affected metal rejections (around 80%), but an increase in sulphate rejection was noticed (29–41 to 42–47%). As explained (see **Figure 8**), the higher fraction of $AlSO_4^+$, whose transport was impeded by the membrane and the lower amount of HSO_4^- in solution limited the transport of sulphate across the membrane. Moreover, H^+ rejections were even lower (from -2 to 9%) than at low Al(III) concentrations (from -3 to 11%), which favoured the recovery of sulphuric acid in the permeate.

The effect of Al(III) concentration was also studied with the Desal DL and HydraCoRe 70pHT NF membranes [46]. Desal DL exhibited metallic rejection higher than 98% over the whole Al(III) concentration range tested (from 0.6 to 1.8 g/L), while sulphate rejection also increased from 60 to 80%. This increase was related to the change in the sulphate speciation. Again, the transport of H^+ was favoured when $Al_2(SO_4)_3$ was added, and its rejection decreased from 40 to 20%. On the other hand, metal rejections barely varied with HydraCoRe 70pHT, whereas sulphate rejections increased from 78 to 84%. Moreover, H^+ rejections marginally decreased from 60 to 57%.

Two different levels of Fe(III) were studied: 0.5 and 2.1g/L Fe(III) at pH 1.0. For the TiO_2 membrane, the addition of 0.5 g/L Fe(III) to the solution implied an increase of sulphate rejection (**Figure 5.e**) in comparison to the case without iron (**Figure 5.a**). Sulphate rejection varied from 16 to 20% over the trans–membrane flux range

evaluated. The higher sulphate rejections were related to the decrease in the concentration of the free anion sulphate forms (i.e. SO_4^{2-} / HSO_4^-) (see **Figure 9**) to give a significant amount of iron complexes (i.e. $FeSO_4^+$, $FeHSO_4^{2+}$ and $Fe(SO_4)_2^-$). The higher rejection of sulphate limited the transport of metals but favoured the transport of H^+. The highest obtained rejections were for Al (35–46%), followed by the ones for Fe(III) (26–37%), whereas H^+ rejections were negative over the whole range (around –10%). As explained before, the main ions (e.g. Al, Fe, H^+ and SO_4) in solution governed the transport of trace ions. REEs(III) rejections increased from 19 to 33%, while rejections of double-charged metals were between 12 and 21%.

The polymeric MPF–34 membrane also showed high rejections of metals (from 70 to 85%), whereas the rejections of sulphate barely varied (31 to 40%) when Fe(III) was added to the solution. Moreover, the addition of Fe(III) was beneficial in terms of H^+ recovery, since lower rejections (from –6 to 1%) were obtained (see **Figure 6.e**).

At 2.1 g/L Fe(III) (see **Figure 5.f**), the TiO_2 membrane exhibited higher rejections of all the ions, which favoured the passage of H^+ across the membrane. Its rejections were lower than in the previous case (around –12%). The increase of metal rejections (a 10% higher than at 0.5 g/L Fe(III)) was related to a lower transport of sulphate across the membrane due to a lower amount of SO_4^{2-} and HSO_4^- fractions (see **Figure 9**).

The addition of Fe(III) to the solution did not show variations in metal rejections for the MPF–34 (see **Figure 6.e and 6.f**). However, sulphate rejections increased due to the lower amount of HSO_4^-, while the amount in the solution of $FeSO_4^+$ and $FeHSO_4^{2+}$ increased. The higher presence of these two cations, which are expected to be rejected by the membrane, explained why sulphate rejection increased. As in the previous case, the higher amount of Fe(III) led to even more negative H^+ rejections.

NF270, Desal DL and HydraCoRe 70pHT membranes were also tested in a previous study to determine how the concentration of Fe (added in chloride form instead of sulphate form) affected on the membrane separation [45]. For NF270 and Desal DL, metal rejections (>95%) were not affected by the addition of Fe (as $FeCl_3$). Besides, the sulphate rejections increased from 70 to 84% for NF270 and from 69 to 81% for Desal DL. The high rejections of metals favoured the transport of H^+ to meet electroneutrality conditions in the permeate, which led to negative rejections. Sulphate rejections also increased using HydraCoRe 70pHT membrane, from 77 to 87%, while metal rejections barely varied (>75%).

Table 5 sums up the rejections of triple and double-charged metals, as well as sulphate and H^+ rejections for TiO_2 ceramic and polymeric (MPF–34, NF270, Desal DL and HydraCoRe 70pHT) membranes. As it can be seen, polyamide polymeric membranes (NF270 and Desal DL) offer good characteristics, in terms of metal rejections and H^+ passage. Nevertheless, their low chemical resistance makes them susceptible to acid attack. The use of acid–resistance polymeric membranes (MPF–34) also offers a good choice for treating AMW, despite exhibiting lower rejections than the polyamide ones. Efforts must be towards the development of narrow TiO_2 ceramic membranes to reduce the convective flux across them so that they can exhibit higher rejections.

3.4. Estimation of ion concentration factors for the TiO_2 and MPF–34 membranes

From the rejections for both membranes, the concentration factors (ratio feed to permeate concentration) at different permeate recovery values (20, 40, 60 and 80%) were estimated (see **Table 6**). These values were calculated for the solution containing 2.1 g/L Fe(III) with the ion rejections at the maximum evaluated TMP values in the experimental part (see **Fig. 5.f** and **6.f**).

As expected, the lowest concentration factor values (<1) for both membranes were obtained for H^+ due to its negative rejections. The concentration factor values for both membranes values did not differ among them. This suggests that the acid was mainly transported across the membrane and, as the %permeate recovery increased, the acidity of the solution decreased. This can be beneficial in terms of saving costs for the acid neutralisation needed in subsequent stages of the treatment. Nevertheless, the concentration factor values for the metals were quite different if both membranes were compared. MPF–34 yielded to higher concentration factors than the TiO_2 ceramic membrane at the same %permeate recovery, since it exhibited higher rejections. To achieve the same concentration factor with the TiO_2 membrane, more permeate should be recovered. For example, the concentration factors for the REEs were 2.10 at 80% of permeate recovery for the TiO_2 membrane; while at 60% of permeate recovery, the concentration factors were 2.20 for the MPF–34. The lack of selectivity of the latter membrane made that all the metals in solution achieve the same concentration factors, while for the more selective TiO_2 membrane, these values varied significantly. For example, at 60 %permeate recovery, the metal concentration factors were around 2.20, while for the TiO_2 membrane ranged between 1.4 (for the Cu) to 1.9 (for the Al).

4. Conclusions

Acid–stable NF membranes have proven to be useful for treating AMW. MPF–34 has shown better results in terms of metal rejection (~80%) than the TiO_2 ceramic membrane (<60%).

Solution composition and speciation were found to have a significant impact on membrane performance, especially those performed with the ceramic membrane. The rejections of metals, sulphate and H^+ by the TiO_2 membrane were highly influenced by the speciation of the ions in solution. The equilibrium shifts towards the formation of metal-sulphate complexes resulted in higher metal rejections. On the other side, the MPF–34 membrane exhibited metal rejections of 80% under all conditions tested, while H^+ and sulphate rejections varied depending on the solution composition.

The high chemical stability of ceramic NF membranes can make them useful for treating AMW. Nevertheless, ceramic NF membranes with smaller pore size need to be developed, in order to reduce the contribution of convective flow to ion transport. This could help ceramic NF membranes to increase ion rejections.

Acknowledgements

This research was supported by the Waste2Product project (CTM2014-57302-R) and by R2MIT project (CTM2017-85346-R) financed by the Spanish Ministry of Economy and Competitiveness (MINECO) and the Catalan Government (2017-SGR-312), Spain. The work of Julio López and Xanel Vecino was supported by MINECO within the scope of the grant (BES-2015-075051) and the Juan de la Cierva contract (IJCI-2016-27445), respectively. We also want to thank the contribution of D. León and R. Pirabed for their help during the experimental work and A. Espriu-Gascón and A. Díaz for the ICP analysis.

References

[1] C. Ayora, F. Macías, E. Torres, A. Lozano, S. Carrero, J.-M. Nieto, R. Pérez-López, A. Fernández-Martínez, H. Castillo-Michel, Recovery of Rare Earth Elements and Yttrium from passive-remediation systems of acid mine drainage, Environ. Sci. Technol. 50 (2016) 8255–8262. doi:10.1021/acs.est.6b02084.

[2] C.A. Cravotta, Dissolved metals and associated constituents in abandoned coal-mine discharges, Pennsylvania, USA. Part 1: Constituent quantities and correlations, Appl. Geochemistry. 23 (2008) 166–202. doi:10.1016/j.apgeochem.2007.10.011.

[3] P.K. Sahoo, S. Tripathy, S.M. Equeenuddin, M.K. Panigrahi, Geochemical characteristics of coal mine discharge vis-à-vis behavior of rare earth elements at Jaintia Hills coalfield, northeastern India, J. Geochemical Explor. 112 (2012) 235–243. doi:10.1016/j.gexplo.2011.09.001.

[4] M. Olías, J.M. Nieto, R. Pérez-López, C.R. Cánovas, F. Macías, A.M. Sarmiento, L. Galván, Controls on acid mine water composition from the Iberian Pyrite Belt (SW Spain), Catena. 137 (2016) 12–23. doi:10.1016/j.catena.2015.08.018.

[5] E. Santofimia, J. Sa, E. Lo, D. Barettino, O. Aduvire, Acid mine drainage in the Iberian Pyrite Belt (Odiel river watershed, Huelva , SW Spain): Geochemistry , mineralogy and environmental implications, Appl. Geochemistry. 20 (2005) 1320–1356. doi:10.1016/j.apgeochem.2005.01.011.

[6] G. Lee, J.M. Bigham, G. Faure, Removal of trace metals by coprecipitation with Fe, Al and Mn from natural waters contaminated with acid mine drainage in the Ducktown Mining District, Tennessee, Appl. Geochemistry. 17 (2002) 569–581. doi:10.1016/S0883-2927(01)00125-1.

[7] U. Wingenfelder, C. Hansen, G. Furrer, R. Schulin, Removal of heavy metals from mine waters by natural zeolites, Environ. Sci. Technol. 39 (2005) 4606–4613. doi:10.1021/es048482s.

[8] B.C. Ricci, C.D. Ferreira, A.O. Aguiar, M.C.S. Amaral, Integration of nanofiltration and reverse osmosis for metal separation and sulfuric acid recovery from gold mining effluent, Sep. Purif. Technol. 154 (2015) 11–21. doi:10.1016/j.seppur.2015.08.040.

[9] S. You, J. Lu, C.Y. Tang, X. Wang, Rejection of heavy metals in acidic wastewater by a novel thin-film inorganic forward osmosis membrane, Chem. Eng. J. 320 (2017) 532–538. doi:10.1016/j.cej.2017.03.064.

[10] B. Vital, J. Bartacek, J.C. Ortega-Bravo, D. Jeison, Treatment of acid mine drainage by forward osmosis : Heavy metal rejection and reverse flux of draw solution constituents, Chem. Eng. J. 332 (2018) 85–91.

doi:10.1016/j.cej.2017.09.034.

[11] M. Nyström, J. Tanninen, M. Mänttäri, Separation of metal sulfates and nitrates from their acids using nanofiltration, Membr. Technol. 2000 (2000) 5–9. doi:10.1016/S0958-2118(00)86633-1.

[12] J. López, M. Reig, O. Gibert, E. Torres, C. Ayora, J.L. Cortina, Application of nanofiltration for acidic waters containing rare earth elements: Influence of transition elements, acidity and membrane stability, Desalination. 430 (2018) 33–44. doi:10.1016/j.desal.2017.12.033.

[13] R. Fornarelli, M. Mullett, D. Ralph, Factors influencing nanofiltration of acid mine drainage, Reliab. Mine Water Technol. (2013) 563–568.

[14] A.R. Guastalli, J. Labanda, J. Llorens, Separation of phosphoric acid from an industrial rinsing water by means of nanofiltration, Desalination. 243 (2009) 218–228. doi:10.1016/j.desal.2008.04.024.

[15] B. Kose Mutlu, B. Cantoni, A. Turolla, M. Antonelli, H. Hsu-Kim, M.R. Wiesner, Application of nanofiltration for Rare Earth Elements recovery from coal fly ash leachate: Performance and cost evaluation, Chem. Eng. J. 349 (2018) 309–317. doi:10.1016/j.cej.2018.05.080.

[16] A.L. Ahmad, B.S. Ooi, A study on acid reclamation and copper recovery using low pressure nanofiltration membrane, Chem. Eng. J. 156 (2010) 257–263. doi:10.1016/j.cej.2009.10.014.

[17] L. Pino, C. Vargas, A. Schwarz, R. Borquez, Influence of operating conditions on the removal of metals and sulfate from copper acid mine drainage by nanofiltration, Chem. Eng. J. 345 (2018) 114–125. doi:10.1016/j.cej.2018.03.070.

[18] S. Platt, M. Nyström, A. Bottino, G. Capannelli, Stability of NF membranes under extreme acidic conditions, J. Memb. Sci. 239 (2004) 91–103. doi:10.1016/j.memsci.2003.09.030.

[19] B.C. Ricci, C.D. Ferreira, L.S. Marques, S.S. Martins, B.G. Reis, M.C.S. Amaral, Assessment of the chemical stability of nanofiltration and reverse osmosis membranes employed in treatment of acid gold mining effluent, Sep. Purif. Technol. 174 (2017) 301–311. doi:10.1016/j.seppur.2016.11.007.

[20] R. Navarro, M.P. González, I. Saucedo, M. Avila, P. Prádanos, F. Martínez, A. Martín, A. Hernández, Effect of an acidic treatment on the chemical and charge properties of a nanofiltration membrane, J. Memb. Sci. 307 (2008) 136–148. doi:10.1016/j.memsci.2007.09.015.

[21] T. Schütte, C. Niewersch, T. Wintgens, S. Yüce, Phosphorus recovery from sewage sludge by nanofiltration in diafiltration mode, J. Memb. Sci. 480 (2015) 74–82. doi:10.1016/j.memsci.2015.01.013.

[22] A. Manis, K. Soldenhoff, E. Jusuf, F. Lucien, Separation of copper from sulfuric acid by nanofiltration, in: Fifth Int. Membr. Sci. Technol. Conf., 2003.

[23] S.M. Samaei, S. Gato-Trinidad, A. Altaee, The application of pressure-driven ceramic membrane technology for the treatment of industrial wastewaters – A review, Sep. Purif. Technol. 200 (2018) 198–220. doi:10.1016/j.seppur.2018.02.041.

[24] V. Gitis, G. Rothenberg, Ceramic Membranes. New opportunities and Practical Applications, 1st ed., Wiley-VCH Verlag GmbH & Co. KGaA, Weinheim, Germany, 2016. doi:10.1002/9783527696550.

[25] S. Benfer, U. Popp, H. Richter, C. Siewert, G. Tomandl, Development and characterization of ceramic nanofiltration membranes, Sep. Purif. Technol. 22–23 (2001) 231–237. doi:10.1016/S1383-5866(00)00133-7.

[26] I. Voigt, G. Fischer, P. Puhlfürß, M. Schleifenheimer, M. Stahn, TiO2-NF-membranes on capillary supports, Sep. Purif. Technol. 32 (2003) 87–91. doi:10.1016/S1383-5866(03)00064-9.

[27] I. Voigt, M. Stahn, S. Wöhner, A. Junghans, J. Rost, W. Voigt, Integrated cleaning of coloured waste water by ceramic NF membranes, Sep. Purif. Technol. 25 (2001) 509–512. doi:10.1007/978-3-642-54734-2.

[28] S.S. Wadekar, R.D. Vidic, Comparison of ceramic and polymeric nanofiltration membranes for treatment of abandoned coal mine drainage, Desalination. 440 (2018) 135–145. doi:10.1016/j.desal.2018.01.008.

[29] K.M. Systems, KMS Flat Sheet Membrane Samples, Massachusetts, 2018. https://www.kochmembrane.com/KochMembraneSolutions/media/Product-Datasheets/Test Products/flat-sheet-sample-datasheet.pdf.

[30] J. Warczok, M. Ferrando, F. López, A. Pihlajamäki, C. Güell, Reconcentration of spent solutions from osmotic dehydration using direct osmosis in two configurations, J. Food Eng. 80 (2007) 317–326. doi:10.1016/j.jfoodeng.2006.06.003.

[31] M.I. Gehan, E.-G. Belal, Recent Drifts in pH-Sensitive Reverse Osmosis, in: T. Yonar (Ed.), Wastewater Water Qual., 1st ed., InTech, 2018. doi:http://dx.doi.org/10.5772/57353.

[32] Mayur Ramesh Dalwani, Thin film composite nanofiltration membranes for extreme conditions, University of Twente, 2011. doi:10.3990/1.9789036532761.

[33] Proyecto Rio Tinto, (n.d.). http://riotinto.atalayamining.com/la-mina/ (accessed June 22, 2017).

[34] I. Puigdomenech, Chemical equilibirum software Hydra/Medusa, (2001). https://sites.google.com/site/chemdiagr/home.

[35] P. Puhlfürß, A. Voigt, R. Weber, M. Morbé, Microporous TiO2 membranes with a cut off <500 Da, J. Memb. Sci. 174 (2000) 123–133. doi:10.1016/S0376-7388(00)00380-X.

[36] T. Van Gestel, C. Vandecasteele, A. Buekenhoudt, C. Dotremont, J. Luyten, R. Leysen, B. Van Der Bruggen, G. Maes, Salt retention in nanofiltration with multilayer ceramic TiO2membranes, J. Memb. Sci. 209 (2002) 379–389. doi:10.1016/S0376-7388(02)00311-3.

[37] P. Dutournié, L. Limousy, J. Anquetil, S. Déon, Modification of the selectivity properties of tubular ceramic membranes after alkaline treatment, Membranes (Basel). 7 (2017) 65. doi:10.3390/membranes7040065.

[38] O. Coronell, M.I. González, B.J. Mariñas, D.G. Cahill, Ionization Behavior, Stoichiometry of Association, and Accessibility of Functional Groups in the Active Layers of Reverse Osmosis and Nanofiltration Membranes, Environ. Sci. Technol. 44 (2010) 6808–6814.

[39] J. Fang, B. Deng, Rejection and modeling of arsenate by nanofiltration : Contributions of convection , diffusion and electromigration to arsenic transport, J. Memb. Sci. 453 (2014) 42–51. doi:10.1016/j.memsci.2013.10.056.

[40] A.E. Yaroshchuk, Non-steric mechanisms of nanofiltration : superposition of

Donnan and dielectric exclusion, Sep. Purif. Technol. 22–23 (2001) 143–158.

[41] R.A. Robinson, R.H. Stokes, Electrolyte Solutions, Second Rev, Dover Books on Chemistry Series, 2002.

[42] D.R. Lide, Handbook of Chemistry and Physics, 87th ed., Boca Raton, FL, USA, 2007.

[43] J.R. Tessman, A.D. Kahn, Electronic Polarizabilities of Ions in Crystals, Phys. Rev. 92 (1953) 890–895. doi:https://doi.org/10.1103/PhysRev.92.890.

[44] A. Yaroshchuk, Dielectric exclusion of ions from membranes, Adv. Colloid Interface Sci. 85 (2000) 193–230.

[45] J. López, M. Reig, O. Gibert, J.L. Cortina, Recovery of sulphuric acid and added value metals (Zn, Cu and rare earths) from acidic mine waters using nanofiltration membranes, Sep. Purif. Technol. 212 (2019) 180–190. doi:10.1016/j.seppur.2018.11.022.

[46] J. López, M. Reig, O. Gibert, J.L. Cortina, Integration of nanofiltration membranes in recovery options of rare earth elements from acidic mine waters, J. Clean. Prod. 210 (2019) 1249–1260. doi:10.1016/j.jclepro.2018.11.096.

[47] J. Tanninen, M. Mänttäri, M. Nyström, Nanofiltration of concentrated acidic copper sulphate solutions, Desalination. 189 (2006) 92–96. doi:10.1016/j.desal.2005.06.017.

[48] J. Tanninen, M. Mänttäri, M. Nyström, Nanofiltration of concentrated acidic copper sulphate solutions, Desalination. 189 (2006) 92–96. doi:10.1016/j.desal.2005.06.017.

[49] H. Diallo, M. Rabiller-Baudry, K. Khaless, B. Chaufer, On the electrostatic interactions in the transfer mechanisms of iron during nanofiltration in high concentrated phosphoric acid, J. Memb. Sci. 427 (2013) 37–47. doi:10.1016/j.memsci.2012.08.047.

[50] L.M. Harwood, T.D.W. Claridge, Introduction to organic spectroscopy, 1st ed., Oxford University Press, Oxford, 1996.

[51] N.I. of S. and Technology, NIST X-ray Photoelectron Spectroscopy Database, (n.d.). https://srdata.nist.gov/xps/Default.aspx.

[52] G. Beamson, D. Briggs, High Resolution XPS of Organic Polymers: The Scienta

ESCA 300 database, Jown Wiley & Sons, Chichester, 1992. doi:10.1002/sia.740200310.

SUPLEMENTARY INFORMATION

	Sulphate	Double-charged metal (M(II))	Triple-charged metal (M(III))
Influence of pH	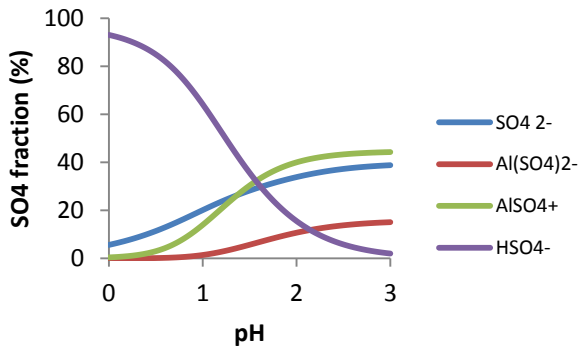	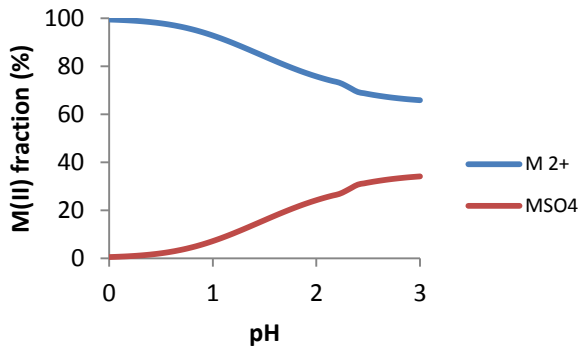	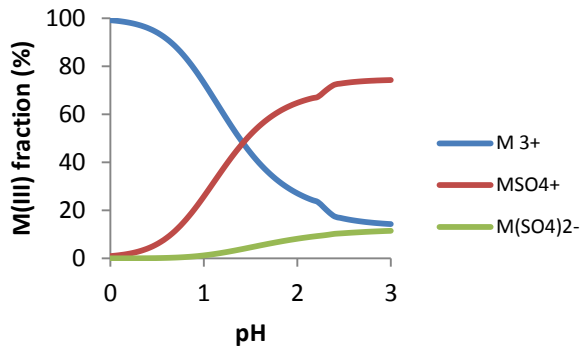
Influence of Al concentration	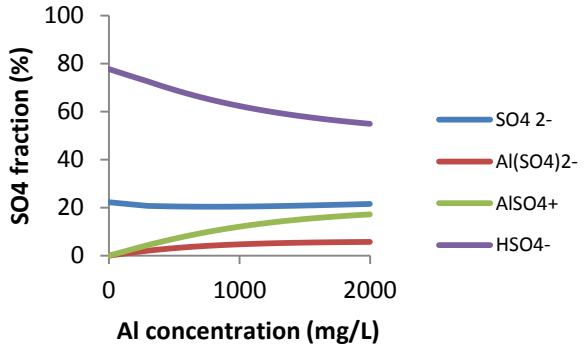	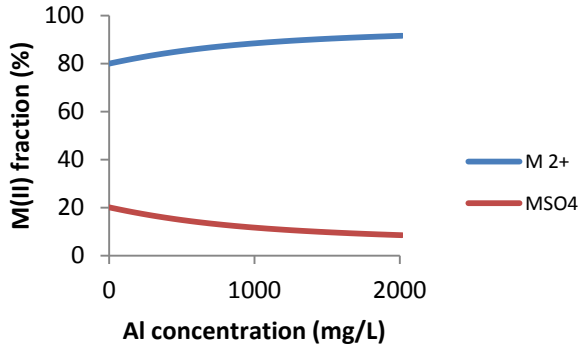	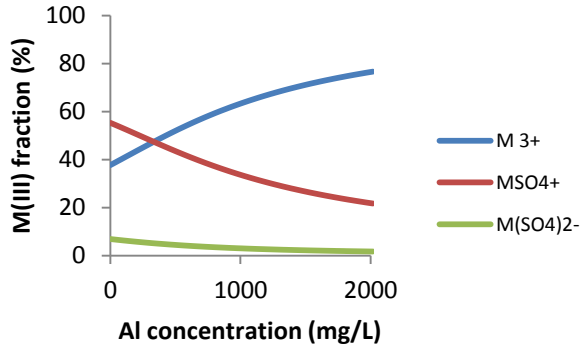

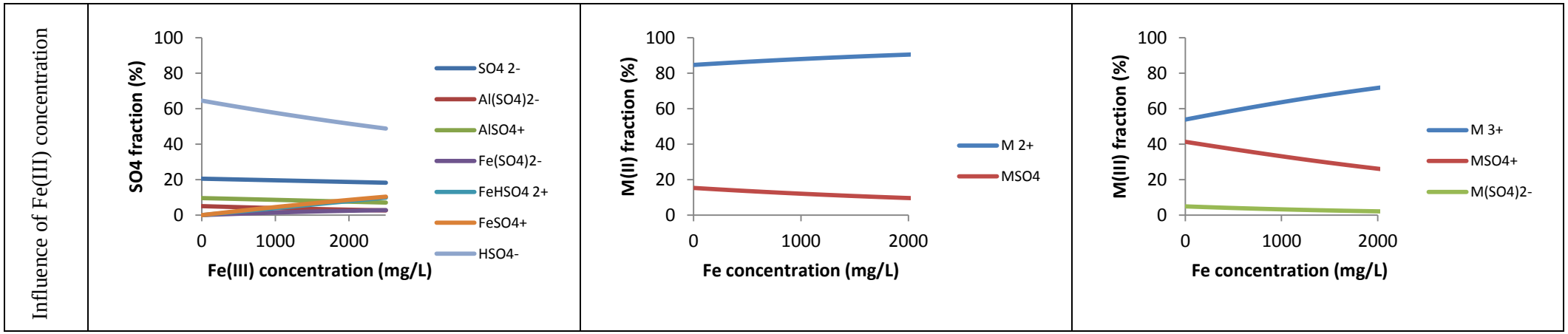

Figure S1. *Sulphate (SO_4), double and triple charged (M(II) and M(III)) fraction diagrams as a function of pH, Al(III) and Fe(III) concentration*

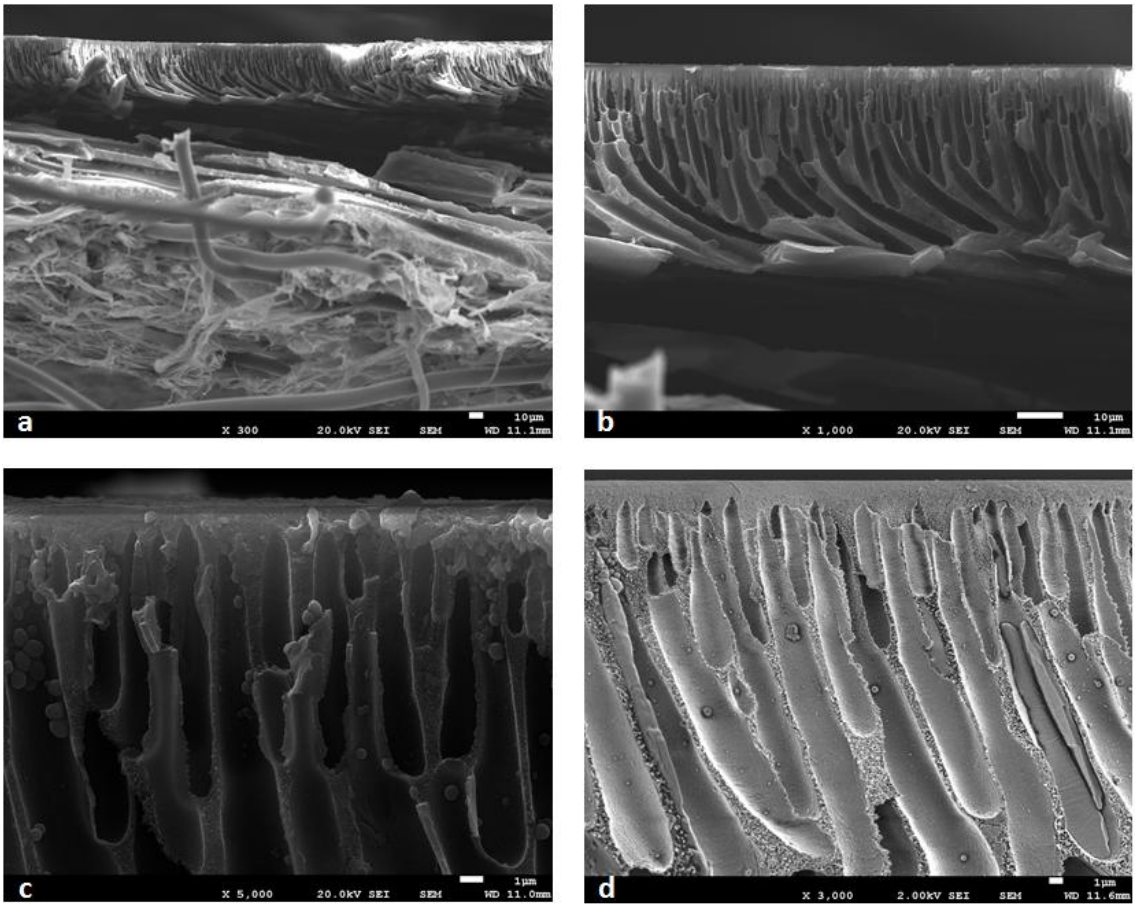

Figure S2. *FESEM images of the MPF-34 membrane profile at: a) x300 amplifications; b) x1000 amplifications; c) x5000 amplifications and; d) x3000 amplifications at 2.00 kV*

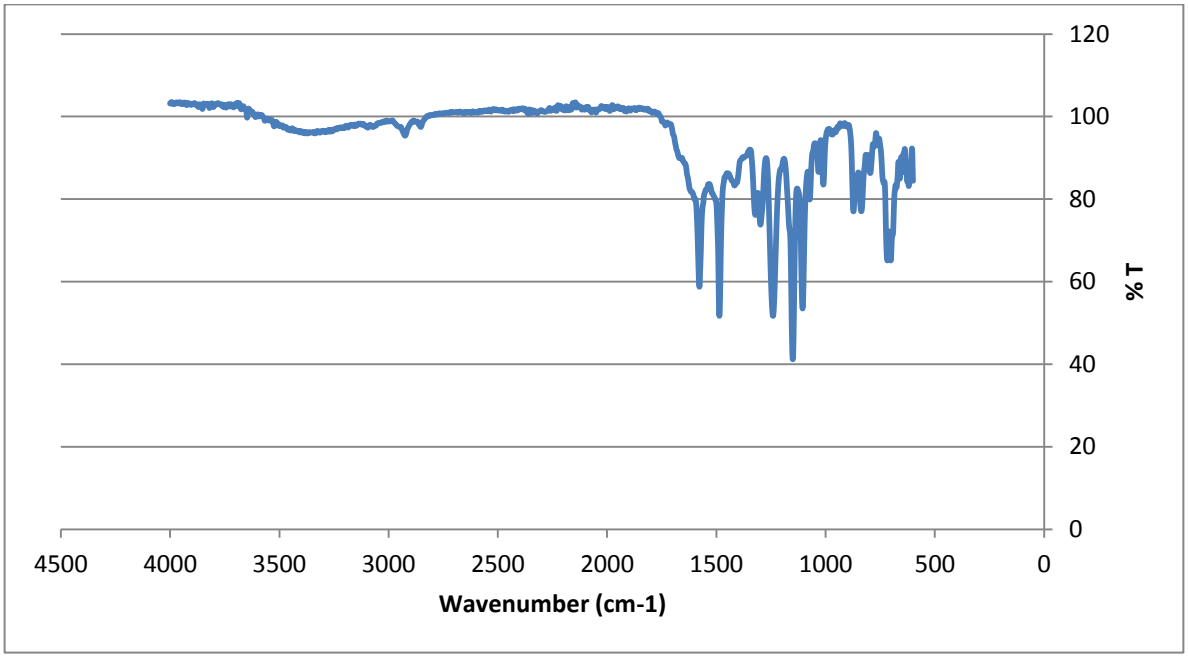

Figure S3. *FTIR-ATR spectra of the MPF-34 membrane. Peak assignments are summarised in Table S1*

Table S1. *Peak assignment for FTIR-ATR spectra of the MPF-34 membrane over 1600–1100 cm^{-1}* [50]

Peak	Range (cm^{-1}) and Intensity	Group and Class	Assignement
1583	1615 – 1590 (m)	Benzene ring in aromatic compounds	Ring stretch, sharp band
1485	1515 – 1485 (m)	Benzene ring in aromatic compounds	Ring stretch, sharp band
1323	1335 – 1295 (vs)	SO_2 in sulfones	SO_2 antisym stretch
1294	1335 – 1295 (vs)	SO_2 in sulfones	SO_2 antisym stretch
1238	1240 – 1070 (s-vs)	C-O-C in ethers	S-O-C stretch
1148	1170 – 1140 (vs)	SO_2 in sulfones	SO_2 sym stretch

Spectra	C1s
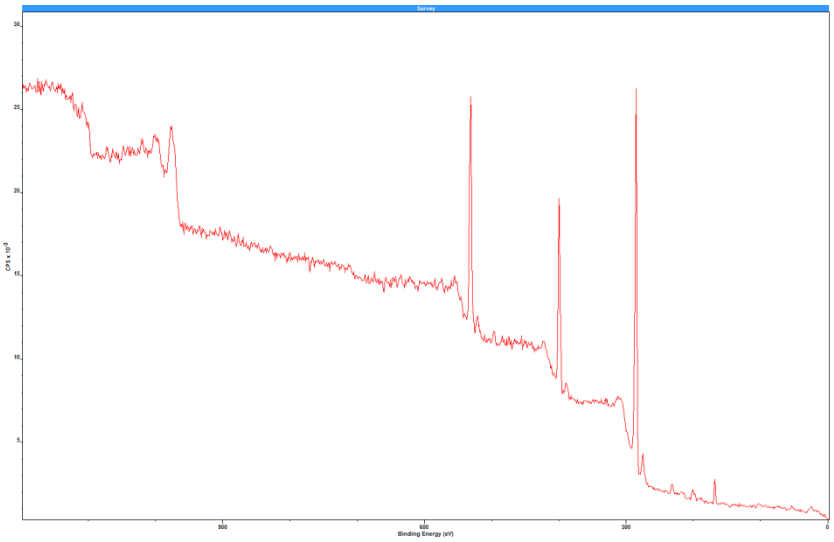	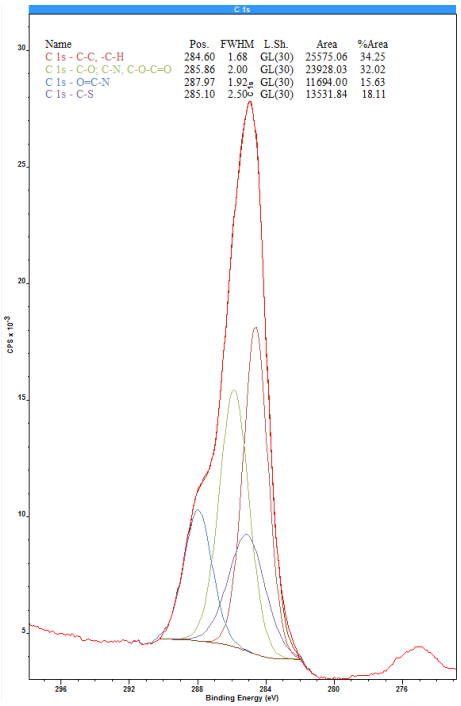

O1s	N1s	S2p
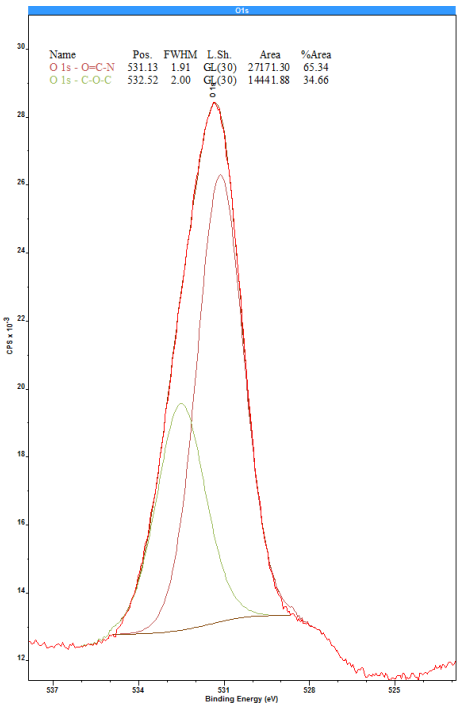	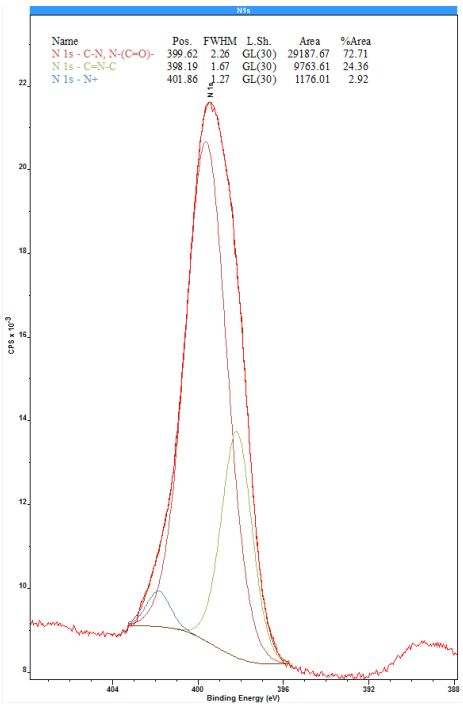	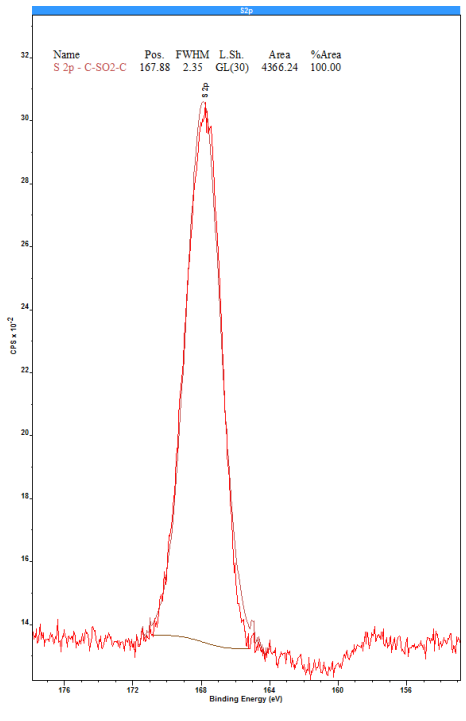

Figure S4. *XPS spectra of the MPF-34 membrane*

Table S2. *Binding energies and relatively amount of functional groups for the MPF-34 membrane* [51,52]

	Binding energy (eV)	%
C 1s		69.53
C-C, C-H	284.6	34.25
C-S, S-SO_2	285.1	18.11
C-O-C, C-CN	285.9	32.02
N-C=O	288.0	15.63
O 1s		10.80
N-C=O, SO_2, SO_3	531.1	65.34
C-O-C	532.5	34.66
N 1s		16.73
C=N-C	398.2	24.36
C-N, N-C=O	399.6	72.71
-NH_3^+	401.9	2.92
S 2p		2.11
C-SO_2-C	167.9	100
Cl 2p		0.83

Comparison of acid-resistant ceramic and polymeric nanofiltration membranes for acid mine waters treatment

J. López [a*], M. Reig [a], X. Vecino [a], O. Gibert [a], J. L. Cortina [a,b]

[a] *Chemical Engineering Department and Barcelona Research Center for Multiscale Science and Engineering, UPC-BarcelonaTECH, C/ Eduard Maristany, 10-14 (Campus Diagonal-Besòs), 08930 Barcelona, Spain*

[b] *Water Technology Center CETaqua, Carretera d'Esplugues 75, 08940 Cornellà de Llobregat, Spain*

* julio.lopez.rodriguez@upc.edu

Abstract

Acid-resistant ceramic and polymeric nanofiltration (NF) membranes have been identified as relevant materials for sustainable management of acidic streams. NF properties such as a high passage of single-charged ions and high rejection of multi-charged ions make NF membranes suitable for acid recovery and metal concentration. In this work, the performance of two acid-resistant membranes: TiO_2 ceramic and MPF–34 (proprietary layer) was tested with solutions mimicking acidic mine waters. Model solutions were composed by Al, Fe, Ca, Cu, Zn and rare earth elements (REEs) such as La, Dy, Sm, Nd, Pr and Yb. The effect of acidity (from pH 1.5 to 1.0), Al(III) (from 0.6 to 1.8 g/L) and Fe(III) (from 0.5 to 2.1 g/L) concentrations was studied. Both membranes allowed the transport of H^+ (negative rejections were obtained), but exhibited differences related to the metallic ions transport. While MPF–34 presented metal rejections around 80% and independent on the concentration of the major components (Al(III) and Fe(III)), the TiO_2 membrane provided a sequence of rejection values from 5 to 30%, with highest values for trivalent transition metals. These differences in the sequence of rejections suggested that the chemical properties of the TiO_2 layer played a relevant role, and that they could only be explained by dielectric effects. From the observed rejections, it was estimated that MPF–34 provided concentration factors for metals up to 4.2 and <1 for the H_2SO_4.

Keywords: acid mine waters; rare earth elements; nanofiltration; TiO_2 active layer; MPF–34; sulphuric acid recovery.

1. Introduction

Mining activities generate a large number of toxic effluents, including acid mine waters (AMW). These streams are characterised by a low pH (<2) and by the presence of dissolved metallic ions (e.g. Al, Fe, and Cu). Among these dissolved metals, rare earth elements (REEs) can be found. The concentration of REEs in AMW can vary between 4 to 80 mmol/L, which is two orders of magnitude higher than in natural waters [1–3]. Nowadays REEs, which are widely used in the high-tech industry [4,5], are mainly produced in China , while the European Union has a lack of mining sites to exploit REEs. Within this framework/context circular economy schemes are being proposed for their recovery.

Nowadays, management of AMW is focused on the recovery of valuable elements (e.g. H^+, REEs, Cu and Zn) by different methods, such as selective precipitation [6], treatment with natural zeolites [7] and membrane technologies (reverse osmosis [8], forward osmosis [9,10], among others). Among the different membrane technologies, nanofiltration (NF) membranes have shown a good performance because of their capacity of allowing the permeance of single-charged ions while rejecting the multi-charged ones. Different studies have demostrated that this selectivity of NF may allow to separate and recover acid (which permeates through the membrane) from metallic impurities (which are retained by the membrane). The latter can be further concentrated and recovered with other technologies [11–17]. Although the recovery of acid is not having a direct economic benefit, it has an indirect cost in the reduction of alkali consumption in the acidy neutralization stages.

The most widely used NF membranes are the thin-film composite (TFC) polymeric ones incorporating a polyamide active layer. However, at the long–term acid exposure, the polyamide active layer can suffer from hydrolysis leading to a loss in selectivity [18–20]. To solve this problem, acid-resistant TFC NF membranes have been developed and commercialised, such as the Duracid (proprietary, from GE Osmonics), MPF–34 (proprietary, from Koch Membrane Systems) and Hydracore 70pHT (proprietary from Hydranautics) ones, which offer as good rejections as the polyamide ones do [8,14,21].

In most of the cases, the composition of the membrane active layer is proprietary, but sulphamides or sulphonated polyethersulphones are used because of their resistance in acidic media. The stability of this acid-resistant membranes has been studied in literature. For example, Manis et al. [22] filtered a copper electroplating effluent with MPF–34 to separate Cu(II) from the H_2SO_4. As H_2SO_4 concentration increased from 0 to 2 M, copper (from 85% to 45%) and H_2SO_4 (from 20% to 15%) rejections decreased. Moreover, they performed a stability test with a polyamide NF membrane (DK) and the MPF–34 in 2 M H_2SO_4 for 8 weeks. After immersion, the DK showed an increase of permeate flux and a decrease in copper rejection, while MPF–34 was able to keep their properties.

In parallel, ceramic membranes, initially developed for ultrafiltration applications, are emerging as an alternative to the polymeric ones due to their higher chemical, mechanical and thermal stability, resulting in a longer duration. Nevertheless, they have to face their high fabrication cost and low selectivity. These facts have made that ceramic NF membranes are still not applied in applications at large scale [23,24]. The most common materials of their active layer are zirconia (ZrO_2) or titania (TiO_2), while the support is usually made of alumina (Al_2O_3). Only a few studies are found in literature with the applicability of ceramic NF membranes. For instance, Benfer et al. [25] evaluated the performance of ZrO_2 and TiO_2 NF membranes synthesised by the sol-gel method. The former exhibited higher rejections for salts (NaCl and Na_2SO_4), while the latter had better solvent fluxes. Pore size measurements revealed that ZrO_2 membrane had smaller pore size and narrower pore size distribution (0.75 – 1.75 nm) than TiO_2 membrane (0.5 – 2.5 nm). Voigt et al. [26] were able to develop TiO_2 NF membranes with a molecular weight cut-off (MWCO) of 250 Da and water flux of 10 L/(m^2·h·bar) by a two-step coating process. The application of TiO_2 membranes (pore size 0.9 nm, MWCO 450 Da) to treat textile wastewater was also evaluated, achieving a decolouring of 70-100% [27]. Wadekar and Vidic [28] compared the performance of a ceramic (TiO_2, MWCO ~ 500 Da, Cerahelix) and a polymeric (NF270, MWCO ~200 to 400 Da) membranes to treat the drainage of an abandoned coal mine (pH 7.8). NF270 was able to reject more than 96% of all the multi-charged ions, except for arsenic (33%), present as a non-charged form of As(III) (H_3AsO_3). On the other hand, the ceramic membrane exhibited much lower rejections (between 50 and 70%), and an arsenic rejection of 20%. No published studies were found about the performance of ceramic NF membranes in complex acidic media as AMW in the scientific literature.

The increasing price and lack of primary resources of REEs have made other sources such as AMWs to be evaluated. NF membranes have proven to be effective for the treatment of AMWs. However, commercial polyamide membranes can suffer hydrolysis, and therefore acid-resistant membranes (polymeric or ceramic) may be preferred. No studies of the performance of ceramic membranes to treat acidic waters are found in literature. The main objective of this work was to evaluate the performance of two acid-resistant NF membranes: a ceramic one containing titania (TiO_2) as a selective layer and polymeric one (MPF–34) to treat metal-containing sulphuric solutions mimicking AMWs from the Iberian Pyrite Belt. This solution presented an acidic pH (<2) and was characterised by the presence of metals (e.g. Al, Fe, Ca, Cu and Zn) and other elements at a low concentration such as REEs (e.g. La, Pr, Nd, Sm, Dy and Yb). The effects of pH (1.5 to 1.0), Al(III) (from 0.6 to 1.8 g/L) and Fe(III) (from 0.5 to 2.1 g/L) concentration in the AMW were studied in terms of acid and metal rejections. Furthermore, both membranes were characterised by different analytical techniques to study their composition and structure. Experimental results were explained with regard to the membrane active layer and its structure, as well as to the solution composition and the effect of complexation reactions. Moreover, a prediction of concentration factors when an AMW was filtered was carried out for both membranes.

2. Materials and Experimental Methodology

2.1. Membrane and solutions

A ceramic membrane with an active area of 44.92 cm^2 was tested. This membrane has a tubular configuration with an internal diameter of 6.5 mm and a thickness of 2 mm. This membrane presents an active layer of TiO_2 supported on Al_2O_3 with a mean pore size of 1 nm. An acid-resistant flat–sheet (140 cm^2) polymeric NF membrane from Koch Membrane Systems (MPF–34) was also tested. The composition of the active layer is patented, and there are no data about its structure in the literature. This membrane presents an MWCO of 200 Da and an isoelectric point (IEP) between 4.5 and 5.5 [29–32].

First of all, experiments were performed with 0.01 M Na_2SO_4 from pH 1 to 11 to determine the IEP of the ceramic NF membrane. Then, solutions mimicking AMWs

generated in a polysulphide mine in Río Tinto (La Poderosa), Huelva province (Southwest of Spain) were tested in the NF membrane set–up. These solutions reproduced the typical compositions of the effluents from the Iberian Pyrite Belt (Southwest of Spain), which is one of the main sulphide deposits worldwide [33]. Feed composition was based on the mean values along one year. Elements with concentrations lower than 10 mg/L were not included in the solution, such as arsenic, cadmium, cobalt and potassium, among others. The composition of these synthetic solutions is given in **Table 1**. The main variations in the composition were for Al and Fe, and then the effect of different variables such as pH and concentration of Al and Fe on the membrane performance was studied. The presence of Fe, usually as a mixture of Fe(II) and Fe(III), may limit the recovery of REEs in the hydrometallurgical industry. For this reason, Fe(II) is usually oxidised to Fe(III) with air and then removed with a low-cost alkali (e.g. CaO or $CaCO_3$) as hydroxide or hydroxyl–sulphate. Then, two scenarios could be found: one with Fe(III) and another one without this metal. In the present study, Fe in solution was Fe(III) (>99,5%). **Fig. S1** in Supplementary Information collects the speciation diagrams of the different elements in solution.

The following solutions and salts were used to prepare the synthetic solutions: Na_2SO_4 (>99%, Sigma-Aldrich); H_2SO_4 (96 wt%, Sigma-Aldrich); $Al_2(SO_4)_3{\cdot}18H_2O$ (55%, Panreac); $Fe_2(SO_4){\cdot}5H_2O$ (98%, Sigma-Aldrich); $CaSO_4{\cdot}2H_2O$ (100%, Scharlau); $CuSO_4$ (100%, Panreac); $ZnSO_4{\cdot}7H_2O$ (100%, Panreac); $La_2(SO_4)_3{\cdot}9H_2O$ (99.9%, Alfa Aesar); $Pr(NO_3)_3{\cdot}6H_2O$ (100% Fluka AG); $NdCl_3{\cdot}6H_2O$ (100%, Fluka AG); $SmCl_3$ (100%, Fluka AG); Dy_2O_3 (99.9%, Fluka AG) and Yb_2O_3 (99.9% Fluka AG).

In order to take into account the solution chemistry, a speciation analysis was performed with the Hydra/Medusa code [34]. **Table 2** collects the main ion–sulphate complexes in solution for all metals present in the synthetic solutions. Al, Fe and REE were found either as free ions (e.g. Al^{3+}, Fe^{3+}, La^{3+}) or complexed with sulphate (e.g. $AlSO_4^+$, $Fe(SO_4)_2^-$, $LaSO_4^+$, $La(SO_4)_2^-$). As seen in Table 1, complexation of all metals with sulphate gives rise to a wide variety of single- and double- charged species (e.g. $AlSO_4^+$, $FeHSO_4^{2+}$). Other metals such as Ca(II), Cu(II) and Zn(II) can also be present in solution either as a free ion (e.g. Ca^{2+}) or forming neutral species with sulphate (e.g. $CaSO_4$).

2.2. Experimental set–up

The set–ups for the polymeric and ceramic membrane tests were the same differing only in their membrane module. **Figure 1** shows a scheme of the experimental set-up. The experiments with the polymeric membrane were carried out with a flat–sheet membrane placed in a cross-flow test cell (GE SEPA™ CF II) with a spacer-filled feed channel, whereas the experiments with the ceramic membrane were performed with a tubular membrane placed on a stainless steel module (from Fraunhofer IKTS).

The NF experimental set–up was equipped with a by–pass (before the entrance of the feed solution in the module) and a needle valve (in the concentrate line), which allowed to vary the cross-flow velocity (cfv) and the trans–membrane pressure (TMP). The feed solution (30 L) was kept in a thermostatic tank at a constant temperature (25 ± 2 °C) and was pumped to the set–up with a high–pressure diaphragm pump (Hydra-Cell, USA). Both outputs of the membrane (permeate and concentrate) were recycled back to the feed tank to keep the same concentration during the whole experiment. Two manometers were allocated before and after the module to monitor the TMP. Just before the discharge of the concentrate in the feed tank, a flow–meter and a pre–filter cartridge were placed. The pre-filter (100 μm, polypropylene) avoided that any erosion product reached the pump. Permeate samples were collected with a three-way valve. Pipes were made of stainless steel.

Before carrying out an experiment, the TiO_2 membrane was tested with deionised water at 13 bar and cfv of 3.5 m/s for 1 h to determine its hydraulic permeability to water. After compactation of the membrane with the solution at the same condition, the experiments were carried out at a pre-fixed cfv (3.5 m/s) and varying TMP from 6 to 13 bar. On the other hand, the MPF–34 membrane was compacted at 22 bar and cfv of 1 m/s, while during the experiments the TMP was varied from 6 to 20 bar at 0.7 m/s. Once the experiment was finished, both set–ups were cleaned with a diluted sulphuric acid solution (pH = 1.0) and with deionised water to remove any impurity that may be left inside.

2.3. Analytical analysis and membrane characterization

Permeate and feed samples were analysed by Inductively Coupled Plasma Mass Spectrometry (7800 ICP-MS from Agilent Technologies) and Optical Emission Spectrometry (5100 ICP-OES from Agilent Technologies). Before ICP analysis,

samples were filtered (0.2 µm) and acidified with 2% HNO_3. Samples taken during the experiments were analysed with a pH–meter (GLP 22, Crison) and a conductivity–meter (GLP 31, Crison) for monitoring purposes. From the measured concentrations, rejection (R) of a given element regardless of its speciation was calculated as follows (Eq. 1):

$$R = 1 - \frac{C_p}{C_f} \quad (1)$$

Where C_p and C_f represent the total concentration regardless of its speciation given by ICP measurements in the feed and permeate streams, respectively. From the obtained rejections, concentration factors were estimated as the ratio between feed concentrations at one %permeate recovery respect to the initial concentration ($C_{\%p,r}/C_f$).

The morphology of the TiO_2 ceramic and MPF–34 membranes was analysed by Scanning Electron Microscopy (SEM) with a JEOL JSM–7001F microscope, operating at an acceleration voltage of 20.0 keV for secondary-electron imaging (SEI). Samples were previously metalised with an alloy of Pt/Pd. Moreover, MPF–34 was analysed by Fourier-transform infrared spectroscopy (FTIR) and X-ray photoelectron spectroscopy (XPS). FTIR was performed by using the Attenuated Total Reflection mode (ATR) directly on the pristine membrane. The FTIR-ATR spectrum was recorded between 4000 and 600 cm^{-1}. (XPS, SPECS) was used to determine the elementary composition of the MPF–34 active layer with an Al anode XR50 source operating at 150 W and a Phoibos MCD-9 detector at vacuum lower than 10^{-8} mbar. The area of analysis was 0.8 mm^2 with a binding energy accuracy of 0.1 eV. Membrane samples were previously dried at 35°C for 12 h before its analysis.

3. Results and Discussion

3.1. Characterisation of the TiO_2 ceramic membrane

3.1.1. Determination of IEP of the TiO_2 membrane

Figure 1 collects the rejection of 0.01 M Na_2SO_4 solution for pH values ranging from 1.0 to 11.0 and for two different TMP values (6 and 13 bar). Solution acidity ranged from pH values below pK_a (HSO_4^-/SO_4^{-2}) = 2.0 (where the predominant species is HSO_4^-) to values above the pK_a (where the predominant species is SO_4^{2-}). Na_2SO_4

rejection values showed a S-shaped curve. At the lower pH values (<3), Na_2SO_4 rejections were around 15% (at 6 bar of TMP) and 20% (at 13 bar of TMP). The increase of pH led to higher rejections values with an inflexion point around pH 5.4±0.5 to reach a plateau with constant rejections values above pH 6 of 72±3% and 85±2% at 6 and 13 bar of TMP, respectively.

The performance of ceramic membranes containing TiO_2 active layers treating 0.01 M Na_2SO_4 solutions has been studied previously [35,36]. Van Gestel et al. [36] also observed the same trend with a TiO_2 with a pore size between 1 and 2 nm, but Na_2SO_4 rejection started to increase at pH 5.5. Puhlfürß et al. [35] observed the transition from low to high rejection values at pH 2 with a TiO_2 membrane (IEP of 3.1) with a mean pore size of 0.55 nm at 6 bar. Values of Na_2SO_4 rejections from both studies are plotted for comparison in **Figure 2**.

The Na_2SO_4 rejection by the membrane can be related to the protonation/deprotonation of the titania active layer surface groups (R–TiOH), which shift from a protonated and positively charged form ($R–TiOH_2^+$) at acid pH to a deprotonated and negatively charged form ($R–TiO^-$) at basic pH, as it is described in equations (2) and (3) [36]:

$$R - TiOH_2^+ \leftrightarrow R - TiOH + H^+ \quad (2)$$

$$R - TiOH \leftrightarrow R - TiO^- + H^+ \quad (3)$$

Van Gestel et al. [36] and Dutounié et al. [37] characterized the acid-base properties of TiO_2 powder by determining the IEP from zeta potential measurements. The IEP value reported by these studies is around 6. As it can be seen in **Figure 2**, the determined IEP values correspond approximately with the pH of the inflexion point of the rejection/pH functions. The IEP determined in the present study for both TMPs tested was 5.4+/-0.5, which fell in the range of reported values by Puhlfürβ et al. [35] and Van Gestel et al. [36].

Table 3 compares the characteristics of TiO_2-based ceramic NF membranes with different average pore sizes of the reported studies. While it does not seem to exist any dependence of water permeability on laver thickness, a relationship between IEP values and average pore size seemed apparent. The decrease of pore size is associated with an increase of the acidity of the TiOH surface groups and consequently a reduction of their pK_a values. The dependence of the acidity of functional groups in TFC NF and reverse osmosis membranes on the free volume has been reported by Coronell et al. [38]. For

polyamide active layer based-membranes, the reduction of the free volume (pore size) is accompanied by a decrease of the acidity of the functional groups.

3.1.2. SEM analysis of the TiO_2 membrane

SEM analysis was performed on various pieces of the ceramic membrane. The top view of the membrane layers is shown in **Figure 3.a** (for the TiO_2 layer) and **3.b** (for the Al_2O_3 layer) at x300. As also described by Dutounié et al. [37] when analysing a similar TiO_2 based membrane, its active layer is constituted by an agglomerate of TiO_2 nanoparticles. This agglomeration was associated with particle sintering arising during thermal treatment.

Figures 3.c and 3.d show a cross-section observation of the tubular membrane at two different enlargements. The membrane profile (**Fig. 3.c**) allowed to see both layers and also the transition zone between them. First, both SEM micrographs showed that the membrane support (α-Al_2O_3) was constituted by several layers with different porosities. The active layer thickness was found to be 21.1 ± 4.6 µm. Moreover, the TiO_2 layer was found to be smooth, and no visible pores were detected in the layer either at magnifications of x300 (Fig 2c) nor x1000 (**Fig. 3.d**).

3.2. Characterisation of the polymeric MPF–34 membrane

MPF–34 is a polymeric membrane with a proprietary active layer of unknown composition. This layer was analysed in the present study by SEM, FTIR-ATR and XPS. **Figure S2 (supplementary information)** shows the SEM images of the MPF–34 membrane. The membrane profile (**Fig. S2.a, b**) allowed to see the three layers of the membrane, including the polyester, the support and the active layer. The following amplification (**Fig S2.c, d**) allowed to see with more detail the support and the active layer, whose thickness was found to be 1.06 ± 0.03 µm. The analysis by SEM-EDX of the MPF–34 membrane revealed the presence of C, N, O and S in the pristine membrane.

In order to determine the functional groups of the membrane, FTIR-ATR and XPS were used. The obtained FTIR-ATR spectrum showed a superposition of the active and the intermediate layers (**Figure S3** and **Table S1** in supplementary information), which was due to a radiation penetration depth higher than the thickness of the active layer. In practice, due to the relative thickness of the two layers, the main signal was from the intermediate layer. From the membrane FTIR-ATR spectra, it was drawn that the

intermediate layer was made of polyether-sulphone or polysulphone, as these two polymers have quite close FTIR spectra. Contrarily, the use of XPS allowed to analyse mainly the active layer and to determine its composition. From the elementary analysis with XPS, it was observed that the active layer was mainly composed by C (69.5%), N (16.8%), O (10.8%) and a minor presence of S (2.1%) and Cl (0.8%). No presence of Si was detected, which discarded the hypothesis that the membrane active layer is polydimethylsiloxane. The high ratios of N/C and the low content of S allowed to postulate as a primary hypothesis the presence of an amide as a functional group in the active layer (**Figure S4** and **Table S2** in Supplementary information). It is discarded the presence of sulphonated groups, due to the lower amount of S. The presence of such groups ($R\text{-}SO_3^-$) provides the membrane a negative surface charge and IEPs below 1, as in the case of the acid-resistant HydraCoRe 70pHT NF membrane. For the case of the MPF–34, IEPs values range between 4.5 and 5.5, which approach most of the polyamide NF membranes [29–32]. Accordingly, the membrane charge will be given by the protonation/deprotonation of the amine and carboxylic groups, as it is described by equations (4) and (5).

$$R - NH_2^+ \leftrightarrow R - NH + H^+ \quad (4)$$

$$R - COOH \leftrightarrow R - COO^- + H^+ \quad (5)$$

Figure 4 shows a scheme of how membrane charge due to the protonation/deprotonation of functional groups affects separation for both membranes. The presence of a positive membrane charge will favour the transport of anions, whereas a negative one will attract the cations in solution.

3.3. Ions rejection from metal-containing AMWs solutions

3.3.1. Influence of solution acidity on membrane performance

The influence of acidity on membrane performance was studied by decreasing the pH of the solution from 1.5 to 1.0 by adding H_2SO_4. **Figures 5.a** and **6.a** show the ion rejection curves as a function of the trans-membrane flux for the solution at pH 1.5 for the TiO_2 and MPF–34 membranes, respectively.

For both membranes, the rejection of H^+ was below 10% (with even negative rejections in the case of MFP-34). With regard to the dominant anionic species (HSO_4^-), rejections were below 20% for TiO_2 membrane and below 52% for the case MPF–34. When the

metal rejections were compared, much higher values (ca. 80%) were measured for MPF–34 than the TiO_2 membrane (values below 30%). Additionally, metal rejections values for the ceramic membrane were dependent on the metal ions properties, being Al(III) the highest rejected, followed by REEs and finally by the transition metal ions (Cu(II), Zn(II)) and Ca(II). Overall, the transport of ions through both membranes was clearly influenced by the active layer membrane properties.

The transport of ions across polymeric NF membranes is described as a combination of diffusion, electromigration and convection processes [39]. Usually, the rejections values tend to increase over the trans–membrane flux. However, in the present study, the rejections given by the TiO_2 membrane barely increased over the evaluated trans–membrane flux, which can be explained by a high contribution of the convection term (i.e. coupling between solvent and ions). Moreover, the difference of dominant ions diffusivities inside the membrane (i.e. Al, SO_4 and H^+) generated an electric potential, which in turn drove the transport of ions traces (i.e. REEs, Ca, Cu and Zn). Dutounié et al. [37] modelled the transport of ions across a TiO_2 membrane assuming the transport as a combination of steric, electric and dielectric effects. Moreover, equilibrium partitioning that implies the equality of generalized chemical potentials on both sides of the membrane-solution interfaces was considered.

As explained in section 3.1, it is expected that, at acidic pH, the TiO_2 layer presented a positively charged sites due to the protonated $TiOH_2^+$ groups. According to the Donnan exclusion phenomenon [40], the transport of cations will be impeded (i.e. metals, protons), while the passage of anions will be favoured (i.e. hydrogen sulphate). The rejections for Al(III) were the highest ones, ranging from 25 to 30% at pH 1.5. REEs(III) rejections varied between 15 and 20%, while Cu(II), Ca(II) and Zn(II) rejections were between 10 and 15%. Although all the metals were partially complexed with sulphate ions (see **Fig. S1** in Supplementary Information), still a significant fraction of them were positively charged. The lowest rejection was for the H^+ (below 5%), due to its small ionic radius (2.82 Å) and high diffusion coefficient ($9.3 \cdot 10^{-9}$ m^2/s) [41].

Dutounié et al. [37] reported similar salt rejection rates, from 20 to 30% for pure salt-water solutions (NaI, NaF, NaCl) at neutral to slightly basic pH values with three TiO_2 based membranes with average pore radius from 1.4 to 2.4 nm. At these pH values, the TiO_2 groups were totally dissociated (R-TiO^- groups), and then a negative charge along

the membrane was expected. In such a scenario, Na^+ ions were preferably transported, and then counter-anions in solution (F^-, Cl^-, I^-) were co-transported to reach electroneutrality conditions. Then, membranes with different pore size distribution provided similar rejections for the three halide salts (around 40% for NaF, 20% for NaCl and <5% for NaI). On the contrary, for non-charged solutes, rejection increased up to 60%. However, they concluded when the salt rejections were compared, the sequence NaF>NaCl>NaI could not be explained by the Stokes radii of halide ions (0.166, 0.121 and 0.120 nm for F^-, Cl^- and I^- respectively) [42], suggesting that, in the present case, steric effects were not the determining phenomenon for salt exclusion. As stressed, the selectivity of ionic species is governed by three phenomena: steric, electric and dielectric exclusion. Since steric exclusion cannot be responsible for ion rejections, the combination of electric and dielectric effects, as well as the acid-base and complexing properties of the TiO_2 groups might have an important influence on the ion rejections. The presence of the protonated TiO_2 groups ($R\text{-}TiO_2^+$) makes that the membrane approaches an anion exchange membrane, so the electric and dielectric effects are responsible for the ion rejections. Then, the rejection followed the sequence Al(III)>REE(III)>Ca(II),Zn(II),Cu(II)>H^+. The higher rejections of Al(III) than of REEs(III) can be explained with the electric and dielectric effects. Ion polarizabilities, defined as the ion ability to relocate its electrical charge to minimize the interaction energy with its environment, can explain the sequence Al(III)>REE(III). The polarizability of Al^{3+} is within the range 0.05–0.07 $Å^3$, whereas for REEs (e.g. La^{3+}) is from 1.0 to 1.3 $Å^3$ [43]. Then, higher rejections for Al(III) than REEs(III) were obtained.

On the contrary, MPF–34 provided higher rejections of all metals (around 80%), whereas sulphate rejection increased from 45 to 52%. Nevertheless, the permeate flux was much lower for the polymeric membrane than for the ceramic one. The rejections from the polymeric membrane were strongly influenced by the Donnan and the dielectric exclusion [40,44]. The pH of the solution is below the IEP (4.5-5.5 [30,31]), so the membrane presented a positively charged surface, which rejected the cations and allowed the anions to permeate. The dielectric exclusion phenomenon is caused because of the interactions between ions and the charged induced in the membrane at the interface solution/membrane with different dielectric constants (i.e. polymeric matrix/bulk solution). The effect of dielectric exclusion is more pronounced than Donnan exclusion since the exclusion energy is proportional to the square of the ion charge, whereas Donnan exclusion is linear with it [44]. Thus, the dielectric exclusion

could explain why the transport of metal-based species, non-complexed (i.e. M^{n+}: Al^{3+}, Ca^{2+} and Cu^{2+}) and complexed forms (i.e. $M(SO_4)_m^{(n-2\cdot m)}$) was more impeded than the one of H^+. However, it should be stressed that metal rejections were independent of their properties (e.g. ionic radii and polarizability), and no differences were observed between divalent and trivalent metal ions. The effect of dielectric exclusion was not used to explain the experimental results of the TiO_2 membrane because its mean pore size was around 1 nm, which makes this phenomenon weak. Rejection values obtained with the MPF-34 membrane in the present study (80%) were lower than those obtained with other polymeric membranes with semi-aromatic polyamides (>98%) as an active layer (e.g. NF270 and Desal DL) reported in a previous study [45].

Figures 5.b and **6.b** show the ion rejection curves for the solution at pH 1.0 for the TiO_2 and MPF–34 membranes, respectively. For the TiO_2 membrane, the shift in pH led to lower rejections of sulphate (4–12 %) and aluminium (21–31%). These variations in rejections could be explained from the speciation diagrams. This variation in the pH in the solution implied a change in the metal-sulphate complexation as it is described in **Figure 7**. When pH decreased from 1.5 to 1.0, the fraction of HSO_4^- increased while the ones of SO_4^{2-}, $AlSO_4^+$ and $Al(SO_4)_2^-$ decreased. The higher amount of HSO_4^- and the positively charged membrane ($R\text{-}TiOH_2^+$) led to lower rejections of sulphate.

Besides, rejections for Ca(II), Cu(II) and Zn(II) with the TiO_2 also decreased to values between 2 and 12% when the acidity of the solution was increased (from pH 1.5 to 1.0). Due to a higher sulphate permeation, more H^+ was transported across the TiO_2 membrane, which conducted to lower rejections than at pH 1.5 (from –2 to 5%). MPF–34 membrane only showed differences in sulphate and H^+ rejections, while metal rejections barely varied (~80%). Sulphate rejections decreased from 45–52% at pH 1.5 to 29–41% at pH 1.0, which was related to the effect of dielectric exclusion phenomena. The fact that at pH 1.0, the sulphate was mainly present as HSO_4^- made it prone to be transported, due to lower exclusion energy than for SO_4^{2-}. This shift in speciation, in addition to the positively charged membrane surface, allowed the transport of sulphate (as HSO_4^-) across the membrane.

Membrane performances were compared with results obtained for similar AMWs when using a semi-aromatic poly(piperazine amides): NF270 [12], Desal DL [46] and a sulphonated polyethersulphone (HydraCoRe 70pHT) [46]. The effect of decreasing the pH (from pH 1.5 to 1.0) was also studied. Both polyamides membranes (NF270 and

Desal DL) at acidic pHs were positively charged, and then metals (i.e. Al, REEs, Cu, among others) were effectively rejected (>95%) by the membranes at the pH range studied (1.5 to 1.0). Moreover, a decrease in sulphate rejection (from 55 to 45% for NF270 and from 80 to 55% for Desal DL) was observed due to the presence of the species HSO_4^- [12,46]. For dense polymeric active layers, the dielectric exclusion mechanism prevails. Because its effect is more pronounced in multivalent ions (e.g. Al^{3+} or SO_4^{2-}) than in monovalent ions (e.g. HSO_4^-), lower sulphate rejections were observed [44]. On the other hand, HydraCoRe 70pHT membrane, which is characterised by a negatively charged surface, was able to reject sulphate at both pHs at a 75%, while metal rejections decreased from 90 to 75% when working at pH 1.5 and 1.0, respectively. Polymeric membranes allowed to obtain higher rejections than the ceramic membrane tested in this study, but the latter was able to obtain higher trans-membrane fluxes at the same TMP.

MPF–34 performances when treating AMWs or acidic solutions containing metals from hydrometallurgical industries were compared [8,47] (**Table 4**). Ricci et al. [8] treated an AMW from a gold mine at pH 1.5 containing metallic impurities (Mg, Fe, Ca, Ni and Cu, among others) with the MPF–34 membrane and obtained metal rejections between 72 and 82%. Tanninen et al. [47] treated an acidic effluent composed by H_2SO_4 and $CuSO_4$. MPF–34 was able to reject an 82% of $CuSO_4$ at 0.1 M H_2SO_4, while acid rejection was near zero. An increase in acid concentration led to lower $CuSO_4$ and higher H_2SO_4 rejections. In both cases, reported metal rejection values were similar to the values reported in this study. No studies of the application of ceramic membranes for treating acidic waters were found.

Mass balances were performed with the composition of feed and permeate samples to determine if any metal was trapped on the membrane. Differences below 1% were found, which were related to analytical errors rather than to metal entrapment and scaling. Moreover, solubility analysis performed with the Hydra/Medusa code [34] revealed that no metal precipitation is expected to occur at pH<1.5.

3.3.2. Influence of Al(III) and Fe(III) concentration

One of the main parameters in the management of AMW is the presence of Al(III) and Fe(III). Both cations have strong acidic properties due to their strong hydrolytic properties in solution. Actually, the acidity of acid mine waters is defined by their concentration in solution. **Figures 5.c-d** and **6.c-d** show the ion rejection curves for the

solution containing 0.6 g/L Al(III) and 1.8 g/L Al(III) for the TiO_2 and MPF–34 membranes, respectively at pH 1.0.

For the TiO_2 membrane, the increase in Al(III) concentration led to higher sulphate rejections, from 4–12 % (**Figure 5.c**) to 13–19% (**Figure 5.d**).This finding was related to an increase in the sulphate fractions of aluminium–sulphate complexes, such as $AlSO_4^+$ and $Al(SO_4)_2^-$ (see **Figure 8**). The addition of Al(III) to the solution was beneficial in terms of acid recovery in the permeate, because it allowed to obtain even lower H^+ rejections, while metal rejections slightly increased. The fact that the dominant ions (i.e. Al, SO_4 and H^+) in solution controlled the transport of traces (i.e. REEs(III), Ca(II), Cu(II) and Zn(II)) resulted in higher rejections of those traces than at the lowest Al(III) concentration tested. For example, REEs(III) rejections varied between 11 to 20% at 1.8 g/L Al(III) (**Figure 5.d**), while ranged between 13 and 21% at 0.60 g/L (**Figure 5.c**). On the other hand, Ca(II), Cu(II) and Zn(II) rejections increased to 13–19%, whereas at 0.6 g/L those rejections were between 4 and 12%.

However, for the MPF–34 the increase in Al concentration barely affected metal rejections (around 80%), but an increase in sulphate rejection was noticed (29–41 to 42–47%). As explained (see **Figure 8**), the higher fraction of $AlSO_4^+$, whose transport was impeded by the membrane and the lower amount of HSO_4^- in solution limited the transport of sulphate across the membrane. Moreover, H^+ rejections were even lower (from -2 to 9%) than at low Al(III) concentrations (from -3 to 11%), which favoured the recovery of sulphuric acid in the permeate.

The effect of Al(III) concentration was also studied with the Desal DL and HydraCoRe 70pHT NF membranes [46]. Desal DL exhibited metallic rejection higher than 98% over the whole Al(III) concentration range tested (from 0.6 to 1.8 g/L), while sulphate rejection also increased from 60 to 80%. This increase was related to the change in the sulphate speciation. Again, the transport of H^+ was favoured when $Al_2(SO_4)_3$ was added, and its rejection decreased from 40 to 20%. On the other hand, metal rejections barely varied with HydraCoRe 70pHT, whereas sulphate rejections increased from 78 to 84%. Moreover, H^+ rejections marginally decreased from 60 to 57%.

Two different levels of Fe(III) were studied: 0.5 and 2.1g/L Fe(III) at pH 1.0. For the TiO_2 membrane, the addition of 0.5 g/L Fe(III) to the solution implied an increase of sulphate rejection (**Figure 5.e**) in comparison to the case without iron (**Figure 5.a**). Sulphate rejection varied from 16 to 20% over the trans–membrane flux range

evaluated. The higher sulphate rejections were related to the decrease in the concentration of the free anion sulphate forms (i.e. SO_4^{2-} / HSO_4^-) (see **Figure 9**) to give a significant amount of iron complexes (i.e. $FeSO_4^+$, $FeHSO_4^{2+}$ and $Fe(SO_4)_2^-$). The higher rejection of sulphate limited the transport of metals but favoured the transport of H^+. The highest obtained rejections were for Al (35–46%), followed by the ones for Fe(III) (26–37%), whereas H^+ rejections were negative over the whole range (around –10%). As explained before, the main ions (e.g. Al, Fe, H^+ and SO_4) in solution governed the transport of trace ions. REEs(III) rejections increased from 19 to 33%, while rejections of double-charged metals were between 12 and 21%.

The polymeric MPF–34 membrane also showed high rejections of metals (from 70 to 85%), whereas the rejections of sulphate barely varied (31 to 40%) when Fe(III) was added to the solution. Moreover, the addition of Fe(III) was beneficial in terms of H^+ recovery, since lower rejections (from –6 to 1%) were obtained (see **Figure 6.e**).

At 2.1 g/L Fe(III) (see **Figure 5.f**), the TiO_2 membrane exhibited higher rejections of all the ions, which favoured the passage of H^+ across the membrane. Its rejections were lower than in the previous case (around –12%). The increase of metal rejections (a 10% higher than at 0.5 g/L Fe(III)) was related to a lower transport of sulphate across the membrane due to a lower amount of SO_4^{2-} and HSO_4^- fractions (see **Figure 9**).

The addition of Fe(III) to the solution did not show variations in metal rejections for the MPF–34 (see **Figure 6.e and 6.f**). However, sulphate rejections increased due to the lower amount of HSO_4^-, while the amount in the solution of $FeSO_4^+$ and $FeHSO_4^{2+}$ increased. The higher presence of these two cations, which are expected to be rejected by the membrane, explained why sulphate rejection increased. As in the previous case, the higher amount of Fe(III) led to even more negative H^+ rejections.

NF270, Desal DL and HydraCoRe 70pHT membranes were also tested in a previous study to determine how the concentration of Fe (added in chloride form instead of sulphate form) affected on the membrane separation [45]. For NF270 and Desal DL, metal rejections (>95%) were not affected by the addition of Fe (as $FeCl_3$). Besides, the sulphate rejections increased from 70 to 84% for NF270 and from 69 to 81% for Desal DL. The high rejections of metals favoured the transport of H^+ to meet electroneutrality conditions in the permeate, which led to negative rejections. Sulphate rejections also increased using HydraCoRe 70pHT membrane, from 77 to 87%, while metal rejections barely varied (>75%).

Table 5 sums up the rejections of triple and double-charged metals, as well as sulphate and H^+ rejections for TiO_2 ceramic and polymeric (MPF–34, NF270, Desal DL and HydraCoRe 70pHT) membranes. As it can be seen, polyamide polymeric membranes (NF270 and Desal DL) offer good characteristics, in terms of metal rejections and H^+ passage. Nevertheless, their low chemical resistance makes them susceptible to acid attack. The use of acid–resistance polymeric membranes (MPF–34) also offers a good choice for treating AMW, despite exhibiting lower rejections than the polyamide ones. Efforts must be towards the development of narrow TiO_2 ceramic membranes to reduce the convective flux across them so that they can exhibit higher rejections.

3.4. Estimation of ion concentration factors for the TiO_2 and MPF–34 membranes

From the rejections for both membranes, the concentration factors (ratio feed to permeate concentration) at different permeate recovery values (20, 40, 60 and 80%) were estimated (see **Table 6**). These values were calculated for the solution containing 2.1 g/L Fe(III) with the ion rejections at the maximum evaluated TMP values in the experimental part (see **Fig. 5.f** and **6.f**).

As expected, the lowest concentration factor values (<1) for both membranes were obtained for H^+ due to its negative rejections. The concentration factor values for both membranes values did not differ among them. This suggests that the acid was mainly transported across the membrane and, as the %permeate recovery increased, the acidity of the solution decreased. This can be beneficial in terms of saving costs for the acid neutralisation needed in subsequent stages of the treatment. Nevertheless, the concentration factor values for the metals were quite different if both membranes were compared. MPF–34 yielded to higher concentration factors than the TiO_2 ceramic membrane at the same %permeate recovery, since it exhibited higher rejections. To achieve the same concentration factor with the TiO_2 membrane, more permeate should be recovered. For example, the concentration factors for the REEs were 2.10 at 80% of permeate recovery for the TiO_2 membrane; while at 60% of permeate recovery, the concentration factors were 2.20 for the MPF–34. The lack of selectivity of the latter membrane made that all the metals in solution achieve the same concentration factors, while for the more selective TiO_2 membrane, these values varied significantly. For example, at 60 %permeate recovery, the metal concentration factors were around 2.20, while for the TiO_2 membrane ranged between 1.4 (for the Cu) to 1.9 (for the Al).

4. Conclusions

Acid–stable NF membranes have proven to be useful for treating AMW. MPF–34 has shown better results in terms of metal rejection (~80%) than the TiO_2 ceramic membrane (<60%).

Solution composition and speciation were found to have a significant impact on membrane performance, especially those performed with the ceramic membrane. The rejections of metals, sulphate and H^+ by the TiO_2 membrane were highly influenced by the speciation of the ions in solution. The equilibrium shifts towards the formation of metal-sulphate complexes resulted in higher metal rejections. On the other side, the MPF–34 membrane exhibited metal rejections of 80% under all conditions tested, while H^+ and sulphate rejections varied depending on the solution composition.

The high chemical stability of ceramic NF membranes can make them useful for treating AMW. Nevertheless, ceramic NF membranes with smaller pore size need to be developed, in order to reduce the contribution of convective flow to ion transport. This could help ceramic NF membranes to increase ion rejections.

Acknowledgements

This research was supported by the Waste2Product project (CTM2014-57302-R) and by R2MIT project (CTM2017-85346-R) financed by the Spanish Ministry of Economy and Competitiveness (MINECO) and the Catalan Government (2017-SGR-312), Spain. The work of Julio López and Xanel Vecino was supported by MINECO within the scope of the grant (BES-2015-075051) and the Juan de la Cierva contract (IJCI-2016-27445), respectively. We also want to thank the contribution of D. León and R. Pirabed for their help during the experimental work and A. Espriu-Gascón and A. Díaz for the ICP analysis.

References

[1] C. Ayora, F. Macías, E. Torres, A. Lozano, S. Carrero, J.-M. Nieto, R. Pérez-López, A. Fernández-Martínez, H. Castillo-Michel, Recovery of Rare Earth Elements and Yttrium from passive-remediation systems of acid mine drainage, Environ. Sci. Technol. 50 (2016) 8255–8262. doi:10.1021/acs.est.6b02084.

[2] C.A. Cravotta, Dissolved metals and associated constituents in abandoned coal-mine discharges, Pennsylvania, USA. Part 1: Constituent quantities and correlations, Appl. Geochemistry. 23 (2008) 166–202. doi:10.1016/j.apgeochem.2007.10.011.

[3] P.K. Sahoo, S. Tripathy, S.M. Equeenuddin, M.K. Panigrahi, Geochemical characteristics of coal mine discharge vis-à-vis behavior of rare earth elements at Jaintia Hills coalfield, northeastern India, J. Geochemical Explor. 112 (2012) 235–243. doi:10.1016/j.gexplo.2011.09.001.

[4] M. Olías, J.M. Nieto, R. Pérez-López, C.R. Cánovas, F. Macías, A.M. Sarmiento, L. Galván, Controls on acid mine water composition from the Iberian Pyrite Belt (SW Spain), Catena. 137 (2016) 12–23. doi:10.1016/j.catena.2015.08.018.

[5] E. Santofimia, J. Sa, E. Lo, D. Barettino, O. Aduvire, Acid mine drainage in the Iberian Pyrite Belt (Odiel river watershed, Huelva , SW Spain): Geochemistry , mineralogy and environmental implications, Appl. Geochemistry. 20 (2005) 1320–1356. doi:10.1016/j.apgeochem.2005.01.011.

[6] G. Lee, J.M. Bigham, G. Faure, Removal of trace metals by coprecipitation with Fe, Al and Mn from natural waters contaminated with acid mine drainage in the Ducktown Mining District, Tennessee, Appl. Geochemistry. 17 (2002) 569–581. doi:10.1016/S0883-2927(01)00125-1.

[7] U. Wingenfelder, C. Hansen, G. Furrer, R. Schulin, Removal of heavy metals from mine waters by natural zeolites, Environ. Sci. Technol. 39 (2005) 4606–4613. doi:10.1021/es048482s.

[8] B.C. Ricci, C.D. Ferreira, A.O. Aguiar, M.C.S. Amaral, Integration of nanofiltration and reverse osmosis for metal separation and sulfuric acid recovery from gold mining effluent, Sep. Purif. Technol. 154 (2015) 11–21. doi:10.1016/j.seppur.2015.08.040.

[9] S. You, J. Lu, C.Y. Tang, X. Wang, Rejection of heavy metals in acidic wastewater by a novel thin-film inorganic forward osmosis membrane, Chem. Eng. J. 320 (2017) 532–538. doi:10.1016/j.cej.2017.03.064.

[10] B. Vital, J. Bartacek, J.C. Ortega-Bravo, D. Jeison, Treatment of acid mine drainage by forward osmosis : Heavy metal rejection and reverse flux of draw solution constituents, Chem. Eng. J. 332 (2018) 85–91.

doi:10.1016/j.cej.2017.09.034.

[11] M. Nyström, J. Tanninen, M. Mänttäri, Separation of metal sulfates and nitrates from their acids using nanofiltration, Membr. Technol. 2000 (2000) 5–9. doi:10.1016/S0958-2118(00)86633-1.

[12] J. López, M. Reig, O. Gibert, E. Torres, C. Ayora, J.L. Cortina, Application of nanofiltration for acidic waters containing rare earth elements: Influence of transition elements, acidity and membrane stability, Desalination. 430 (2018) 33–44. doi:10.1016/j.desal.2017.12.033.

[13] R. Fornarelli, M. Mullett, D. Ralph, Factors influencing nanofiltration of acid mine drainage, Reliab. Mine Water Technol. (2013) 563–568.

[14] A.R. Guastalli, J. Labanda, J. Llorens, Separation of phosphoric acid from an industrial rinsing water by means of nanofiltration, Desalination. 243 (2009) 218–228. doi:10.1016/j.desal.2008.04.024.

[15] B. Kose Mutlu, B. Cantoni, A. Turolla, M. Antonelli, H. Hsu-Kim, M.R. Wiesner, Application of nanofiltration for Rare Earth Elements recovery from coal fly ash leachate: Performance and cost evaluation, Chem. Eng. J. 349 (2018) 309–317. doi:10.1016/j.cej.2018.05.080.

[16] A.L. Ahmad, B.S. Ooi, A study on acid reclamation and copper recovery using low pressure nanofiltration membrane, Chem. Eng. J. 156 (2010) 257–263. doi:10.1016/j.cej.2009.10.014.

[17] L. Pino, C. Vargas, A. Schwarz, R. Borquez, Influence of operating conditions on the removal of metals and sulfate from copper acid mine drainage by nanofiltration, Chem. Eng. J. 345 (2018) 114–125. doi:10.1016/j.cej.2018.03.070.

[18] S. Platt, M. Nyström, A. Bottino, G. Capannelli, Stability of NF membranes under extreme acidic conditions, J. Memb. Sci. 239 (2004) 91–103. doi:10.1016/j.memsci.2003.09.030.

[19] B.C. Ricci, C.D. Ferreira, L.S. Marques, S.S. Martins, B.G. Reis, M.C.S. Amaral, Assessment of the chemical stability of nanofiltration and reverse osmosis membranes employed in treatment of acid gold mining effluent, Sep. Purif. Technol. 174 (2017) 301–311. doi:10.1016/j.seppur.2016.11.007.

[20] R. Navarro, M.P. González, I. Saucedo, M. Avila, P. Prádanos, F. Martínez, A. Martín, A. Hernández, Effect of an acidic treatment on the chemical and charge properties of a nanofiltration membrane, J. Memb. Sci. 307 (2008) 136–148. doi:10.1016/j.memsci.2007.09.015.

[21] T. Schütte, C. Niewersch, T. Wintgens, S. Yüce, Phosphorus recovery from sewage sludge by nanofiltration in diafiltration mode, J. Memb. Sci. 480 (2015) 74–82. doi:10.1016/j.memsci.2015.01.013.

[22] A. Manis, K. Soldenhoff, E. Jusuf, F. Lucien, Separation of copper from sulfuric acid by nanofiltration, in: Fifth Int. Membr. Sci. Technol. Conf., 2003.

[23] S.M. Samaei, S. Gato-Trinidad, A. Altaee, The application of pressure-driven ceramic membrane technology for the treatment of industrial wastewaters – A review, Sep. Purif. Technol. 200 (2018) 198–220. doi:10.1016/j.seppur.2018.02.041.

[24] V. Gitis, G. Rothenberg, Ceramic Membranes. New opportunities and Practical Applications, 1st ed., Wiley-VCH Verlag GmbH & Co. KGaA, Weinheim, Germany, 2016. doi:10.1002/9783527696550.

[25] S. Benfer, U. Popp, H. Richter, C. Siewert, G. Tomandl, Development and characterization of ceramic nanofiltration membranes, Sep. Purif. Technol. 22–23 (2001) 231–237. doi:10.1016/S1383-5866(00)00133-7.

[26] I. Voigt, G. Fischer, P. Puhlfürß, M. Schleifenheimer, M. Stahn, TiO2-NF-membranes on capillary supports, Sep. Purif. Technol. 32 (2003) 87–91. doi:10.1016/S1383-5866(03)00064-9.

[27] I. Voigt, M. Stahn, S. Wöhner, A. Junghans, J. Rost, W. Voigt, Integrated cleaning of coloured waste water by ceramic NF membranes, Sep. Purif. Technol. 25 (2001) 509–512. doi:10.1007/978-3-642-54734-2.

[28] S.S. Wadekar, R.D. Vidic, Comparison of ceramic and polymeric nanofiltration membranes for treatment of abandoned coal mine drainage, Desalination. 440 (2018) 135–145. doi:10.1016/j.desal.2018.01.008.

[29] K.M. Systems, KMS Flat Sheet Membrane Samples, Massachusetts, 2018. https://www.kochmembrane.com/KochMembraneSolutions/media/Product-Datasheets/Test Products/flat-sheet-sample-datasheet.pdf.

[30] J. Warczok, M. Ferrando, F. López, A. Pihlajamäki, C. Güell, Reconcentration of spent solutions from osmotic dehydration using direct osmosis in two configurations, J. Food Eng. 80 (2007) 317–326. doi:10.1016/j.jfoodeng.2006.06.003.

[31] M.I. Gehan, E.-G. Belal, Recent Drifts in pH-Sensitive Reverse Osmosis, in: T. Yonar (Ed.), Wastewater Water Qual., 1st ed., InTech, 2018. doi:http://dx.doi.org/10.5772/57353.

[32] Mayur Ramesh Dalwani, Thin film composite nanofiltration membranes for extreme conditions, University of Twente, 2011. doi:10.3990/1.9789036532761.

[33] Proyecto Rio Tinto, (n.d.). http://riotinto.atalayamining.com/la-mina/ (accessed June 22, 2017).

[34] I. Puigdomenech, Chemical equilibirum software Hydra/Medusa, (2001). https://sites.google.com/site/chemdiagr/home.

[35] P. Puhlfürß, A. Voigt, R. Weber, M. Morbé, Microporous TiO2 membranes with a cut off <500 Da, J. Memb. Sci. 174 (2000) 123–133. doi:10.1016/S0376-7388(00)00380-X.

[36] T. Van Gestel, C. Vandecasteele, A. Buekenhoudt, C. Dotremont, J. Luyten, R. Leysen, B. Van Der Bruggen, G. Maes, Salt retention in nanofiltration with multilayer ceramic TiO2membranes, J. Memb. Sci. 209 (2002) 379–389. doi:10.1016/S0376-7388(02)00311-3.

[37] P. Dutournié, L. Limousy, J. Anquetil, S. Déon, Modification of the selectivity properties of tubular ceramic membranes after alkaline treatment, Membranes (Basel). 7 (2017) 65. doi:10.3390/membranes7040065.

[38] O. Coronell, M.I. González, B.J. Mariñas, D.G. Cahill, Ionization Behavior, Stoichiometry of Association, and Accessibility of Functional Groups in the Active Layers of Reverse Osmosis and Nanofiltration Membranes, Environ. Sci. Technol. 44 (2010) 6808–6814.

[39] J. Fang, B. Deng, Rejection and modeling of arsenate by nanofiltration : Contributions of convection , diffusion and electromigration to arsenic transport, J. Memb. Sci. 453 (2014) 42–51. doi:10.1016/j.memsci.2013.10.056.

[40] A.E. Yaroshchuk, Non-steric mechanisms of nanofiltration : superposition of

Donnan and dielectric exclusion, Sep. Purif. Technol. 22–23 (2001) 143–158.

[41] R.A. Robinson, R.H. Stokes, Electrolyte Solutions, Second Rev, Dover Books on Chemistry Series, 2002.

[42] D.R. Lide, Handbook of Chemistry and Physics, 87th ed., Boca Raton, FL, USA, 2007.

[43] J.R. Tessman, A.D. Kahn, Electronic Polarizabilities of Ions in Crystals, Phys. Rev. 92 (1953) 890–895. doi:https://doi.org/10.1103/PhysRev.92.890.

[44] A. Yaroshchuk, Dielectric exclusion of ions from membranes, Adv. Colloid Interface Sci. 85 (2000) 193–230.

[45] J. López, M. Reig, O. Gibert, J.L. Cortina, Recovery of sulphuric acid and added value metals (Zn, Cu and rare earths) from acidic mine waters using nanofiltration membranes, Sep. Purif. Technol. 212 (2019) 180–190. doi:10.1016/j.seppur.2018.11.022.

[46] J. López, M. Reig, O. Gibert, J.L. Cortina, Integration of nanofiltration membranes in recovery options of rare earth elements from acidic mine waters, J. Clean. Prod. 210 (2019) 1249–1260. doi:10.1016/j.jclepro.2018.11.096.

[47] J. Tanninen, M. Mänttäri, M. Nyström, Nanofiltration of concentrated acidic copper sulphate solutions, Desalination. 189 (2006) 92–96. doi:10.1016/j.desal.2005.06.017.

[48] J. Tanninen, M. Mänttäri, M. Nyström, Nanofiltration of concentrated acidic copper sulphate solutions, Desalination. 189 (2006) 92–96. doi:10.1016/j.desal.2005.06.017.

[49] H. Diallo, M. Rabiller-Baudry, K. Khaless, B. Chaufer, On the electrostatic interactions in the transfer mechanisms of iron during nanofiltration in high concentrated phosphoric acid, J. Memb. Sci. 427 (2013) 37–47. doi:10.1016/j.memsci.2012.08.047.

[50] L.M. Harwood, T.D.W. Claridge, Introduction to organic spectroscopy, 1st ed., Oxford University Press, Oxford, 1996.

[51] N.I. of S. and Technology, NIST X-ray Photoelectron Spectroscopy Database, (n.d.). https://srdata.nist.gov/xps/Default.aspx.

[52] G. Beamson, D. Briggs, High Resolution XPS of Organic Polymers: The Scienta

ESCA 300 database, Jown Wiley & Sons, Chichester, 1992. doi:10.1002/sia.740200310.

SUPLEMENTARY INFORMATION

	Sulphate	Double-charged metal (M(II))	Triple-charged metal (M(III))
Influence of pH	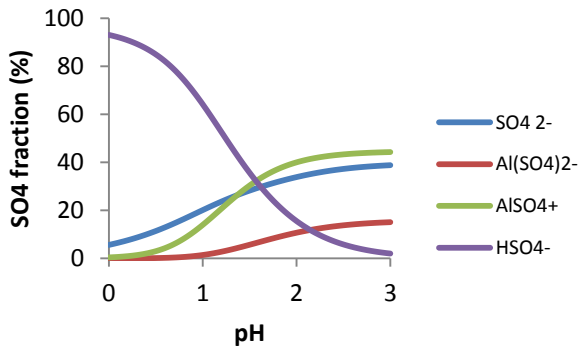	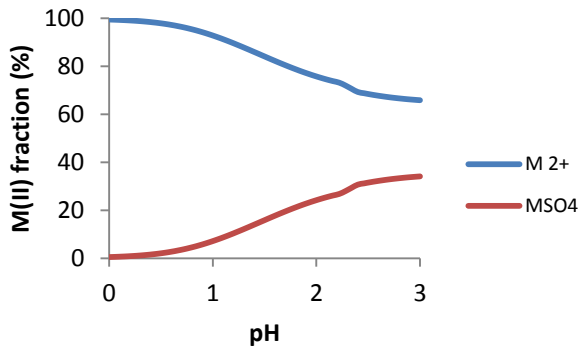	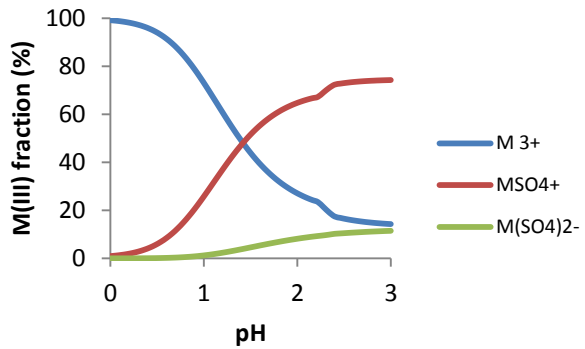
Influence of Al concentration	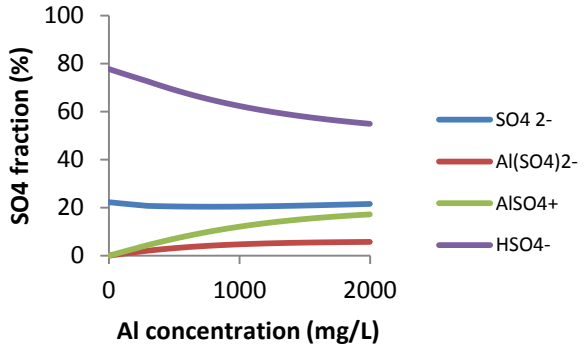	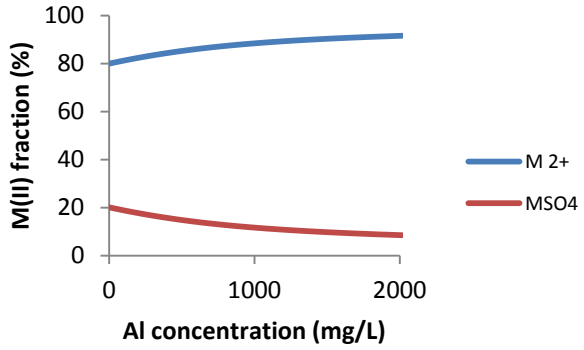	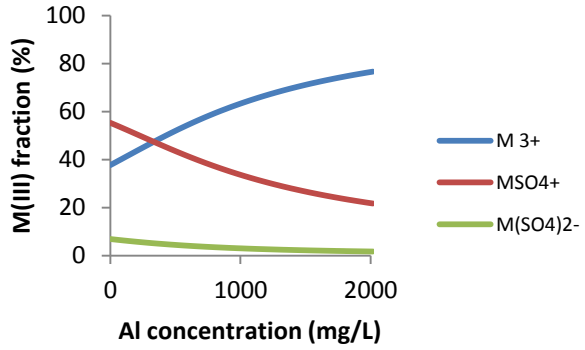

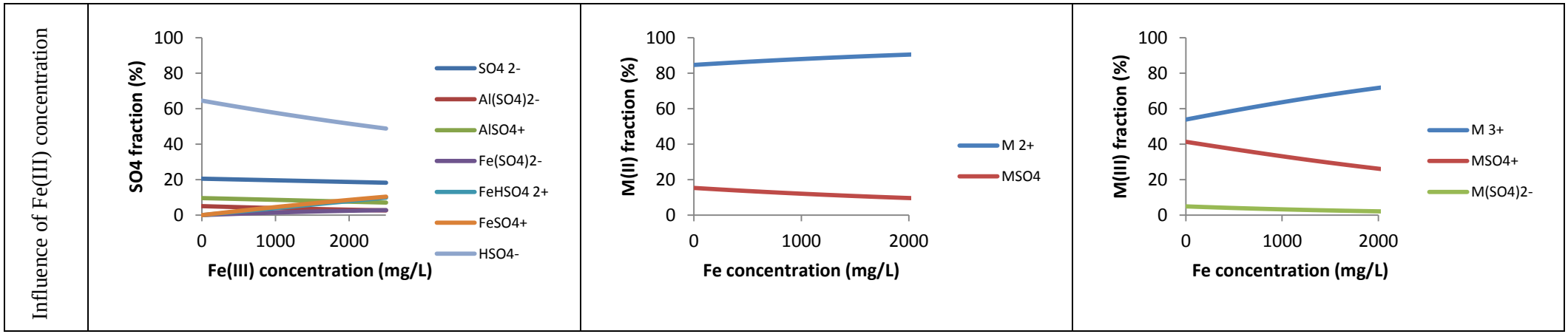

Figure S1. *Sulphate (SO_4), double and triple charged (M(II) and M(III)) fraction diagrams as a function of pH, Al(III) and Fe(III) concentration*

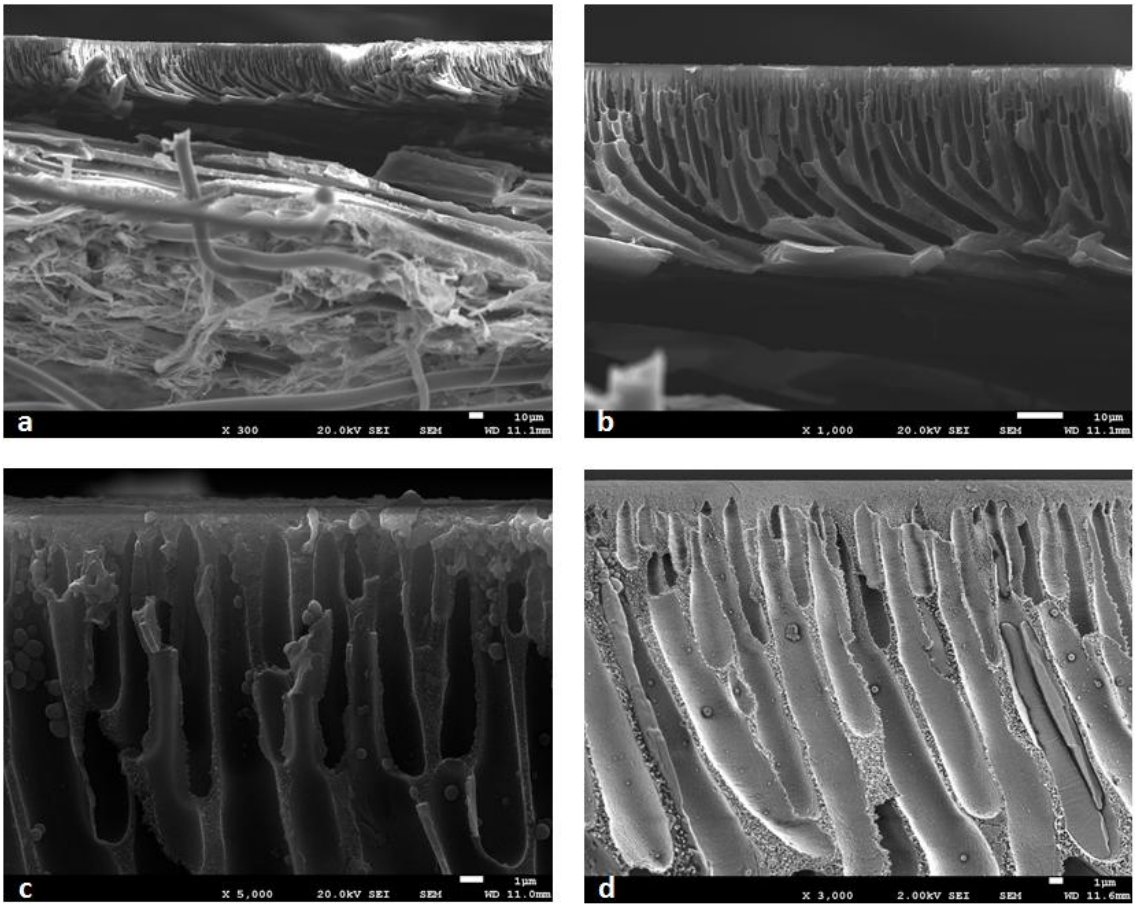

Figure S2. *FESEM images of the MPF-34 membrane profile at: a) x300 amplifications; b) x1000 amplifications; c) x5000 amplifications and; d) x3000 amplifications at 2.00 kV*

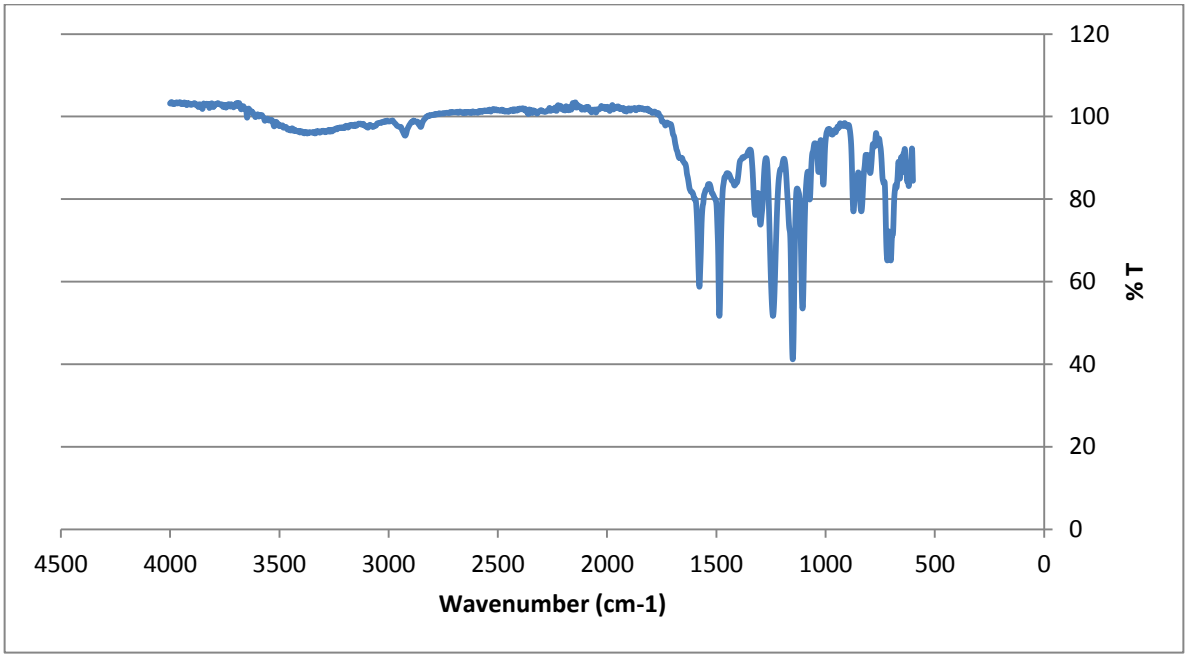

Figure S3. *FTIR-ATR spectra of the MPF-34 membrane. Peak assignments are summarised in Table S1*

Table S1. *Peak assignment for FTIR-ATR spectra of the MPF-34 membrane over 1600–1100 cm^{-1}* [50]

Peak	Range (cm^{-1}) and Intensity	Group and Class	Assignement
1583	1615 – 1590 (m)	Benzene ring in aromatic compounds	Ring stretch, sharp band
1485	1515 – 1485 (m)	Benzene ring in aromatic compounds	Ring stretch, sharp band
1323	1335 – 1295 (vs)	SO_2 in sulfones	SO_2 antisym stretch
1294	1335 – 1295 (vs)	SO_2 in sulfones	SO_2 antisym stretch
1238	1240 – 1070 (s-vs)	C-O-C in ethers	S-O-C stretch
1148	1170 – 1140 (vs)	SO_2 in sulfones	SO_2 sym stretch

Spectra	C1s
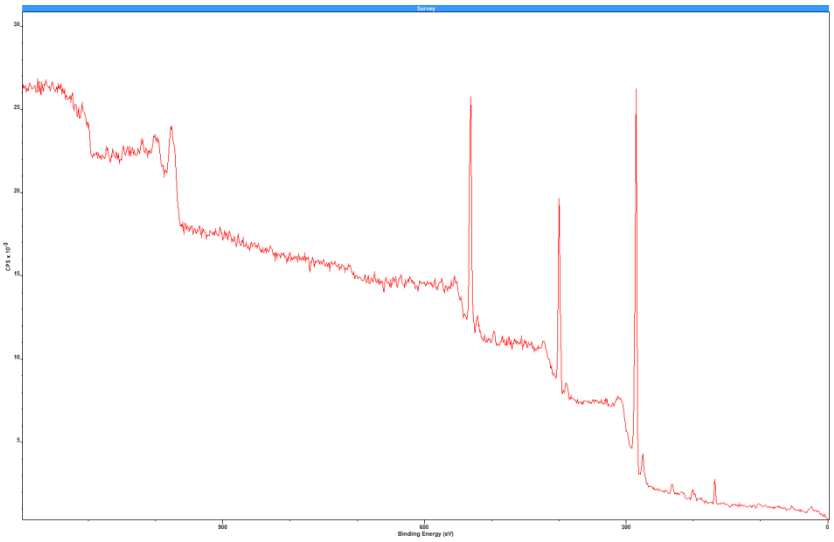	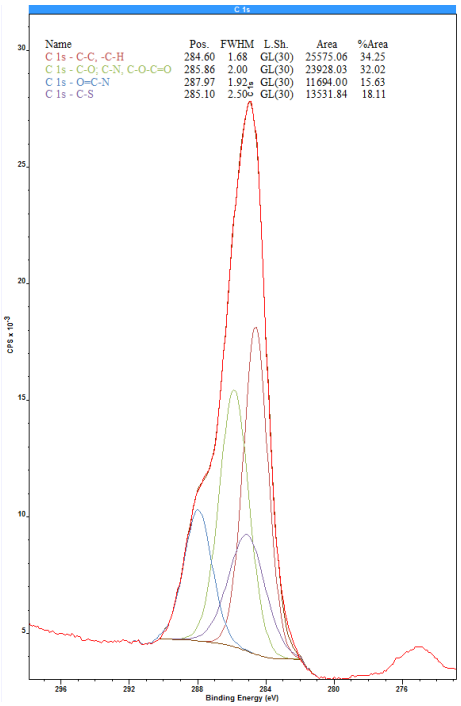

O1s	N1s	S2p
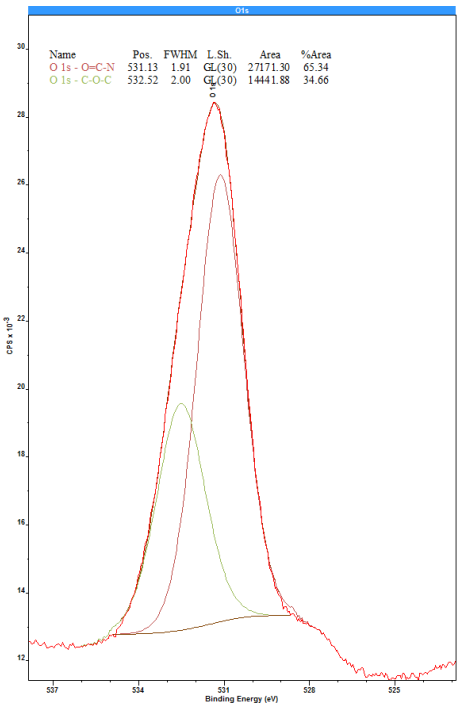	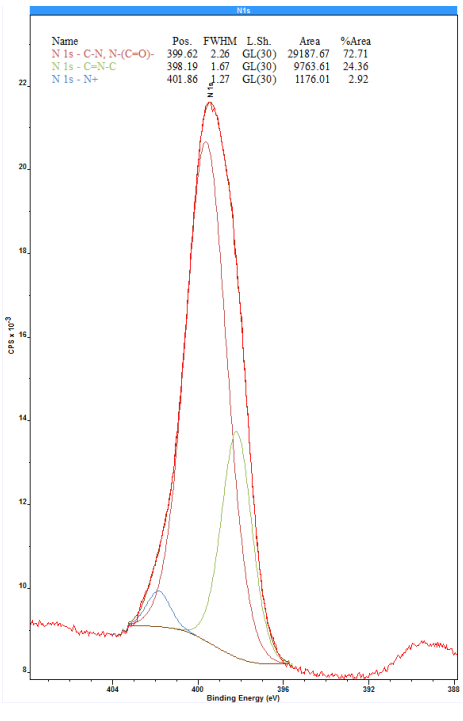	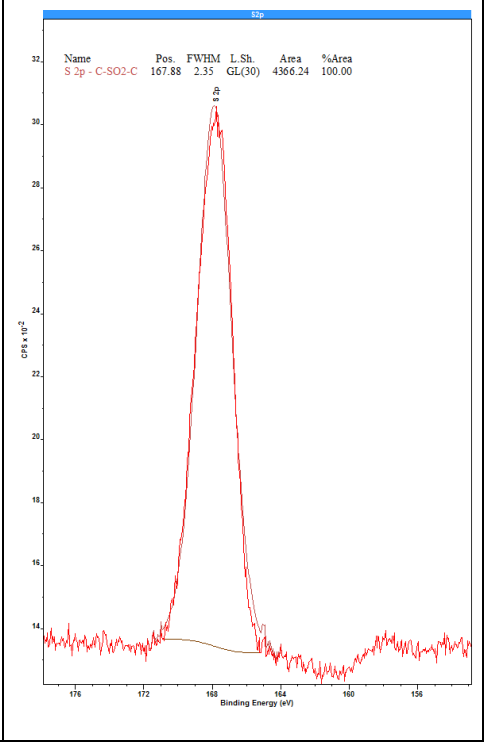

Figure S4. *XPS spectra of the MPF-34 membrane*

Table S2. *Binding energies and relatively amount of functional groups for the MPF-34 membrane* [51,52]

	Binding energy (eV)	%
C 1s		69.53
C-C, C-H	284.6	34.25
C-S, S-SO_2	285.1	18.11
C-O-C, C-CN	285.9	32.02
N-C=O	288.0	15.63
O 1s		10.80
N-C=O, SO_2, SO_3	531.1	65.34
C-O-C	532.5	34.66
N 1s		16.73
C=N-C	398.2	24.36
C-N, N-C=O	399.6	72.71
-NH_3^+	401.9	2.92
S 2p		2.11
C-SO_2-C	167.9	100
Cl 2p		0.83

Table

Table 1*. Composition of the synthetic solutions, as total concentrations, mimicking AMWs from the Iberian Pyrite Belt in Huelva province (Southwest of Spain) (mg/L)*

	pH	Al(III)	Fe(III)	Ca(II)	Cu(II)	Zn(II)	REEs[1](III)
Influence of pH	1.5	600	-	25	40	46	60
	1.0	600	-	25	40	46	60
Influence of Al(III) concentration	1.0	600	-	25	40	46	60
	1.0	1800	-	25	40	46	60
Influence of Fe (III) concentration	1.0	600	500	25	40	46	60
	1.0	600	2125	25	40	46	60

[1] The term REEs includes the following metals: La(III), Pr(III), Nd(III), Sm(III), Dy(III) and Yb(III) (10 mg/L each one)

***Table 2**. Chemical equilibrium constants for the main species present in solution (HYDRA database* [34]*)*

Chemical reaction	$\log K_i$	Chemical reaction	$\log K_i$
$H^+ + SO_4^{2-} \leftrightarrow HSO_4^-$	2.0	$La^{3+} + SO_4^{2-} \leftrightarrow LaSO_4^+$	3.6
$Al^{3+} + SO_4^{2-} \leftrightarrow AlSO_4^+$	3.5	$La^{3+} + 2\,SO_4^{2-} \leftrightarrow La(SO_4)_2^-$	5.1
$Al^{3+} + 2\,SO_4^{2-} \leftrightarrow Al(SO_4)_2^-$	5.0	$Pr^{3+} + SO_4^{2-} \leftrightarrow PrSO_4^+$	3.6
$Al^{3+} + H^+ + SO_4^{2-} \leftrightarrow AlHSO_4^{2+}$	2.5	$Pr^{3+} + 2\,SO_4^{2-} \leftrightarrow Pr(SO_4)_2^-$	4.9
$Fe^{3+} + SO_4^{2-} \leftrightarrow FeSO_4^+$	4.1	$Nd^{3+} + SO_4^{2-} \leftrightarrow NdSO_4^+$	3.6
$Fe^{3+} + 2\,SO_4^{2-} \leftrightarrow Fe(SO_4)_2^-$	5.4	$Nd^{3+} + 2\,SO_4^{2-} \leftrightarrow Nd(SO_4)_2^-$	5.1
$Fe^{3+} + H^+ + SO_4^{2-} \leftrightarrow FeHSO_4^{2+}$	4.5	$Sm^{3+} + SO_4^{2-} \leftrightarrow SmSO_4^+$	3.6
$Ca^{2+} + SO_4^{2\pm} \leftrightarrow CaSO_4$	2.30	$Sm^{3+} + 2\,SO_4^{2-} \leftrightarrow Sm(SO_4)_2^-$	5.2
$Ca^{2+} + H^+ + SO_4^{2-} \leftrightarrow CaHSO_4^+$	3.1	$Dy^{3+} + SO_4^{2-} \leftrightarrow DySO_4^+$	3.6
$Cu^{2+} + SO_4^{2-} \leftrightarrow CuSO_4$	2.3	$Dy^{3+} + 2\,SO_4^{2-} \leftrightarrow Dy(SO_4)_2^-$	5.1
$Zn^{2+} + SO_4^{2-} \leftrightarrow ZnSO_4$	2.4	$Yb^{3+} + SO_4^{2-} \leftrightarrow YbSO_4^+$	3.6
$Zn^{2+} + 2\,SO_4^{2-} \leftrightarrow Zn(SO_4)_2^{2-}$	3.3	$Yb^{3+} + 2\,SO_4^{2-} \leftrightarrow Yb(SO_4)_2^-$	5.1

***Table 3**. Properties of the TiO_2 ceramic NF membranes found in the literature*

Active layer	TiO_2	TiO_2	TiO_2	TiO_2
Support	α- Al_2O_3	n.a.	α- Al_2O_3	Al_2O_3
Average pore size (nm)	2	0.9	1.4 – 2.3	1
IEP	6	3.3	6	5.4±0.5
Water permeability ($L/(m^2 \cdot h \cdot bar)$)	20	15 – 25	n.a.	27
Ref.	Van Gestel et al. [36]	Puhlfürβ et al. [35]	Dutournié et al. [37]	This work

n.a. not available

***Table 4**. Comparison of the MPF–34 performance when filtering acidic waters containing metals*

Solution composition (g/L)	Permeate flux/TMP	Rejections (%)	Reference
pH = 1.46 Mg: 2.43 Fe: 0.43 Ca: 0.42 Al: 0.34	10 bar 10% recovery	pH = 1.29 Mg: 91 Fe: 91 Ca: 80 Al: 93	Ricci et al. [8]
H_2SO_4: 25 Cu: 2	10 L/(m^2 h)	H_2SO_4: 20 Cu: 75	Manis et al. [22]
H_2SO_4: 200 Cu: 2	10 L/(m^2 h)	H_2SO_4: 15 Cu: 75	Manis et al. [22]
H_2SO_4: 80 $CuSO_4$: 76	14 L/(m^2 h)	H_2SO_4: 15 $CuSO_4$: 69	Tanninen et al. [48]
H_3PO_4: 580 $FeCl_3$: 2	40 bar	H_3PO_4: 0 Fe: 60 Cl: -25	Diallo et al. [49]
H_3PO_4: 12 $FeCl_3$: 2	40 bar	H_3PO_4: 60 Fe: 98 Cl: 10	Diallo et al. [49]

***Table 5**. Variation of triple-charged (M(III), i.e. Al, Fe(III) and REEs) and double-charged metals (M(II), i.e. Ca, Cu and Zn); sulphate and H^+ for ceramic (TiO_2) and polymeric (MPF–34, NF270, Desal DL and HydraCoRe 70pHT) membranes*

Membrane	pH	Metal content (g/L)	M(III) rejection (%)	M(II) rejection (%)	SO_4 rejection (%)	H^+ rejection (%)
TiO_2 (this work)	1.5	Al:0.6	25–30	10–15	10–15	2–7
	1.0	Al: 0.6	21–31	2–12	4–12	-2–5
		Al: 1.8	23–31	13–19	13–19	-1–2
		**Fe: 0.5	26–46	12–21	16–20	-10
		**Fe: 2.1	32–58	23–34	26–30	-12
MPF–34 (this work)	1.5	Al: 0.6	~80	~80	45–52	-6–3
	1.0	Al: 0.6	~80	~80	29–41	-3–11
		Al: 1.8	~80	~80	42–47	-2–9
		**Fe: 0.5	72–85	72–85	31–40	-6–2
		**Fe: 2.1	72–81	72–81	43–50	-13
NF270 * [12,45]	1.0	Al: 0.6	>99	>99	39–52	-6–12
		**Fe: 0.5	>99	>99	56–64	-10–9
		**Fe: 2.1	>99	>99	71–85	-20–-15
Desal DL * [45,46]	1.5	Al: 0.6	>98	>98	82–90	6–48
	1.0	Al: 0.6	>98	>98	52–71	20–48
		Al: 1.8	>98	>98	65–79	-1–32
		**Fe: 0.5	>98	>98	59–76	10–35
		**Fe: 2.1	90–98	87–98	69–85	2–15
HydraCoRe 70pHT * [45,46]	1.5	Al: 0.6	73–96	31–90	60–95	52–85
	1.0	Al: 0.6	66–88	53–74	51–70	41–66
		Al: 1.8	68–96	56–89	60–88	40–70
		**Fe: 0.5	79–89	63–80	69–82	34–55
		**Fe: 2.1	77–93	40–76	70–90	-2–30

* In the experiments performed with Fe(III), this metal was added as chloride ($FeCl_3$)

** This experiments also contained 0.6 g/L Al(III)

Table 6. *Estimation of concentration factors for the different ions in solution at different %permeate recovery values for the solution at pH 1.0 containing 0.6 g/L Al and 2.1 g/L Fe(III)*

Membrane	%permeate recovery	Concentration factor						
		H^+	Al	Fe	Ca	Cu	Zn	REEs[1]
TiO_2	20	0.97	1.14	1.11	1.07	1.06	1.07	1.07
	40	0.93	1.38	1.30	1.19	1.17	1.19	1.18
	60	0.84	1.86	1.68	1.42	1.38	1.43	1.41
	80	0.57	3.29	2.82	2.12	2.02	2.15	2.10
MPF–34	20	0.97	1.20	1.20	1.20	1.20	1.20	1.20
	40	0.93	1.53	1.54	1.53	1.52	1.52	1.53
	60	0.83	2.20	2.20	2.20	2.18	2.18	2.20
	80	0.55	4.19	4.21	4.20	4.14	4.14	4.20

[1] The term REEs includes the mean value of the following metals: La, Pr, Nd, Sm, Dy and Yb

FIGURE CAPTIONS

Figure 1. Scheme of the experimental set-up

Figure 2. Rejection of 0.01 M Na_2SO_4 with TiO_2 ceramic membrane (1 nm) from pH 1.0 to 11.0 at TMP of 6 (blue) and 13 bar (red). Triangular green points correspond to the data from Van Gestel et al. [36], and the circular violet ones were taken from Puhlfürß et al. at TMP 6 bar (0.55 nm) [35].

Figure 3. SEM images of the ceramic membrane: a) internal surface (TiO_2); b) external surface (Al_2O_3); c) membrane profile at x300 amplifications and; d) membrane profile at x1000 amplifications

Figure 4. Schematic representation of the membrane protonation/deprotonation. A^- and C^+ represent the anions and cations in solution, respectively. Green and red arrows represent attractive and repulsive forces between the ions and the membrane.>

Figure 5. Rejection curves for the ions in solutions for the TiO_2 ceramic membrane at different solution compositions: (a,b) influence of pH (1.5 and 1.0); (c,d) influence of Al(III) concentration (0.6 and 1.8 g/L) without Fe(III) and; (e,f) influence of Fe(III) concentration (0.5 and 2.1 g/L) containing 0.6 g/L Al(III)

Figure 6. Rejection curves for the ions in solutions for the MPF–34 membrane at different solution compositions: (a,b) influence of pH (1.5 and 1.0); (c,d) influence of Al(III) concentration (0.6 and 1.8 g/L) without Fe(III) and; (e,f) influence of Fe(III) concentration (0.5 and 2.1 g/L) containing 0.6 g/L Al(III)

Figure 7. Sulphate (SO_4) fraction as a function of pH for a solution containing 0.6 mg/L Al(III). The vertical lines in the speciation diagram refer to the pH values evaluated experimentally.

Figure 8. Sulphate (SO_4) fraction as a function of Al concentration for a solution at pH 1.0

Figure 9. Sulphate (SO_4) fraction as a function of Fe concentration for a solution at pH 1.0 containing 0.6 g/L Al(III)

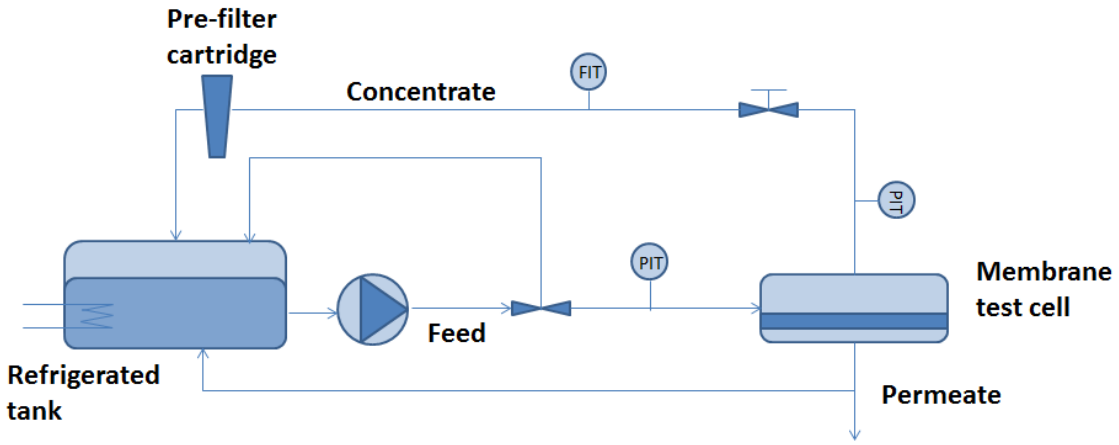
Pre-filter
cartridge
Concentrate
FIT
PIT
PIT
Membrane
test cell
Feed
Refrigerated
tank
Permeate

Figure 1

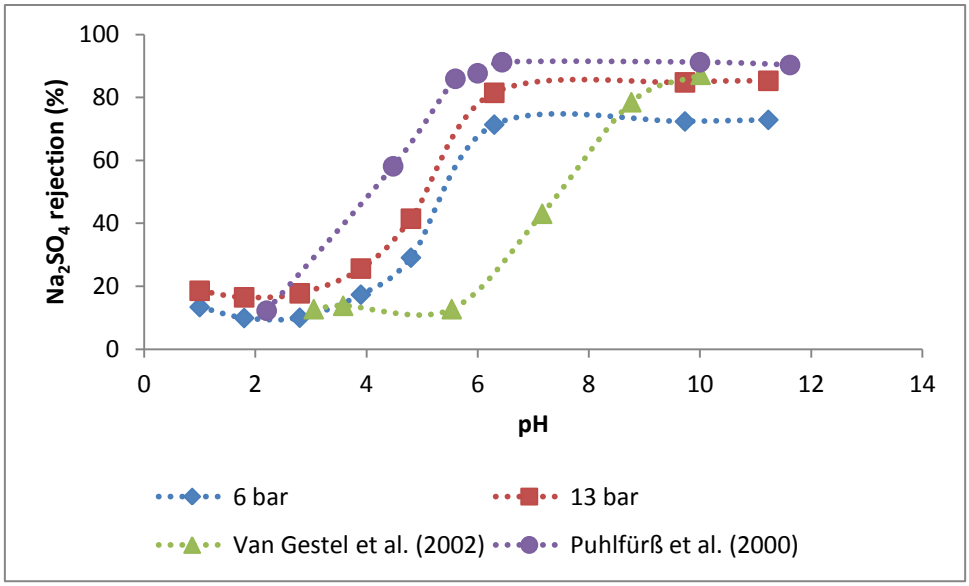
100
80
60
40
20
0
0
2
4
6
8
10
12
14
Na2SO4 rejection (%)
pH
6 bar
13 bar
Van Gestel et al. (2002)
Puhlfürß et al. (2000)

Figure 2

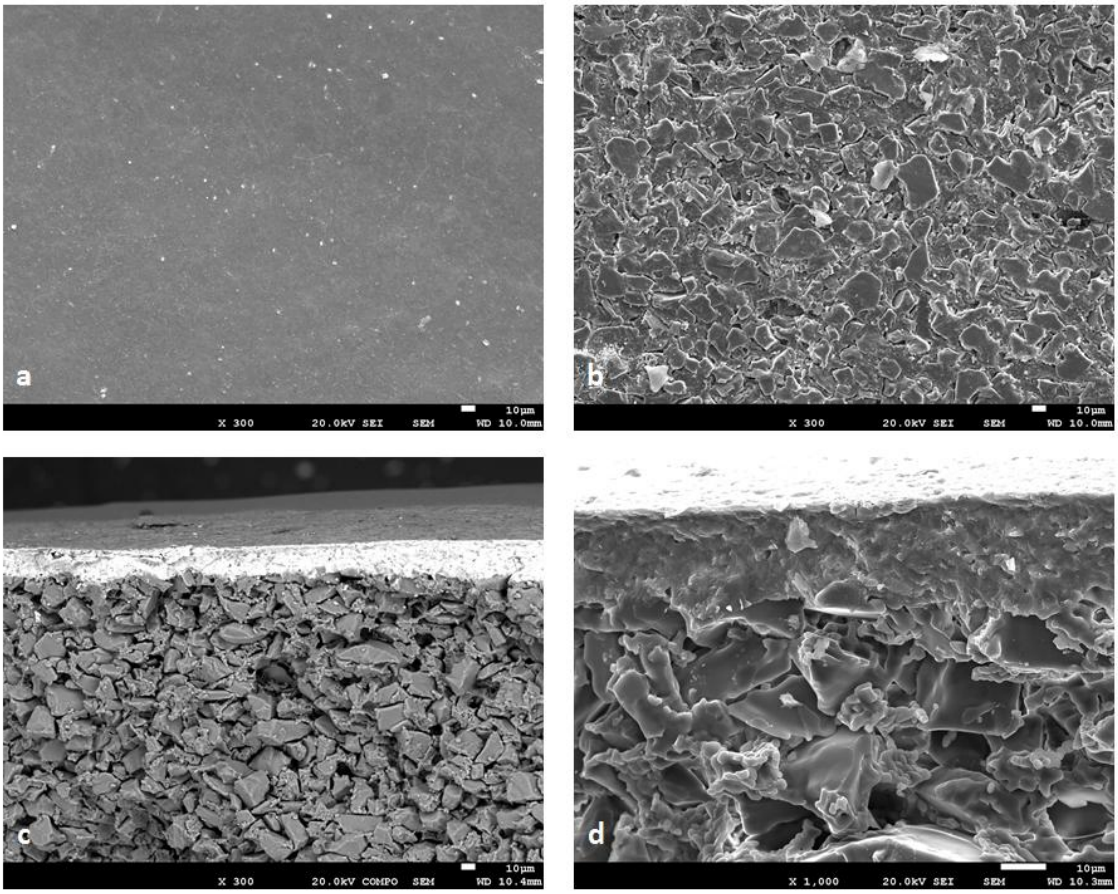
a
X 300 20.0kV SEI SEM WD 10.0mm
10μm
b
X 300 20.0kV SEI SEM WD 10.0mm
10μm
c
X 300 20.0kV COMPO SEM WD 10.4mm
10μm
d
X 1,000 20.0kV SEI SEM WD 10.3mm
10μm

Figure 3

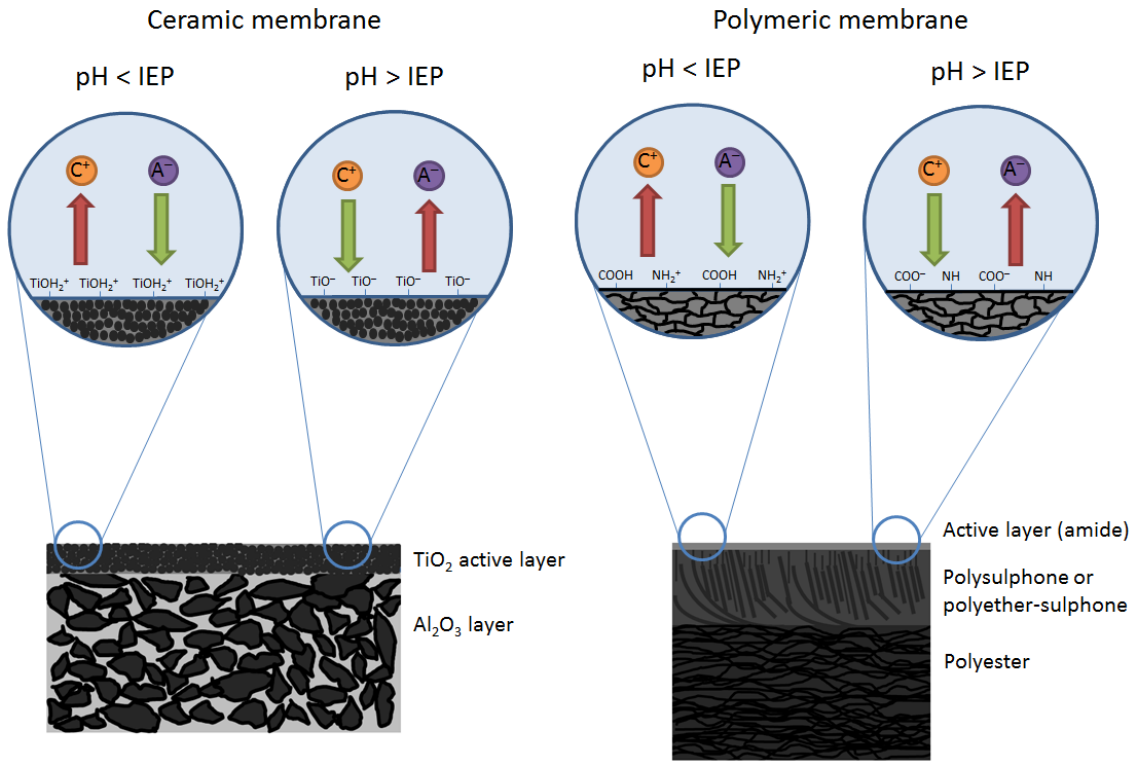
Ceramic membrane
Polymeric membrane
pH < IEP
pH > IEP
pH < IEP
pH > IEP
C+
A−
TiOH2+ TiOH2+ TiOH2+ TiOH2+
TiO− TiO− TiO− TiO−
COOH NH2+ COOH NH2+
COO− NH COO− NH
TiO2 active layer
Al2O3 layer
Active layer (amide)
Polysulphone or
polyether-sulphone
Polyester

Figure 4

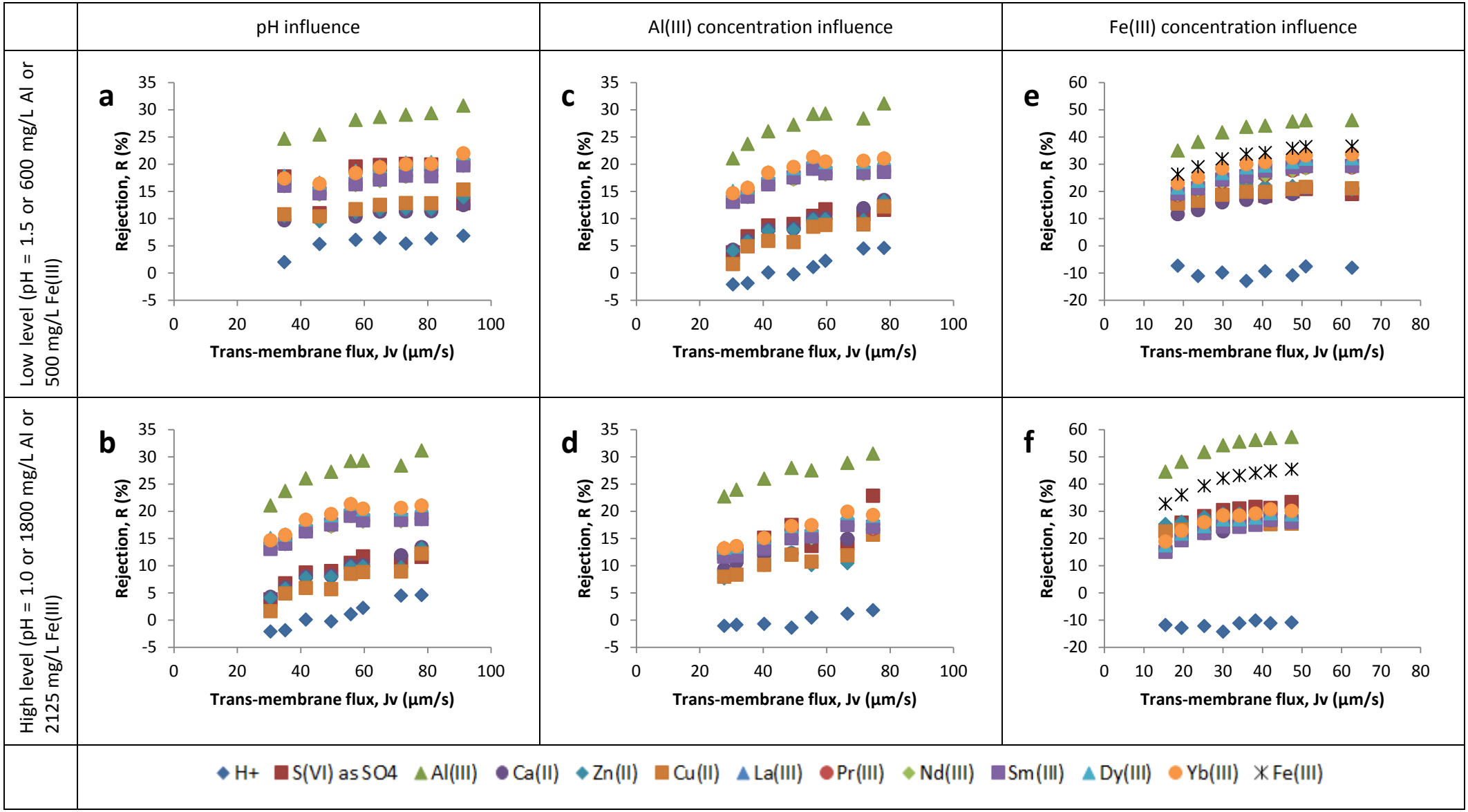
pH influence
Al(III) concentration influence
Fe(III) concentration influence
Low level (pH = 1.5 or 600 mg/L Al or 500 mg/L Fe(III)
High level (pH = 1.0 or 1800 mg/L Al or 2125 mg/L Fe(III)
a
b
c
d
e
f
Rejection, R (%)
Trans-membrane flux, Jv (µm/s)
H+
S(VI) as SO4
Al(III)
Ca(II)
Zn(II)
Cu(II)
La(III)
Pr(III)
Nd(III)
Sm(III)
Dy(III)
Yb(III)
Fe(III)

Figure 5

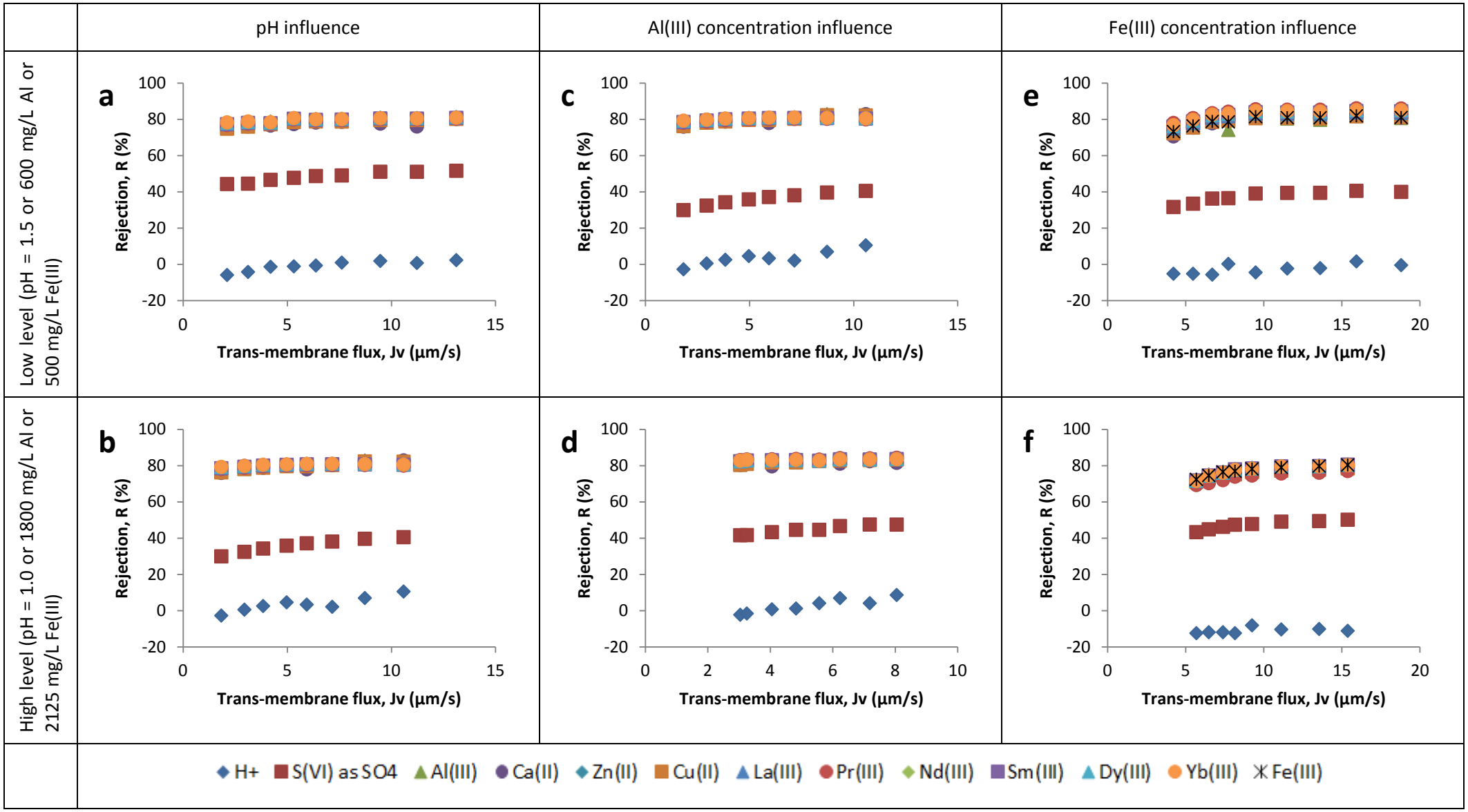
pH influence
Al(III) concentration influence
Fe(III) concentration influence
Low level (pH = 1.5 or 600 mg/L Al or 500 mg/L Fe(III)
High level (pH = 1.0 or 1800 mg/L Al or 2125 mg/L Fe(III)
a
b
c
d
e
f
Rejection, R (%)
Trans-membrane flux, Jv (µm/s)
H+
S(VI) as SO4
Al(III)
Ca(II)
Zn(II)
Cu(II)
La(III)
Pr(III)
Nd(III)
Sm(III)
Dy(III)
Yb(III)
Fe(III)

Figure 6

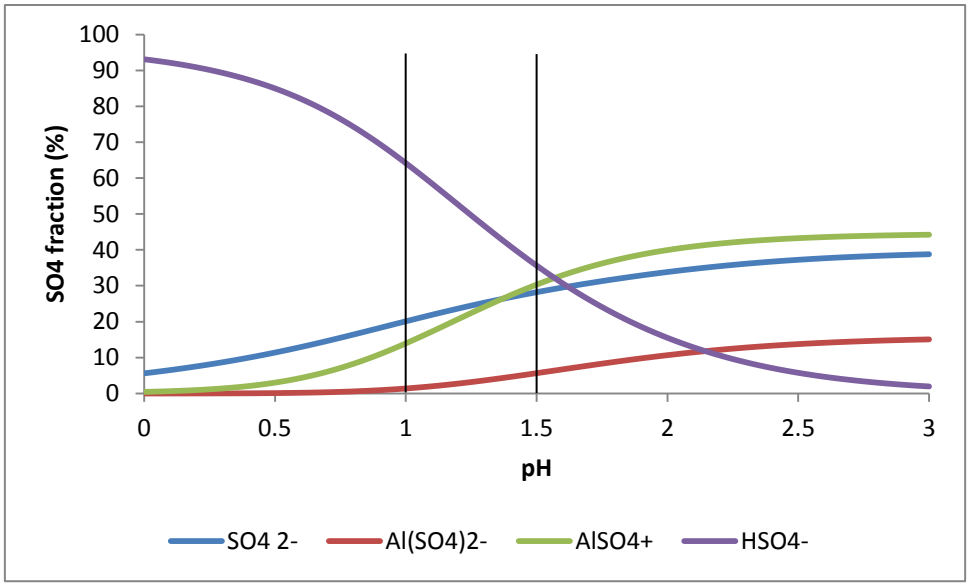
100
90
80
70
60
50
40
30
20
10
0
SO4 fraction (%)
0
0.5
1
1.5
2
2.5
3
pH
SO4 2-
Al(SO4)2-
AlSO4+
HSO4-

Figure 7

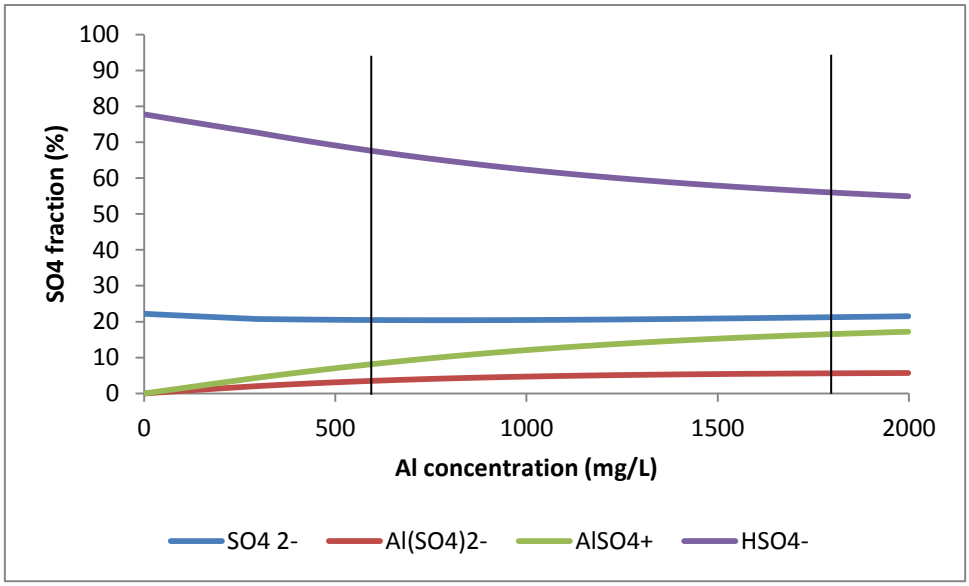
100
90
80
70
60
50
40
30
20
10
0
SO4 fraction (%)
0
500
1000
1500
2000
Al concentration (mg/L)
SO4 2-
Al(SO4)2-
AlSO4+
HSO4-

Figure 8

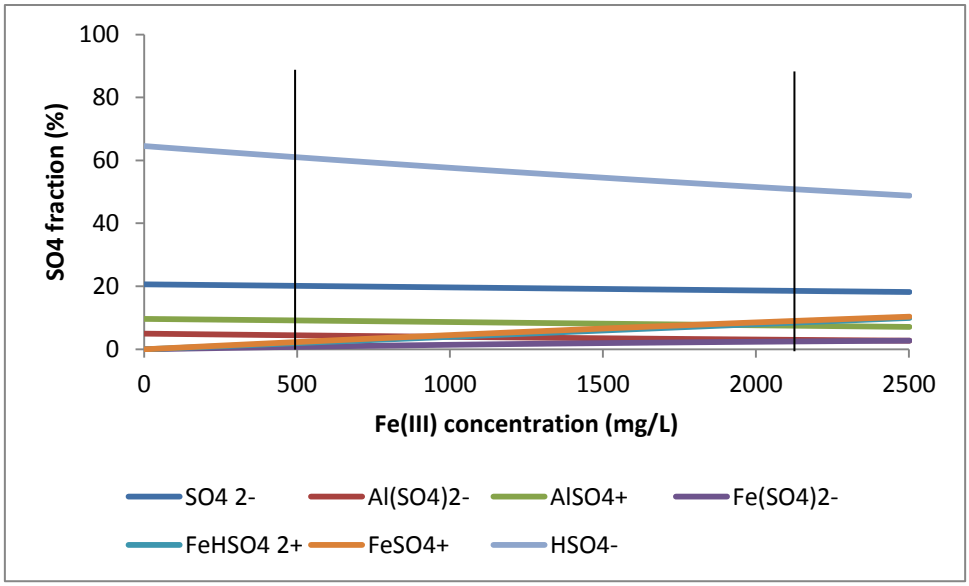
100
80
60
40
20
0
SO4 fraction (%)
0
500
1000
1500
2000
2500
Fe(III) concentration (mg/L)
SO4 2-
Al(SO4)2-
AlSO4+
Fe(SO4)2-
FeHSO4 2+
FeSO4+
HSO4-

Figure 9